STRATEGIES TO TARGET ESTROGEN-RELATED TUMOR PROMOTING MECHANISMS IN LUNG CANCER

by

Natalie J. Rothenberger

Bachelor of Arts, University of Pittsburgh, 2014

Submitted to the Graduate Faculty of

University of Pittsburgh School of Pharmacy

in partial fulfillment of the requirements for the degree of

Master of Science

UNIVERSITY OF PITTSBURGH

School of Pharmacy

This thesis was presented

by

Natalie Rothenberger

It was defended on

August 4th 2017

and approved by

Dr. Wen Xie, MD, PhD,

Interim Chair of Pharmaceutical Sciences, The Joseph Koslow Endowed Chair,

Professor, Department of Pharmaceutical Sciences

Thesis Advisor: Dr. Paul P. Johnston, PhD,

Research Associate Professor,

Department Pharmaceutical Sciences

Thesis Advisor: Laura P. Stabile, PhD,

Associate Professor,

Department of Pharmacology & Chemical Biology

STRATEGIES TO TARGET ESTROGEN-RELATED TUMOR PROMOTING MECHANISMS IN LUNG CANCER

Natalie Rothenberger, M.S.

University of Pittsburgh, 2017

Despite clinical advancements with targeted and immune therapies, lung cancer remains the leading cause of cancer related deaths in the United States. Scant improvements in the five-year survival rate over the past decade necessitate the development of more efficacious therapeutic approaches. Epidemiological reports and preclinical studies have demonstrated involvement of the estrogen pathway, mediated through estrogen receptor β-1 (ERβ), in the development and promotion of lung tumorigenesis. Strategies for targeting the estrogen pathway include anti-estrogens and aromatase inhibitors (AIs), either as single agents or combined with other therapies. The primary objective of this study was to identify and target interactions between the estrogen signaling pathway and the fibroblast growth factor (FGF) pathway and identify additional estrogen-related tumor promoting mechanisms in non-small cell lung cancer (NSCLC). Fibroblast growth factor receptor 1 (FGFR1) was significantly over-expressed in ERβ high tumors, while the decoy receptor, fibroblast growth factor receptor like-1 (FGFR5), was down-regulated. NSCLC cell lines lacking FGFR1 amplification expressed multiple FGFRs and secreted several FGFs. β-estradiol (E2) treatment significantly enhanced FGF2 release, an effect blocked by the anti-estrogen fulvestrant. Furthermore, co-targeting the E2 and FGF pathways with fulvestrant and the pan-FGFR inhibitor AZD4547 resulted in greater anti-tumor effects both *in vitro* and *in vivo* compared to single pathway inhibition. These results demonstrate crosstalk between the two pathways in NSCLC, and suggest clinical utility of a pan-FGFR inhibitor in combination with an anti-estrogen in a subset of NSCLC patients. Previous reports of aromatase

expression in pulmonary tumor macrophages, and up-regulation of anti-oxidant signaling with AIs, indicate a potential interaction between estrogen signaling and inflammation in lung cancer. Utilizing an *in vivo* NSCLC xenograft model, the AIs exemestane and letrozole significantly inhibited tumor proliferation, reduced Ki67 expression, altered tumor histology, and increased anti-inflammatory signaling. Finally, we demonstrated fulvestrant enhanced therapeutic sensitivity and inhibited the migration of NSCLC cells resistant to the heat shock protein 90 (HSP90) inhibitor ganetespib, but not through a reversal of epithelial-mesenchymal transition. Together, the results of this study highlight the pervasive role of estrogen signaling in lung cancer and provide rationale for combinatorial strategies involving hormonal agents for lung cancer treatment.

TABLE OF CONTENTS

LIST OF TABLES

LIST OF FIGURES

ACKNOWLEDGEMENTS

I would like to thank all members of the Stabile laboratory, especially Autumn Gaither-Davis for her unwavering encouragement and friendship both in the lab and in life. I would also like to personally thank Bea Kanterewicz for her assistance with animal experimentation and continued willingness to help with scientific projects at any and all times. I would also like to thank Dr. Timothy Burns and all members of the Burns laboratory for their scientific and morale support. I would also like to extend gratitude to Dr. Jill Siegfried and all members of her laboratory for their collaboration and experimental support with the FGFR project.

I would also like to sincerely thank my thesis advisor and mentor Dr. Laura Stabile for providing me not only the opportunity to work in her laboratory, but also continued mentorship, guidance, and opportunities for personal and professional growth throughout my winding academic journey. I would also like to thank my co-thesis advisor Dr. Paul Johnston for his scientific and academic assistance during my master's program. I am also very grateful for the guidance and support from my committee member Dr. Wen Xie.

Most of all, I would like to extend my deepest gratitude to my parents, family, and friends for their unconditional love, support, and encouragement as I continue to pursue my goals.

1. INTRODUCTION

1.1 LUNG CANCER INCIDENCE AND EPIDEMIOLOGY

Lung cancer remains the leading cause of cancer related deaths in the United States (U.S.) and worldwide [1]. Despite declining trends in incidence since the 1990's for men and 2000's for women, lung cancer is the second most prevalent carcinoma with an estimated 222,500 new cases in 2017 alone [1]. While advancements in early detection with the use of low-dose computed tomography for high-risk patients and the development of targeted therapies and immunotherapies have improved therapeutic options and patient outcomes [2-4], the five-year survival rate for lung cancer remains a dismal 17% for all stages combined [1]. Scarce improvements in the survival rate over last decade indicate the need to further identify risk factors and mechanisms driving lung carcinogenesis to enable the development of more personalized and efficacious therapeutic strategies.

Lung cancer is broadly classified as one of two forms: small cell lung cancer (SCLC) and non-small cell lung cancer (NSCLC). NSCLC accounts for the majority of lung cancer cases (85%) and can be further differentiated into histologically unique subtypes including adenocarcinomas, squamous cell carcinomas, and large cell carcinomas (Figure 1).

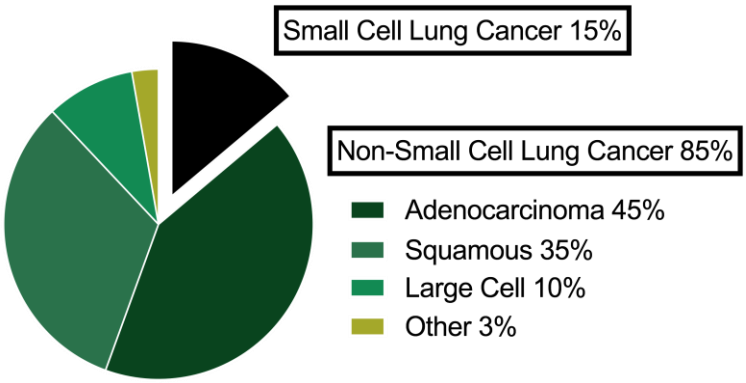

Figure 1. Lung Cancer Histological Subtypes

NSCLCs harbor more genetic abnormalities compared to SCLC, are less responsive to chemotherapy, and the subtype adenocarcinoma is the most common form of lung cancer in patients who have never smoked [5]. Interestingly, as smoking prevalence declined over the past few decades incidence of squamous cell carcinomas declined among men, while incidence of adenocarcinomas increased among both men and women [6]. This variation in subtype incidence has partially been attributed to ventilation in cigarette filters [7]; however, other individual genetic and environmental factors are being investigated to better understand this observation.

Among identified risk factors for the development of lung cancer, cigarette smoking and tobacco inhalation account for the majority of cases and reportedly 80% of lung cancer deaths in the U.S. [1]. Exposure to environmental toxins such as radon gas, asbestos, and polycyclic aromatic hydrocarbons (PAH) have also been implicated in lung tumorigenesis [8]. Comorbidities such as chronic obstructive inflammatory disease (COPD) may also act as oncogenic drivers through increased cell proliferation, exposure to inflammatory cytokines, and oxidative stress [9]. Viral infections such as such as human papilloma virus (HPV), Simian Virus 40 (SV40), and Epstein Bar Virus (EBV) have also been implicated as potential contributors to lung cancer development [10]. While additional correlative studies are still required, the presence of HPV

strain 16/18 DNA in circulating blood was reported to be associated with increased risk of lung cancer development in non-smoking females, and both SV40 and EBV have suggested roles in mesothelioma pathogenesis [10-12]. Furthermore, while a specific genetic link has yet to be identified, studies have observed an increased risk of lung cancer incidence in patients who have a family history of the disease suggesting genetic factors are involved [13]. Moreover, studies assessing familial aggregations of lung cancer have found that affected individuals tend to be younger at the age of onset and female [14]. In addition to familial aggregation trends, several other sex differences have been observed in the epidemiology and presentation of lung cancer suggesting endogenous and exogenous hormones may also act as risk factors for the disease [15].

1.2 TREATMENT STRATEGIES FOR LUNG CANCER

Significant advancements in the diagnosis and treatment of lung cancer have been made over the past few decades. Differential clinical response based on histology to the nitrogen mustard chemotherapy cyclophosamide observed in 1969 was among the first evidence that lung tumors varied in location, histology, biology, and therapeutic response [16]. Chemotherapy options diversified over the next 30 years with the development of anti-mitotic vinca alkaloids such as vinorelbine, mitotic inhibiting taxanes paclitaxel and docetaxel, and platinum-based regimens cisplatin and carboplatin [17]. It wasn't until the early 2000's, however, that a shift in the oncology therapeutic paradigm occurred with the use of molecular profiling to identify and target genetic abnormalities driving an individual's disease.

For both early and advanced SCLC patients, however, platinum-based chemotherapy combinations remain the standard of care, most commonly cisplatin plus etoposide or carboplatin plus etoposide [18]. Four randomized clinical trials have been conducted to compare cisplatin

efficacy to carboplatin in these patients, and a recent meta-analysis of individual patient data from these studies found no statistically significant survival advantage of one therapy over the other [19]. Compared to NSCLC patients, significantly higher (50-80%) response rates are observed in SCLCs treated with these therapies, however due to frequent and early relapse the five-year survival rate for both NSCLC and SCLC advanced stage patients remain similar (1-5%) [20,21]. Clinical strategies for SCLC are restrained to these systemic regimens, however, with failed clinical development of targeted therapies and a dearth of identified molecular events other than *TP53* and *RB1* inactivation in these patients [20]. Although, early occurrence of chemotherapy-resistant disease has led to "non-cross-resistant" approaches and multi-drug combinations incorporating cytotoxic taxanes such as paclitaxel to be administered in later cycles to improve clinical benefit [18].

The general therapeutic approach for patients diagnosed with NSCLC significantly varies from that of SCLC patients. Surgical resection is the standard treatment option for eligible early-stage patients, with adjuvant radiation or chemotherapy depending on localization and staging of the disease [17]. For advanced-stage NSCLC patients, several considerations are made regarding therapy regimens due to the development and approval of targeted and immune therapies.

1.2.1 Targeting Oncogenic Molecular Drivers in Advanced NSCLC

Paul Ehrlich's theory for the development of "magic bullet" therapies selectively targeting molecular drivers of disease led to the century-long evolution of targeted small molecule anti-cancer agents [22]. Currently 13 targeted agents, including small molecule inhibitors and monoclonal antibodies, that selectively interfere with molecular targets propagating uncontrolled

proliferation, angiogenesis, and cell survival are approved for the treatment of metastatic NSCLC with several more in the pipeline.

Preclinical investigations and molecular profiling have identified several genetic oncogenic driver mutations and alterations among the various NSCLC histologies as shown in Figure 2. The frequency and distribution of these genetic drivers indicates lung cancer is a complex and heterogeneous disease, and the development of small molecule inhibitors targeting specific alterations within an individual patient's disease allows for a more directed and efficacious treatment strategy.

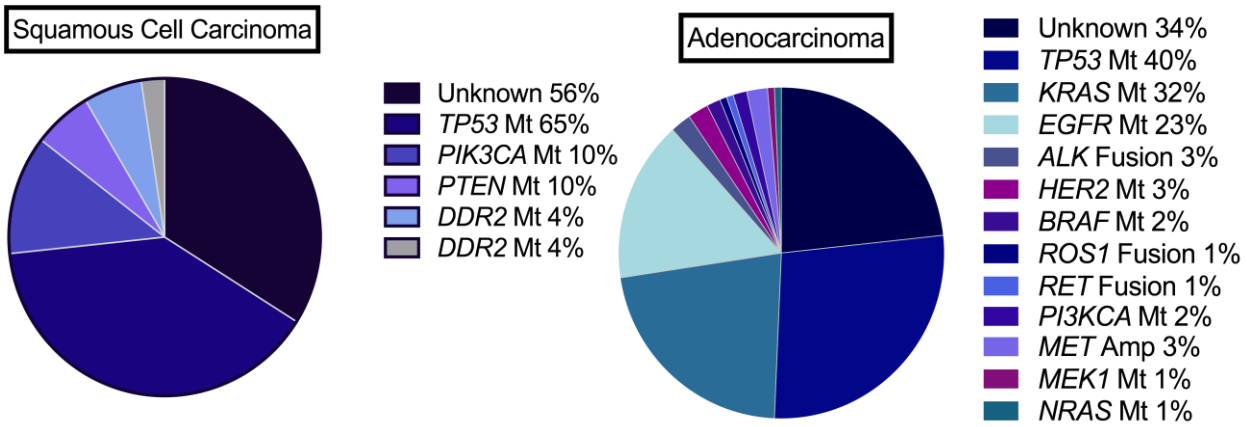

Figure 2. Molecular Alterations in NSCLC by Histology. Frequency of molecular alterations including gene amplification, mutations and fusions in NSCLC based on histological subtype. Data adapted from references [23,24].

Therapies targeted against epidermal growth factor receptor (EGFR), anaplastic lymphoma kinase (ALK), ROS1, and BRAF are FDA-approved for the treatment of NSCLC in patients whose tumors express these alterations, while off-label use of agents targeting HER2, MET and RET is also pursued for NSCLC patients who have progressed on standard therapies. With the incorporation of genotyping, improved screening technology, and enhancements in pathological

techniques, physicians are now able to acquire a much more comprehensive analysis of each patient's carcinoma. Improved diagnosing coupled with the development of novel targeted agents has enabled treatment strategies to be stratified based on histology, staging, driver mutations and most recently expression of the immune regulatory protein programmed death-ligand 1 (PD-L1) as shown in Figure 3 [17].

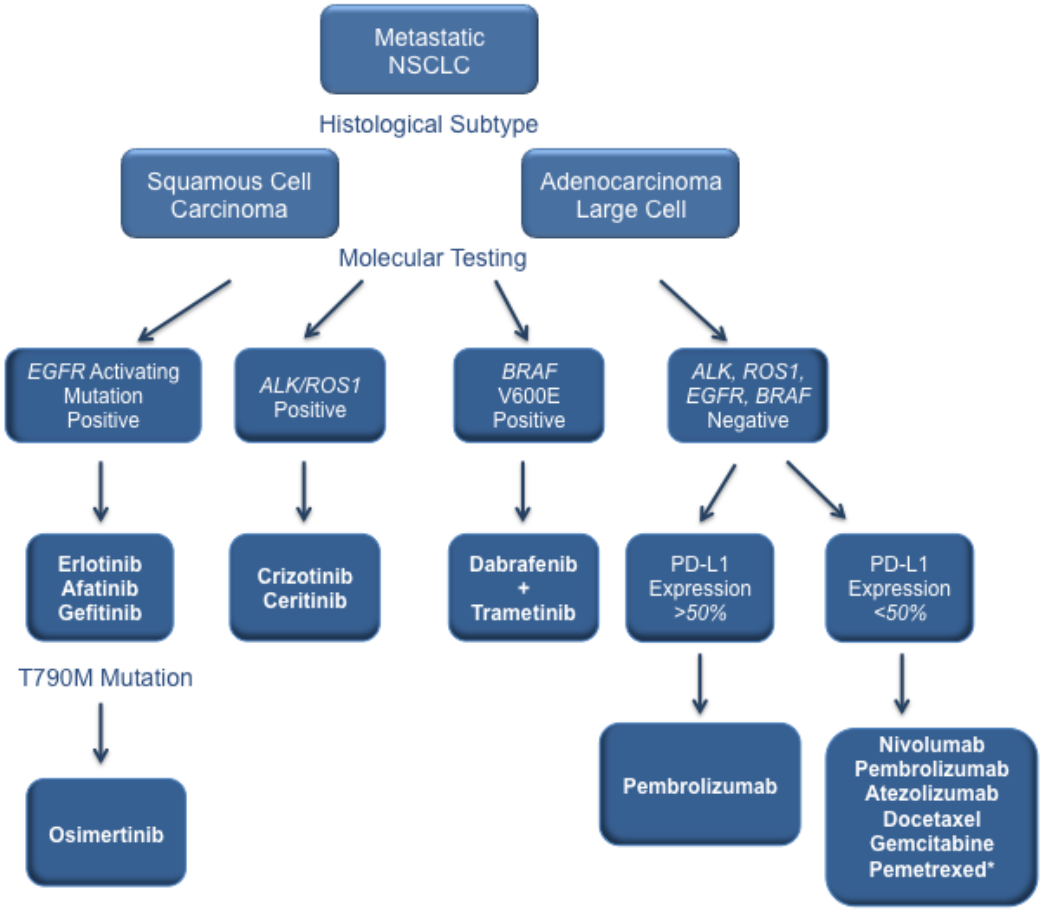

Figure 3. First-line Treatment Strategies for Advanced NSCLC Based on Molecular Testing. Adapted from NCCN guidelines and literature search as of July 7th, 2017 for FDA approved treatment strategies for metastatic NSCLC [17]. *Pemetrexed is only indicated for adenocarcinoma and large cell histological subtypes.

Following *TP53* and *KRAS*, mutations in the *EGFR* gene are among the most commonly observed molecular alterations in NSCLC. Widely expressed in a majority of epithelial cells, EGFR signaling is fundamental in supporting normal development and physiology [25]. EGFR is activated by numerous ligands such as epidermal growth factor (EGF) and transforming growth factor alpha (TGF-α) leading to receptor homo- and hetero-dimerization and subsequent activation of downstream effector molecules that mediate cellular proliferation, invasion, and survival [26]. Overexpression of EGFR is reported in multiple malignancies including lung cancer, and often correlated with poor prognosis and shorter survival prompting the development of EGFR tyrosine kinase inhibitors (TKIs) [27-29]. Following broad approval of EGFR TKIs gefitinib and erlotinib in refractory NSCLC patients, the discovery of *EGFR* sensitizing mutations in exons 19 and 21 conferring increased response rates revolutionized NSCLC EGFR treatment strategies [30,31]. The FDA ultimately re-labeled these agents for restricted use only in patients harboring these mutations. As such, erlotinib is now given as a first-line monotherapy to patients with an activating *EGFR* mutation. A meta-analysis of 13 clinical trials assessing EGFR TKI efficacy confirmed therapeutic benefit of the targeted agents in mutant patients observing significantly improved progression-free survival (PFS) among *EGFR* mutant patients receiving EGFR TKIs compared to wild-type patients [32]. However, with the advent of targeted therapies came the discovery of intrinsic and acquired resistance mechanisms such as the EGFR T790M mutation observed in approximately 60% patients previously treated and whom initially responded to an EGFR TKI [17,33]. The prevalence of this acquired resistance mutation led to the development and recent approval of the third-generation EGFR TKI, osimertinib and second generation afatanib which target tumors harboring T790M [17].

In addition to EGFR inhibitors, agents targeted against the fusions of the anaplastic lymphoma kinase (*ALK*) gene and rearrangement of the proto-oncogene *ROS1* have also been

approved for treatment of NSCLC patients harboring these genetic alterations. *ALK* gene fusions are observed in 3-7% of NSCLC cases. Fusion of the *ALK* gene to the echinoderm microtubule-associated protein-like 4 (*EML4*) gene leads to constitutive activation of the kinase domain and downstream pathways promoting proliferation and tumor progression [34,35]. ALK kinase inhibitors crizotinib, and second-generation ceritinib, were clinically developed revealing a robust response in ALK-positive patients with superior clinical benefit compared to chemotherapy [36]. These clinical observations led to the approval of crizotinib as a first-line therapy for advanced and metastatic NSCLC with the fusion gene mutation. Due to 77% amino acid homology in the ATP binding sites in both ALK and ROS1, crizotinib was also identified as a potent inhibitor of the ROS1 kinase [37-39]. *ROS1* rearrangements are observed in approximately 1% of NSCLC patients, and upon clinical investigation of crizotinib therapy in 50 patients harboring this mutation, the therapy received FDA approval with reports that 66% of patients experienced either partial or complete responses [37].

Drug discovery efforts have initiated the development of several other therapies targeting the molecular alterations referenced in Figure 2. Mutations in the tumor suppressor *p53* gene are the most frequently observed genetic alterations in lung cancer with increased mutation frequency associated with tobacco consumption [40]. While several research efforts have focused on developing therapies to deplete mutant *p53* or restore wild-type function, the challenging chemical structure of the transcription factor has hindered the clinical development of pharmacologic inhibitors and activators [41,42]. Moreover, several efforts have focused on targeting the RAS-Raf-MEK-ERK and the PI3K-Akt-mTOR signaling cascades as they are two of the most commonly dysregulated networks involved in the promotion of lung tumorigenesis. Mutations in the effector molecules of these pathways account for the largest percentage identified molecular alterations in NSCLC making them attractive targets for selective inhibition. While therapies

targeted against *KRAS* (Kirsten-rous avian sarcoma) mutations have had limited success, targeting downstream proteins such as BRAF and MEK have been more successful. Dabrafenib, a potent inhibitor of wild-type and V600E mutant *BRAF*, combined with the MEK1/2 inhibitor trametinib, revealed synergistic anti-proliferative effects *in vitro* prompting a recent phase II multi-center trial assessing the combination in *BRAF* V600E-mutant NSCLC patients. The study reported a 63% overall response rate in *BRAF* mutant patients leading to the recent FDA approval of dabrafenib plus tramedinib for advanced NSCLC patients with this mutation [43,44].

Agents targeting phosphatidylinositide 3-kinases (PI3K) have also been studied in NSCLC, but have failed to demonstrate efficacy as a monotherapy. Akt and dual PI3K-mTOR inhibitors have also been developed and are in early clinical development as combination strategies in NSCLC [45]. Amplification of fibroblast growth factor receptor 1 (FGFR1), conferring sensitivity to FGFR inhibitors, is reported in 23% of squamous cell carcinomas and pan-FGFR inhibitors such as AZD4547 are in early phase I/II clinical evaluation in NSCLC (NCT02965378, NCT01824901, NCT02664935). Several other inhibitors targeting HER2, RET DDR2, PTEN, and EPH have also been developed but await further clinical evaluation in NSCLC.

1.2.2 Immunotherapy for the Treatment of NSCLC

Lung cancer has been historically considered nonimmunogenic due to a loss of major histocompatibility complex (MHC) antigen expression, secretion of immunosuppressive cytokines, and suppression of cytotoxic T-cells [46-48]. However, the field of immuno-oncology is rapidly evolving and various therapeutic strategies have been investigated in lung cancer to override the disease's evasion of immunosurveillance. Among these strategies check-point blockade antibodies inhibiting the programmed cell death-1 (PD-1) receptor and PD-1 ligand (PD-

L1) have revealed great clinical benefit in patients with tumors expressing elevated levels of PD-L1 [3,49,50]. The PD-1 receptor is expressed on T cells, natural killer (NK) cells, and some B cells and recognizes both the PD-L1 and PD-L2 ligands commonly expressed on a range of antigen-presenting cells, tumor cells, and cells within the tumor microenvironment [48]. The binding of the PD-1 receptor to its ligands induces inhibition of T-cell activation down regulating the immune response. Elevated PD-L1 expression has been reported in 13-70% of lung cases, which led to the clinical development of PD-1 inhibitors nivolumab and pembrolizumab which consistently reveal improved overall response rates compared to chemotherapy in NSCLC PD-L1 positive (PD-L1 expression >50%) patients [49,50]. The promising results of these studies led to the approval of pembrolizumab as a first line agent in advanced NSCLC patients lacking driver mutations with at least 50% PD-L1 positive tumor cells, and nivolumab for advanced NSCLC who have progressed on or after platinum-based regimens [17]. Monoclonal antibodies targeted against PD-L1 including BMS936559, Medi-4736 and MPDL3280 are also in early phase I or phase II clinical development in combination with other therapies.

Additional immunogenic therapies undergoing clinical investigation in lung cancer include ipilimumab, a cytotoxic T-lymphocyte antigen-4 (CTLA-4) antibody, along with tumor antigen specific vaccines and whole tumor vaccines. CTLA-4 is a checkpoint protein expressed on activated T-cells that trigger immune resistance by competitively binding to CD80 and CD86, blocking CD28 T-cell activation [51]. Assessment of CTLA-4 antibodies in preclinical murine models revealed synergy when combined with chemotherapies [52,53]. These preclinical results led to the current phase III clinical evaluation of ipilimumab in combination with chemotherapy in NSCLC and SCLC patients and FDA approval of the therapy in metastatic melanoma patients (NCT01285609, NCT01450761).

Lung cancer vaccines have also been developed to induce *de novo* anti-tumor immunity. Developed against either specific lung tumor antigens such as melanoma-associated antigen-A3 (MAGE-A3), membrane-associated glycoprotein (MUC-1), and EGFR, or against whole tumor cells such as tergenpumatucel-L composed of genetically altered NSCLC cells [51]. While early clinical results for vaccines are modest and variable, these therapies represent novel approaches for stimulating patients' innate and adaptive immune responses for enhanced elimination of neoplastic cells.

Incredible advancements in precision medicine with molecular profiling and the development of targeted TKIs and immunotherapies have significantly improved the treatment options available for lung cancer patients. However, the lack of improvement in overall clinical benefit indicates a need for the continued discovery of novel oncogenic targets and development of more effective treatment strategies.

1.3 SEX DIFFERENCES IN LUNG CANCER

The rise of lung cancer incidence in women between the 1950's to 1980's was so severe that the 1980 Surgeon General's report declared smoking-related lung cancer an epidemic among women [54]. However, as smoking prevalence declined among men and women during the 1990's corresponding declines in lung cancer incidence were observed in men, but not in women [55]. Instead female lung cancer cases continued increasing during this time (Figure 4), precipitating multiple investigations to identify potential sex differences in the epidemiology of lung cancer.

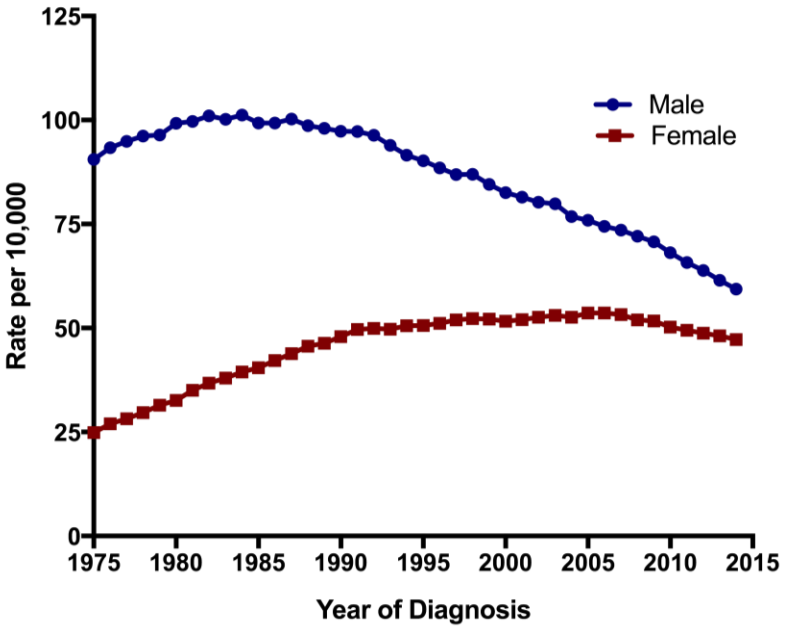

Figure 4. Lung Cancer Incidence Rates Among Men and Women in U.S. Lung cancer incidence rates stratified by sex from 1975 to 2014 adapted from National Cancer Institute Surveillance, Epidemiology, and End Results Program [55]. Red squares=female; blue circles=male.

Several cohort studies have subsequently assessed whether women are more susceptible than men to the development of smoking-related lung cancer. While earlier results reported increased risk in women compared to men upon adjustment for age and smoking history, more recent studies challenge these findings by showing both sexes may have comparable risk of tobacco-induced incidence [56-59]. Alternatively, cohort studies assessing lung cancer incidence in never-smokers have consistently observed significantly 2.25-fold increased incidence of the disease in women compared to men ($P<0.0001$) [60,61]. As mentioned previously women are more susceptible to the disease in the event of familial aggregation, and tend to be diagnosed at a younger age. Upon diagnosis, however, female patients have significantly improved 5-year survival outcomes compared to male patients ($P=0.001$) [56,62,63].

Altered metabolism of carcinogens is another clinical characteristic reportedly predisposing women to lung cancer. Some tobacco carcinogens including PAHs are inhaled as pro-carcinogens requiring activation by phase 1 cytochrome P450 enzymes such as CYP1A1. Oxidation of PAHs and other pro-carcinogens generates reactive epoxide species that when not conjugated and detoxified by phase II enzymes can bind to DNA forming adducts causing irreversible DNA damage [64]. Female lung cancer patients have been shown to have higher levels of DNA adducts correlating with increased expression of CYP1A1 compared to male patients [65,66]. DNA adduct levels are considered a measure carcinogen metabolism comparing phase 1 activation to phase II detoxification. Elevated PAH-DNA adduct levels and upregulated expression of CYP1A1, coupled with decreased DNA repair capacity, put women at a significantly greater risk of tobacco-induced lung carcinogenesis than men with an odds ratio of 7.6 ($P<0.001$). [67]. Furthermore, while relatively few studies have evaluated the effects of testosterone levels on lung cancer risk and incidence a recent *in vitro* analysis showed that female sex hormones had more potent inhibitory effects on tobacco-carcinogen detoxification in NSCLC cell lines compared to testosterone [68]. These results, in addition to the fact that circulating serum estrogen levels are up to 7.5 times greater (1.5nM) in premenopausal women compared to men, support the hypothesis that sex differences in lung cancer development and incidence may be attributed more so to female hormones as opposed to androgens [68].

Further investigations into sex differences in the presentation of lung cancer have also identified distinctly varying histological and biological characteristics between men and women. Compared to men, women are diagnosed more frequently with adenocarcinoma than any other histological subtype accounting for up to 60% of cases[15]. Albeit a heterogeneous disease, trends in mutation profiles have also been identified between sexes. Female patients diagnosed with adenocarcinomas are more likely to have activating *EGFR* mutations [69]. This observation may

in part relate to the demonstrated crosstalk between the estrogen receptor (ER) and EGFR pathways in lung cancer and suggest that females may gain more therapeutic benefit from EGFR inhibitors than males due to *EGFR* mutant patients responding better to targeted EGFR therapies compared to wild-type [70,71]. Furthermore, while the *KRAS* mutation frequency is 32% in adenocarcinoma NSCLC, genotyping of over 3,000 lung adenocarcinomas revealed the *KRAS* G12C transversion mutation is significantly more common in women than men (P=0.007) [72]. Female patients with this *KRAS* variant were younger on average and smoked less than males harboring the same mutation [72]. Taken together theses genetic and biological variations in presentation of lung cancer between men and women suggest hormones, specifically estrogens, impact the development and progression of the disease.

1.4 ENDOCRINE THERAPIES AND LUNG CANCER RISK AND MORTALITY

Further evidence of a hormonal influence in lung cancer comes from multiple cohort studies assessing the effects of hormone replacement therapy (HRT) on subsequent lung cancer incidence in women. The first study to suggest a potential role of estrogens in lung cancer was the 1973 Coronary Drug Project Trial. The trial was designed to assess the influence of various therapies including equine estrogens on long-term treatment of coronary artery disease in men with a history of myocardial infarction. Patients were randomly assigned to receive either estrogen or placebo, and interestingly the study observed a significantly increased risk of lung cancer mortality in the estrogen treated group leading to early termination of the treatment arm in the study [73]. Over a decade later, Wu et.al. reported a potential link between HRT use and lung cancer risk in a case-control study where differences in risk were observed between women who used HRT and those who did not [74]. Adami et.al. reported similar findings of increased lung cancer risk among

women who used HRT in a much larger population study of over 20,000 women [75]. Following these initial reports, multiple case-control, cohort, and retrospective studies looked to further assess a link between HRT and lung cancer risk in women. While some subsequent studies demonstrated a significant correlation between HRT and lung cancer [76], and HRT and decreased overall survival (OS) in female lung cancer patients [77], others studies have alternatively reported a protective effect, or no effect at all, of HRT use against lung cancer development and mortality [78-80].

While type and duration of HRT use were not accounted for in these earlier cohort studies, the recent Vitamins and Lifestyle large-scale population based cohort study adjusted for confounding variables such as smoking, age, HRT formulation and duration. The study assessed a prospective cohort of 36,588 women among which 344 were diagnosed with lung cancer and observed a duration-dependent positive association between estrogen plus progestin (E+P) use and lung cancer incidence [81]. A separate, randomized, double-blind, placebo-controlled trial conducted by the Women's Health Initiative (WHI) also evaluated lung cancer risk associated with specific HRT formulations. The trial enrolled over 16,000 healthy post-menopausal women who were randomly assigned to either E+P therapy or matching placebo. While the results of the study did not indicate increased incidence of lung cancer with E+P treatment, increased mortality was observed[82]. Interestingly, these negative effects of HRT use were only observed in the E+P treated groups and not estrogen alone. Progesterone receptor (PR) expression is reported to have a protective effect in lung cancer, with multiple studies observing improved clinical outcome with elevated PR expression compared to low [83,84]. Circulating progesterone levels in post-menopausal women are typically inadequate for PR activation [84] and with not knowing the PR status of the women in these studies it is impossible to make conclusive remarks regarding these observations. Finally, while a correlation study has yet to be conducted, leveling lung cancer

incidence trends among women beginning during the early 2000's, as shown in Figure 4, may coincide with a reported 18% decline in HRT use among post-menopausal women from 1999-2010 (P=0.004) [85].

Alternatively, studies assessing lung cancer risk associated with antiestrogen use have further supported the role of estrogen signaling in development of the disease. A recent prospective cohort study assessing over 6,000 women diagnosed with breast cancer registered in the Geneva Cancer Registry, reported a significantly (P<0.001) decreased lung cancer mortality rate among women who received antiestrogen therapy compared to rates of the general population [86]. Similar findings were reported by a retrospective cohort analysis of 2,320 female patients diagnosed with NSCLC in the Manitoba Cancer Registry. The study reported a significant decrease in lung cancer mortality among female patients who received antiestrogen therapy before and/or after diagnosis and remained constant across age and disease staging [87]. Furthermore, a study evaluating lung cancer incidence and mortality in 6,361 female breast cancer patients treated at Sun Yat-Sen Cancer Center reported longer OS in patients diagnosed with lung cancer who received antiestrogen therapy compared to those who did not [88]. In addition to observations of improved survival with antiestrogen use, a recent population study investigating subsequent lung cancer incidence in 40,900 breast cancer patients in the Taiwan National Health Insurance database reported significantly decreased incidence among women ≥50 who received antiestrogen therapy compared to women who did not [89]. Together, antiestrogens' protective effect against lung cancer incidence and mortality coupled with the adverse risks associated with HRT therapy highlight the integral role of estrogens in lung tumorigenesis prompting investigation of estrogenic mechanisms underlying lung cancer pathology.

1.5 ROLE OF ESTROGEN SIGNALING IN LUNG CANCER

Several preclinical studies have elucidated the role of estrogen signaling as a driver of NSCLC. The estrogen receptors are requisite mediators of intracellular estrogen signaling, of which there are two isoforms: estrogen receptor α (ERα) and estrogen receptor β (ERβ). ERα overexpression is well documented and characterized in breast cancer, but has been variable and less frequently reported in NSCLC tissue [84,90-92]. Alternatively, ERβ, which was not discovered until the late 1990's, has been identified as the predominant isoform found in NSCLC among both men and women [90,92-95]. In addition to differential expression among tissues, ERα and ERβ are both expressed in the nucleus and cytoplasm of lung tumor cells. Cellular localization of ER expression is an important distinction to make, due to varying clinicopathological correlations between nuclear ER and cytoplasmic ER in lung cancer. While copy number alterations and activating mutations of ERβ have yet to be identified in lung tumors, some studies have reported nuclear ERβ expression as a positive prognostic indicator, whereas survival analysis of 183 NSCLC primary tumors revealed elevated cytoplasmic ERβ expression is a poor prognostic indicator [84,91,96].

ER signaling is activated following ligand-receptor interaction with one of three endogenous estrogens: 17β-estradiol (E2), estrone (E1), and estriol (E3). E2 is the primary estrogen found in both sexes, and synthesized not only by Leydig and granulosa cells in the male and female reproductive tracts, but also locally within NSCLC lung tumors. Significantly elevated levels (2.2-fold, P=0.002) of E2 have been reported in NSCLC tumor tissue when compared to adjacent healthy epithelial tissue [90]. The cytochrome-P450 enzyme aromatase, CYP19A1, is responsible for catalyzing the conversion of testosterone into estradiol. Acting as an integral enzyme in estradiol synthesis, multiple studies have evaluated aromatase expression in lung tumors

and reported elevated co-expression of aromatase and E2, and aromatase and ERβ [84,90,97,98], while increased aromatase expression is clinically associated with poorer prognosis and female NSCLC patients [99].

1.5.1 Estrogen Signaling Drives Lung Tumorigenesis

ER expression in both the nucleus and cytoplasm allows estrogen to exert both genomic and non-genomic receptor-mediated effects. Liganded ERβ dimerizes and undergoes a conformational change in the AF-2 domain enabling a surface for interaction with coactivator proteins such as GRIP1/TIF2 [100]. Ligand-bound ERβ then translocates to the nucleus where the receptor binds directly to estrogen response elements (ERE) or AP-1 sites located in the promoter region to induce transcription of target genes [93,101]. Genomic ER signaling promotes cellular proliferation in lung cancer in part through increased transcription of cell cycle regulatory genes such as cyclin D1 and c-myc [100].

The oncogenic effects of non-genomic ER signaling in lung cancer largely occur through interactions with other growth factor receptor pathways such as EGFR. EGFR, as previously mentioned, is a prominent pathway in lung cancer pathogenesis due to activation of downstream mitogen-activated protein kinase (MAPK) and PI3K signaling cascades that promote cell survival and proliferation [26]. Crosstalk between the ER and EGFR pathways in lung cancer was established through *in vitro* observations that E2 rapidly stimulated activation of MAPK signaling and release of EGFR ligands HB-EGF and TGFα [70] Furthermore, co-targeting the ER and EGFR signaling pathways enhanced inhibition of proliferation *in vitro* and *in vivo* [70]. Co-inhibition of these interacting pathways was further validated as a viable therapeutic strategy in lung cancer with synergy reported between the aromatase inhibitor (AI) anastrozole and gefitinib, and re-

sensitization of gefitinib-resistant lung cancer cells with the addition of the anti-estrogen fulvestrant [102,103].

1.5.2 Strategies to Target Estrogen Signaling in Lung Cancer

Anti-estrogen therapies have made arguably the most pivotal improvement in the treatment and prevention of hormonal positive breast cancers, reducing the mortality rate by 28% over the past 35 years and becoming the first-line standard of care treatment [1]. Clinical evaluation of anti-estrogens in NSCLC are currently under way as well. Strategies for targeting the estrogen signaling pathway include estrogen blocking agents: anti-estrogens and AI's. Anti-estrogens include selective estrogen receptor modulators (SERMs) such as fulvestrant and tamoxifen. However, following reports that tamoxifen exhibits partial agonist properties in some tissues, including lung, use of ER-antagonists in lung cancer evaluations is now limited to fulvestrant [104]. ER turnover is frequent and rapid with a reported 3-5 hour half-life regulated by ligand-induced ubiquitination following recruitment of coactivator proteins [105]. Fulvestrant acts as an ER-downregulator by selectively interacting with ERs leading to immobilization and similar methods of receptor degradation by independent activation of the ubiquitination-proteosomal pathway [106].

AIs on the other hand inhibit estrogen synthesis by targeting the enzyme responsible for converting hormonal precursors to estrogens (Figure 5).

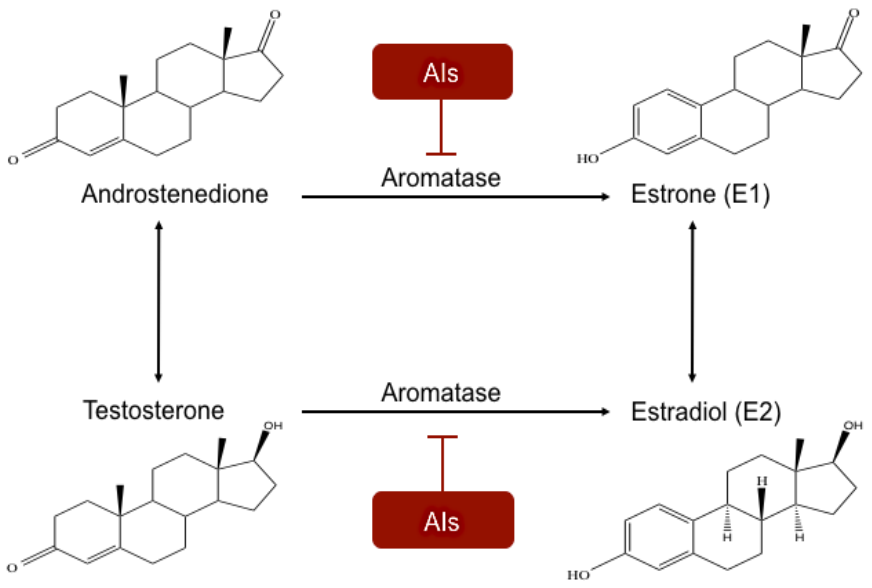

Figure 5. Role of Aromatase Inhibitors in Estrogen Synthesis. Adapted from Figure 1 published in reference [107]. Both steroidal and nonsteroidal AIs block activity of the enzyme that converts androstenedione and testosterone into estrogens.

AIs are classified based on chemical structure as either steroidal or nonsteroidal. Steroidal inhibitors such as exemestane are covalent and irreversible inhibitors of the aromatase enzyme, while nonsteroidal inhibitors such as letrozole interfere noncovalently and reversibly [107]. Both classes of compounds potently inhibit estrogen synthesis, but are clinically reserved for postmenopausal female patients.

Increasing reports of interactions between estrogen signaling and several other tumor promoting pathways and biological mechanisms provide evidence for combination treatments with hormonal therapies as well. For example, following preclinical evidence of crosstalk between EGFR and ER signaling, a phase 1 trial demonstrated safety and tolerability and a phase II trial evaluated early efficacy of combined targeting with the EGFR TKI erlotinib and fulvestrant treatment. While statistically significant clinical benefit was not observed with the combination treatment, the trial was conducted before the advent of molecular profiling to identify patients with

EGFR activating mutations. Retrospective analysis of the enrolled patients did reveal significantly improved PFS and OS for patients positive for EGFR-sensitizing mutations [108]. Furthermore, additional clinical trials are assessing AIs alone (NCT02666105) and in combination with chemotherapy regimens in metastatic patients as well (NCT01664754).

As hormonal therapies inhibiting ER signaling undergo early clinical evaluation in NSCLC, preclinical studies further elucidating the pathway's carcinogenic mechanisms indicate single-agent inhibition may not be sufficient in all lung cancer settings. Therefore, the aim of this investigation was to utilize estrogen-blocking agents to identify additional pathways and mechanisms propagating lung tumorigenesis through cross-communication with estrogen signaling.

2.0 TARGETING CROSSTALK BETWEEN THE ESTROGEN RECEPTOR AND FIBROBLAST GROWTH FACTOR RECEPTOR PATHWAYS IN NSCLC

2.1 INTRODUCTION

Albeit an integral pathway in normal embryonic development, dysregulation of the fibroblast growth factor receptor (FGFR) pathway has been implicated in multiple carcinomas, including NSCLC [109-111]. The FGFR family consists of 18 ligands and 5 receptors and ligand-bound activation of FGFR signal transduction is reliant on docking proteins recruited to the cytoplasmic juxtamembrane domain such as fibroblast growth factor receptor substrate 2 (FRS2). FRS2 is a critical mediator of FGFR signal transduction interacting with effector molecules for subsequent activation of RAS-Raf-ERK and PI3K-Akt-mTOR signaling (Fig. 6) [112].

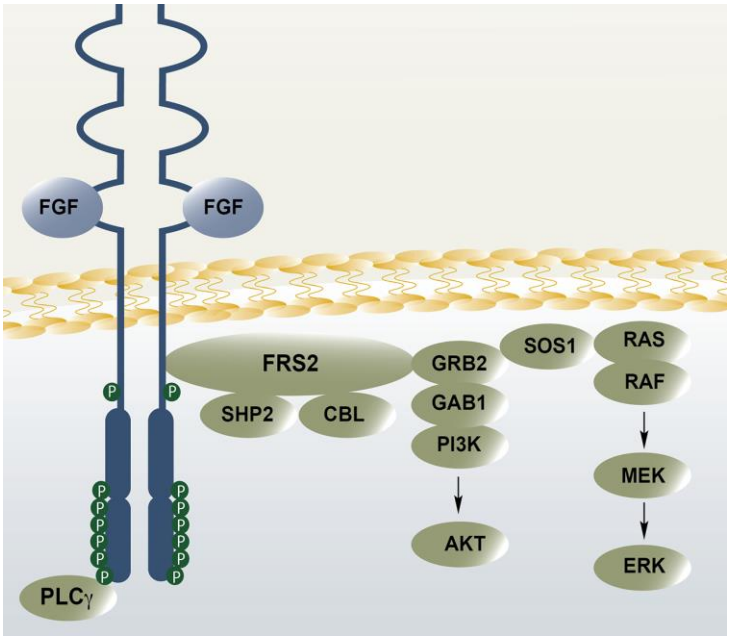

Figure 6. FGFR Signal Transduction in NSCLC. Adapted from Figure 1 in reference [113]. Diagram of ligand-activated FGFR signaling resulting in phosphorylation of docking protein FRS2 leading to downstream activation of ERK and AKT signaling cascades.

Clinically, amplification of the *FGFR1* gene is reported in approximately 20% of squamous cell lung carcinomas and serum levels of its associated pro-angiogenic ligand FGF2 are significantly elevated ($P<0.05$) in NSCLC patients compared to healthy controls, both of which are adverse prognostic biomarkers associated with aggressive disease [114-116]. Genetic alterations in the *FGFR2* and *FGFR3* genes have also been reported at a combined mutation frequency of 6% in NSCLC [117]. Preclinical studies evaluating activating *FGFR2* and *FGFR3* mutations and *FGFR3* gene fusions revealed constitutive activation of the signaling pathway promoting tumor proliferation in xenograft mouse models and enhanced sensitivity to pan-FGFR inhibitors [117,118]. Co-expression of FGF ligands and their corresponding receptors observed in NSCLC cell lines also suggest an autocrine signaling loop within the tumor microenvironment providing further evidence that the FGFR signaling axis is an attractive molecular target for lung cancer [111]. Several selective FGFR kinase inhibitors have been developed, among which AZD4547 (Figure 7) has shown significant preclinical efficacy and currently undergoing evaluation in a phase II clinical trial for NSCLC with FGFR genetic abnormalities (NCT02664935) [119].

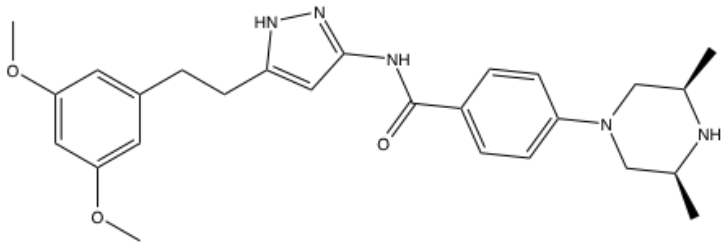

Figure 7. AZD4547 Chemical Structure

Individually the estrogen and FGF signaling pathways have identified roles in the promotion of lung tumorigenesis with several preclinical studies demonstrating the anti-tumor

effects of targeted inhibition. Recent studies in breast cancer cells have also suggested a potential interaction between the two signaling axes and an opportunity for co-inhibition. In ERα-positive breast cancer cells, FGF2 and E2 treatments both increased cellular proliferation, while the addition of anti-estrogens fulvestrant and tamoxifen significantly inhibited FGF2-induced proliferation [120]. Fillmore et.al., also showed estrogen induced FGF-dependent cancer stem cell-like (CSC) phenotypes and induced secretion of multiple FGF ligands including FGF2 [121]. Furthermore, in *FGFR1* amplified breast cancer cell lines FGFR signaling has been identified as a potential compensatory mechanism of resistance to endocrine therapies by increasing activation of the downstream ERK and AKT signaling pathways [122]. Clinical investigation for co-targeting these pathways using AZD4547 in combination with AIs is underway in advanced stage breast cancer patients (NCT01791985).

Recent evidence of crosstalk between the ER and FGFR pathways in breast cancer, in addition to the pre-existing evidence for each pathway's role within lung cancer led us to investigate whether a druggable interaction exists within NSCLC as well. In this study, we evaluated inhibition of the FGFR pathway in NSCLC using AZD4547 in combination with the anti-estrogen fulvestrant under the hypothesis that co-targeting these pathways would provide greater clinical benefit for patients who lack *FGFR* genetic alterations. The experimental design for this project was done in collaboration with Dr. Jill Siegfried's laboratory at the University of Minnesota and published in Oncotarget. For a more detailed view of these methods, results, and additional related data see reference [123].

2.2 METHODS AND MATERIALS

2.2.1 Cell Lines and Reagents

NSCLC H1703, H1581, H520, A549, and H23 were purchased from American Type Culture Collection (ATCC; Manassas, VA). 128-88T, 273T, and 201T cell lines were established in our laboratory from primary lung tumor specimens [124]. Cells were cultured in either Basal Medium Eagle (BME) +10% fetal bovine serum (FBS) or RPMI 1640 + 10% FBS and maintained at 37^0C in 5% CO_2. E2 and fulvestrant were both purchased from Sigma-Aldrich (St. Louis, MO) and diluted in water and ethanol respectively to create 100mM and 10μM stock solutions. AZD4547 was purchased from ChemieTek (Indianapolis, IN) and reconstituted in DMSO to create 10mM stock solutions [123].

2.2.2 Microarray Gene Expression Analysis

The High Pure FFPE RNA Isolation Kit (Roche) was used to isolate RNA from formalin fixed paraffin-embedded (FFPE) sections from 64 lung cancer specimens that we have previously stratified based on high ERβ (n = 15) and low ERβ (n = 49) protein expression using immunohistochemistry (IHC). Tumors were stratified using the Allred IHC scoring system taking into account cytoplasmic ERβ staining positivity and intensity and classified as either low or high expressing tumors based on a median cutoff score of $\leq$7 or >7, respectively [84]. mRNA profiles were compared in the ERβ high versus ERβ low expressing lung tumors using the Illumina Whole-Genome DASL Assay (HT-12 V4 Bead Chip platform) and analyzed using BeadStudio software and Biometric Research Branch (BRB) array tools Version 4.2.1. TaqMan q-RT-PCR was used to validate FGFR1/FGFRL1 expression in ERβ high expressing tumors [123].

2.2.3 Fluorescence *In Situ* Hybridization

Following fixation of cells on glass slides, slides were denatured in hybridization buffer (Agilent Technologies, CA), and 0.5ng of FGFR1 (8p11) probe (Kreatech, Leica Biosystems) at 70 ^{0}C for 12 minutes and then incubated overnight in a 37 ^{0}C humidified chamber. Following hybridization, slides were washed at 45 ^{0}C with 2x sodium citrate buffer multiple times, blocked, and then counterstained with 4′,6-diamidine-2′-phenylindole (DAPI). Gene copy number was determined by comparing the number of centromeres to number of gene copies and anything greater than two was considered amplified.

2.2.4 Protein Extraction and Western Blotting Analysis

Determination of basal FGFR and ERβ protein levels was conducted using cells grown to 80-90% confluency in T75 flasks. Cells were washed 2x with cold phosphate-buffered saline (PBS) and lysed using RIPA lysis buffer (1X PBS, 1% NP40, 0.5% sodium deoxycholate, 0.1% SDS containing 0.5 protease inhibitor cocktail/5ml buffer (Roche Diagnostics, Indianapolis, IN)) and briefly sonicated. The insoluble cellular debris was pelleted using centrifugation at 10,000 rpm for 10 minutes at 4^{0}C. The BCA 200 Protein Assay Kit (Pierce, Rockford, IL) was then used to quantitate protein concentrations in the lysate supernatant. Equal amounts of protein (40μg) were loaded and separated on 10% Tris-glycine SDS-PAGE gels and transferred to nitrocellulose membranes. Membranes were then blocked with 10 mM Tris-HCl (pH 7.4), 150 mM NaCl, and 0.1% Tween-20 (1X TBST) containing 5% nonfat dry milk at room temperature (RT) for1 hour. Primary antibodies were then diluted in 1X TBST containing 5% non-fat milk or 5% bovine serum albumin (BSA) and added to membranes for an overnight incubation at 4^{0}C on an orbital shaker. Primary antibodies and dilutions used included: FGFR1 (1:1000; 3427s; Cell Signaling

Technology), FGFR2 (1:500; ab58201; Abcam), FGFR3 (1:1000; ab52246, Abcam), FGFR4 (1:1000; 8562s; Cell Signaling Technology), FGFR5 (1:500; ab95940; Abcam), ERβ (1:500;Clone 68-4; Millipore), pFRS2 (1:1000; ab195826; Abcam), GAPDH (1:5000; 2188s, Cell Signaling Technology) and β-actin (1:5000; Clone C4; Millipore). Following incubation with primary antibodies, membranes were rinsed with 1X TBST 3x for 10 minute intervals. Next HRP coupled anti-mouse or rabbit secondary antibodies were applied to membranes for 2 hours at RT. Protein bands were visualized using SuperSignal West Pico Chemiluminescent Substrate (Thermo Fisher Scientific, Waltham, MA) and autoradiography. For pFRS2 experiment, cells were seeded at 75% confluency and serum-deprived in phenol-red-free/serum-free BME for 24 hours post attachment. Cells were then subjected to DMSO, AZD4547 (2μM), fulvestrant (2μM), or the combination. Cells were harvested 72 hours following treatment and used for immunoblotting in the same manner as other FGFRs [123].

2.2.5 FGF Enzyme Linked Immunosorbent Assays

NSCLC cell lines were seeded onto 100mm tissue culture treated dishes at 75% confleuncy. Following 24 hours, cells were serum-starved in phenol-red-free/serum-free BME+ 10% charcoal-stripped serum for 48 hours at 37^0C at which point conditioned media was collected. Collected media was concentrated using Amicon®Ultra-4 Centrifugal Filter Devices (Millipore) by centrifugation at 4000 x *g* for 5 minutes at RT. Concentrated conditioned media was evaluated using commercially available enzyme-linked immunosorbent assay (ELISA) kits for FGF 2, 9, and 19 from R&D systems (Minneapolis, MN), for FGF 3, 6 and 10 from Antibodies Online (Atlanta, GA), for FGF4 from Abcam and for FGF8 from USCN Life Sciences. The corresponding cells from the conditioned media were harvested for each sample to normalize FGF secretion to protein

concentration. Assays were performed in triplicate for each sample. Estrogen-induced FGF2 secretion experiments were performed by treating cells with 10nM of E2 or vehicle control (sterile water) for 15 minutes to 6 hours following 48 hour serum deprivation with conditioned media and protein lysates collected at each time point. For fulvestrant *in vitro* studies a dose of 5μM was chosen based on previous studies in our laboratory and others that show the IC_{50} for fulvestrant is well above 10μM in NSCLC cells, with no cytostatic or cytotoxic effect at the selected concentration [103,123,125]. A 24-hour fulvestrant pre-treatment was selected based on previous unpublished results in our laboratory identifying this as a standard time period to elicit inhibition of biological ligand release in NSCLC.

2.2.6 Cell Proliferation Assay

Cells were seeded on 96-well plates at a concentration of 10,000 cells per well and incubated overnight at 37^0C to allow for attachment. To determine the IC_{50} for each line, cells were then treated with a serial-dilution of AZD4547 compound (0-25μM) in triplicate with each assay performed a minimum of three times. Anti-proliferative effects of fulvestrant treatment in combination with AZD4547 was evaluated by treating cells after attachment with 5μM of fulvestrant with and without AZD4547 at concentrations below the determined IC_{50} for each cell line. Fulvestrant dose was selected based on the ligand-release studies and previous publications indicating 5μM was capable of inducing biological effects, but not impacting cell viability [103,125]. Following 72 hour treatment Cell Titer96 AQueous One Solution Cell Proliferation Assay (Promega, Madison, WI) was added to each well and cells were analyzed at 490nm using a Biorad microplate absorbance reader (Hercules, CA).

2.2.7 *In vivo* NSCLC Cell Line Tumor Xenograft Model

Female immunocompromised athymic nude mice were purchased from Harlan (Indianapolis, IN). A549 and 273T NSCLC tumor cells were grown, harvested, and resuspended in a 50% sterile serum-free PBS/50% matrigel (BD Biosciences, San Jose, CA). Cells ($1x10^6$) were then injected into the rear flank on both sides of each mouse. Tumors were grown to approximately $100mm^3$ at which point mice were randomized into four treatment groups: (a) vehicle control, (b) AZD4547, (c) fulvestrant, and (d) AZD4547 plus fulvestrant. AZD4547 was administered daily via oral gavage at a dose of 12.5 mg/kg in 0.2mL of the vehicle 4% DMSO/30%PEG in sterile deionized water. Fulvestrant (30mg/kg) or vehicle control (peanut oil) was administered twice a week by subcutaneous injection. Tumor volume was measured twice a week and recorded as a relative tumor volume calculated ($l \times w \times h$) (mm^3), where l is length, w is width, and h is height of the tumor. At the completion of the treatment period the mice were sacrificed and tumors were collected [123]. Animal care was in agreement with IACUC and University of Pittsburgh guidelines.

2.2.8 Immunohistochemistry

Fixed xenografts were paraffin embedded, sliced, and mounted on slides. Paraffin was removed from slides using xylenes and slides were then subjected to rehydration, antigen retrieval, and incubation with 3% hydrogen peroxide for 15 minutes to quench endogenous peroxidase. Slides were stained with hematoxylin and eosin (H&E) and analyzed for Ki67 expression. For Ki67, ERα, and ERβ staining, slides were rinsed with PBS and blocked in 1.3% goat serum (MOM Kit, Vector Labs), then incubated with Ki67 (ab833; Abcam), ERα (SC-543; Santa Cruz), ERβ (MCA1974ST; AbD Serotec) overnight in a humidified 4^0C chamber. Slides were then incubated

for 1 hour with horseradish peroxidase labeled secondary antibody (1:200) and cell nuclei were counterstained with hematoxylin. Bright field images were taken using 40X magnification using the 4000B LED Leica microscope and LASv4.7 software (Leica Biosystems). Four images were captured from three separate animals per treatment group and Ki67 cell proliferation index was determined by counting the number of Ki67 positive cells per field divided by the total tumor cell count per field [123].

2.2.9 Statistical Analyses

All values are expressed as the mean ± standard error of the mean (S.E.M.). Analyses were performed using GraphPad Prism software version 7 for Mac (GraphPad Software, San Diego California USA). Statistical significance was determined using unpaired *t*-tests or ANOVA with a 95% confidence interval ($P<0.05$).

2.3 RESULTS

2.3.1 FGFR1 is Highly Expressed in NSCLC Tumors Expressing High ERβ

We previously published that elevated ERβ protein expression is a poor prognostic indicator for NSCLC patients [84]. To identify additional biological factors interacting with ER signaling in lung cancer, we performed an mRNA analysis using the Illumina HT-12 V4 Bead Chip comparing RNA from patient samples identified for having high ERβ expression versus patient samples with low ERβ expression. The mRNA analysis revealed that 165 genes were significantly differentially expressed between the two groups ($P<0.001$). The top ten differentially

expressed genes are reported in Table 1. and show that the fibroblast growth factor receptor 1 (*FGFR1*) gene was one of the most significantly upregulated genes (2.41-fold change) in the ERβ high expressing tumors, while the decoy-receptor, fibroblast growth factor receptor like 1 (*FGFRL1* or *FGFR5*), was among the most down-regulated genes (0.54-fold change).

Symbol	Gene	P Value	Fold Change
ZNF334	Zinc Finger Protein 334	1.00E-06	2.7
FGFR5	FGF receptor-like 1 (decoy receptor)	8.00E-06	0.54
ARMCX1	Armadillo repeat-containing protein	1.40E-05	1.59
POFUT1	Protein O-fucosyltransferase 1	2.77E-05	2.16
TNKS	Tankyrase	3.10E-04	1.84
PIAS	Protein inhibitor of STAT,1	5.90E-04	1.92
SFTPB	Surfactant protein B	2.57E-03	0.38
FGFR1	FGF receptor 1	3.51E-03	2.41
SLIT2	Slit homolog 2	3.59E-03	0.44
TNRSF13B	TNF receptor superfamily, member 13B	7.25E-03	0.35

Table 1. Top Ten Differentially Expressed Genes Between ERβ High and ERβ Low Expressing Tumors. Most significantly differentiated genes listed according to P value identified by Illumina HT-12 V4 Bead Chip comparing RNA between high ERβ expressing tumors and low ERβ expressing tumors.

While genes such as *TNKS* and *SLIT2*, have potential implications in lung carcinogenesis, we further pursued investigation of *FGFR1* based on its well-established role in lung cancer and the identified interaction with ER signaling in breast cancer. Furthermore, Ingenuity Pathway Analyses of the ten genes in Table 1 showed they form one interacting network with FGF signaling identified as one of the top canonical pathways (P=0.00072). Quantitative RT-PCR of tumor RNA from the same tumor cohorts confirmed the Illumina microarray results with observed increased levels of *FGFR1* mRNA (P=0.004) and down-regulated levels of *FGFRL1* mRNA (P= 0.0116) in ERβ high expressing tumors compared to low (data not shown).

2.3.2 *FGFR1* is Amplified in Some NSCLC Cell Lines Characterized

In order to elucidate potential communication between the ER and FGFR pathways in NSCLC we first determined *FGFR1* amplification status in eight NSCLC cell lines. In collaboration with the University of Pittsburgh Molecular Pathology Lab, amplification status was determined using fluorescence in situ hybridization (FISH) analysis to examine the gene copy number in each cell line (Table 2). Any cell line with a gene copy number greater than two was classified as amplified, and three of the eight lines were identified as *FGFR1* amplified.

Cell Line	Histology	FGFR1 Gene Copy Number	Amplification Status
NCI-H1703	Squamous	21.00	Amplified
NCI-H1581	Large Cell	6.70	Amplified
NCI-H520	Squamous	10.00	Amplified
273T	Squamous	1.31	Not Amplified
A549	Bronchiolo alveolar	1.24	Not Amplified
128-88T	Squamous	1.10	Not Amplified
201T	Adenocarcinoma	1.01	Not Amplified
NCI-H23	Adenocarcinoma	0.95	Not Amplified

Table 2. NSCLC Cell Line Histology and FGFR1 Gene Amplification Status. Gene amplification status was determined by FISH analysis. Gene copy numbers were calculated based on the ratio of the number of copies of the gene to the number of centromeres of the associated chromosome found within the nucleus of each cell line. Copy number greater than two was classified as amplified.

2.3.3 NSCLC Cell Lines Express Multiple FGFRs and Secrete Multiple FGF Ligands

Protein expression of all 5 FGFR family members was assessed in the five non-amplified cell lines by western blotting analysis. Since amplification of the gene leads to constitutive activation of the FGFFR signaling pathway, identification an interacting pathway is less prominent and more challenging. At least three FGFRs were expressed in each cell line, with all lines expressing detectable levels of FGFR2, FGFR3 and the decoy receptor FGFRL1. Furthermore, each of the lines were assessed for ERβ and revealed moderate and invariable expression of the protein. No correlation was observed between ERβ protein levels and FGFR expression (Fig.8). In order to fully characterize the FGF/FGFR profile for each NSCLC cell line we also evaluated basal levels of FGF ligand secretion. Relative un-stimulated levels of FGF ligand release for each cell line as measured by ELISA is shown in Fig. 9 and summarized in Table 3.

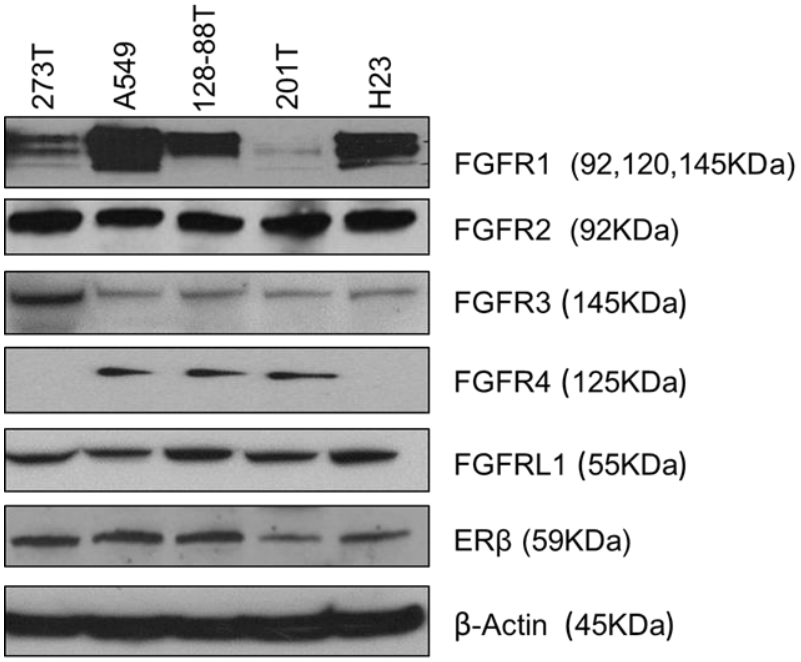

Figure 8. FGFR and ERβ Protein Expression in NSCLC Cell Lines. Each of the five non-amplified NSCLC cell lines were analyzed for basal FGFR and ERβ protein expression using whole cell lysate immunoblotting with β-actin assessed as a loading control.

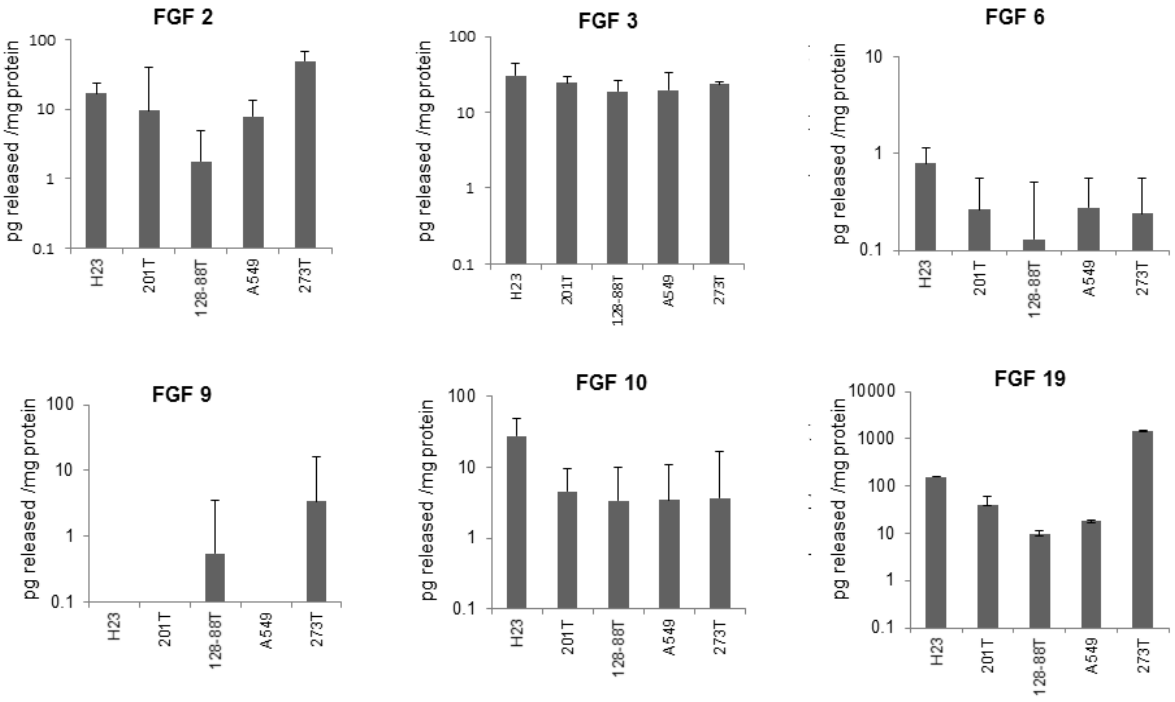

Figure 9. FGF Ligand Secretion in NSCLC Cell Lines. Following 48 hour serum-deprivation conditioned media was collected from each cell line and analyzed using ELISAs for FGF2,3,4,6,8,9,10 and 19. Corresponding whole cell lysates were collected and quantitated for normalization of FGF release to total protein content.

	FGF2	FGF3	FGF4	FGF6	FGF8	FGF9	FGF10	FGF19
273T	++	++	ND	+	ND	+	+	+++
A549	++	++	ND	+	ND	ND	+	++
128-88T	+	++	ND	+	ND	+	+	+
201T	+	++	ND	+	ND	ND	+	++
H23	++	++	ND	+	ND	ND	++	+++

Table 3. Summary of Basal FGF Ligand Secretion in NSCLC Cell Lines. ND= not detectable; + = 0.1-10pg/mg protein; ++ = 11-100pg/mg protein; +++ = >100pg/mg protein

FGF ligand release was variable across cell lines. FGF2, 3 and 19 had the highest overall secretion levels among all cell lines, while FGF4 and FGF8 were not detectable. FGF3 and 10, both ligands for the FGFR1 and FGFR2 receptors, had a detectable range of 18.9-30.7 pg/mg protein and 3-27.5pg/mg protein respectively. FGF2, a ligand with affinity for each FGFR receptor, release ranged from 1.8-49.3 pg/mg of protein. FGF19, a FGFR4 ligand, release was greatest in 273T and H23 cells reaching a maximum secretion of 1459.6 pg/mg protein with the lowest concentration observed in 128-88T cells at 9.9 pg/mg protein. Finally, FGF6 was minimally detected at a concentration below 1 pg/mg protein, while FGF9 was minimal and variable and FGF4 and FGF8 were not detected in any of the lines.

2.3.4 E2 Stimulates FGF2 Release in NSCLC Cells

Indicative of crosstalk between the ER and FGFR pathways in breast cancer, E2 has been shown to induce FGF2 secretion in breast cancer cell lines [121]. We evaluated whether E2 would stimulate FGF2 release in NSCLC. With previous observations of rapid stimulation of growth factor release in NSCLC cells in response to 10nM E2, a time-course from 15 minutes to 6 hours (Appendix 1, Figure 28) was performed. A 10nM concentration of E2 was selected based on previous studies by our laboratory having reported optimal biological responses and ERβ receptor selectively with 10nM E2 compared to 1 and 100nM concentrations [70,126] In this experiment, following E2 exposure, conditioned media was analyzed using a FGF2 ELISA and normalized to total protein content of the cells. Significant increases in FGF2 release upon estrogen stimulation were observed at 1-2 hours in all three cell lines tested (Fig. 10). The most significant effect occurred in 201T cells at 2 hours (Fig. 10B) with a 3.8-fold increase compared to control and a nearly 2-fold increase at 2 hours in A549 cells (Fig.10C). Furthermore, fulvestrant treatment prior

to E2 exposure completely inhibited E2-induced FGF2 secretion as observed in A549 cells (Fig. 10D).

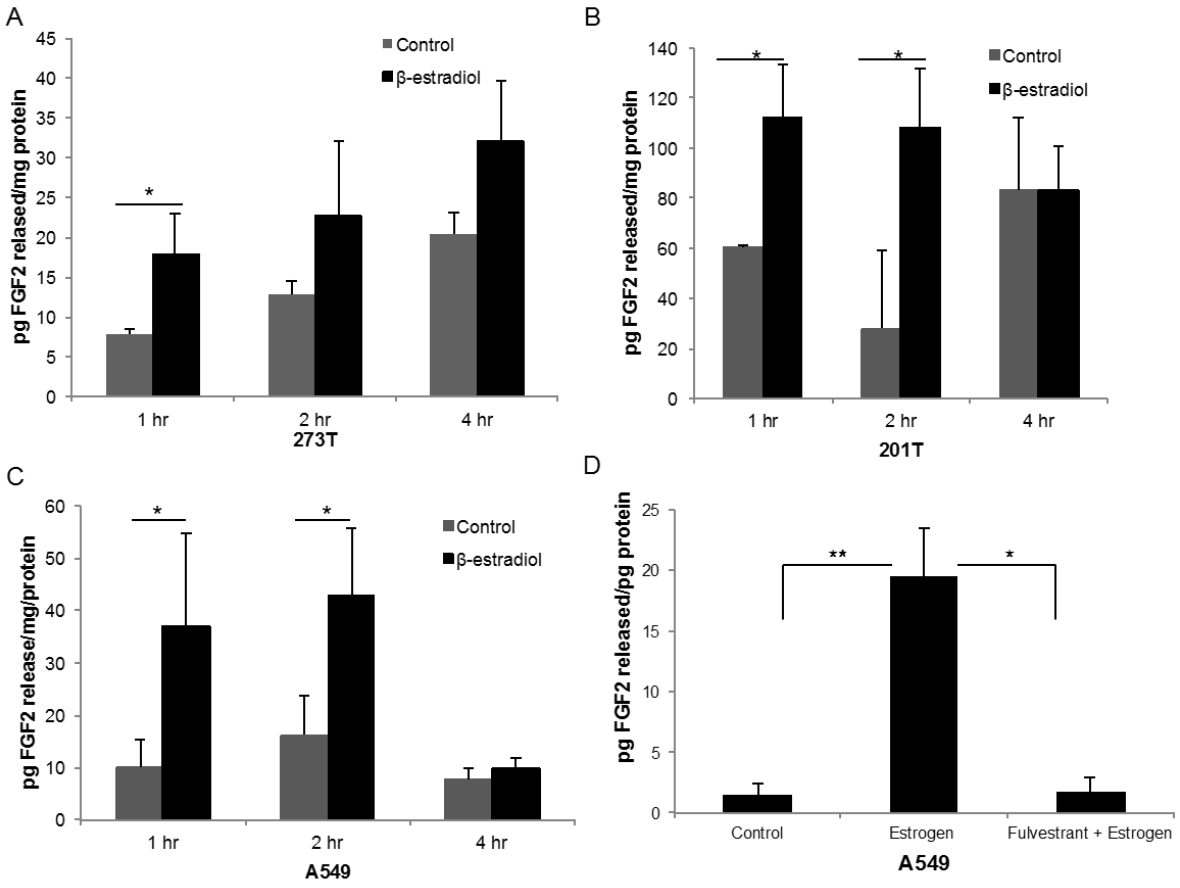

Figure 10. E2 Stimulates FGF2 Secretion in NSCLC Cell Lines while Fulvestrant Inhibits E2-induced FGF2 Release. Cells were treated with 10nM of E2 following 48 hour serum-deprivation. Conditioned media and whole cell lysates were collected at 1, 2, and 4 hours after E2 treatment in A. 273T, B. 201T, and C. A549 cell lines. FGF2 release was evaluated by ELISA and normalized to the protein concentration of each sample. D. A549 cells were serum-deprived and pre-treated with 5μM of fulvestrant 24 hours prior to E2 treatment for 2 hours. Media was collected, concentrated, analyzed by ELISA, and normalized to total protein. Results are the mean ± S.E.M of three independent samples and reported as picogram FGF2 released per milligram protein. *P< 0.05, **P < 0.01.

2.3.5 Fulvestrant Increases the Anti-Proliferative Effects of Pan-FGFR Inhibitor AZD4547

FGFR and ER are both known to promote cellular proliferation, and based on the hypothesis of these two pathways interact, we evaluated the effect of co-inhibition using the anti-estrogen fulvestrant and pan-FGFR inhibitor AZD4547 on NSCLC cellular proliferation. The IC_{50} of AZD4547 was determined for both amplified and non-amplified cell lines (data not shown) and revealed that NSCLC cells lacking FGFR genetic abnormalities were less sensitive to the inhibitor with IC_{50} values ranging from 7μM in 273T to 18μM in A549 cells (Fig.11A). The addition of fulvestrant, however, significantly enhanced the sensitivity of these cell lines to the anti-proliferative effects of AZD4547. Combination treatment was evaluated and compared to single agent therapies in each of the cell lines that revealed E2-induced FGF2 secretion. To evaluate efficacy of co-inhibition, a concentration of AZD4547 that produced 30-40% inhibition was used singularly and in combination with 5μM fulvestrant. Dose-responses to fulvestrant alone were previously performed (data not shown) in each cell line as well and showed minimal cytostatic effect at the selected concentration which we pursued further following ligand-release studies. Significant inhibition was observed in the combination treatments compared to control and single agents in all three cell lines ($P<0.01$, Fig. 11). 201T cells showed a 70.7% inhibition with combination treatment compared to control, while a 61.4% inhibition was observed in 273T cells and 59.9% in A549.

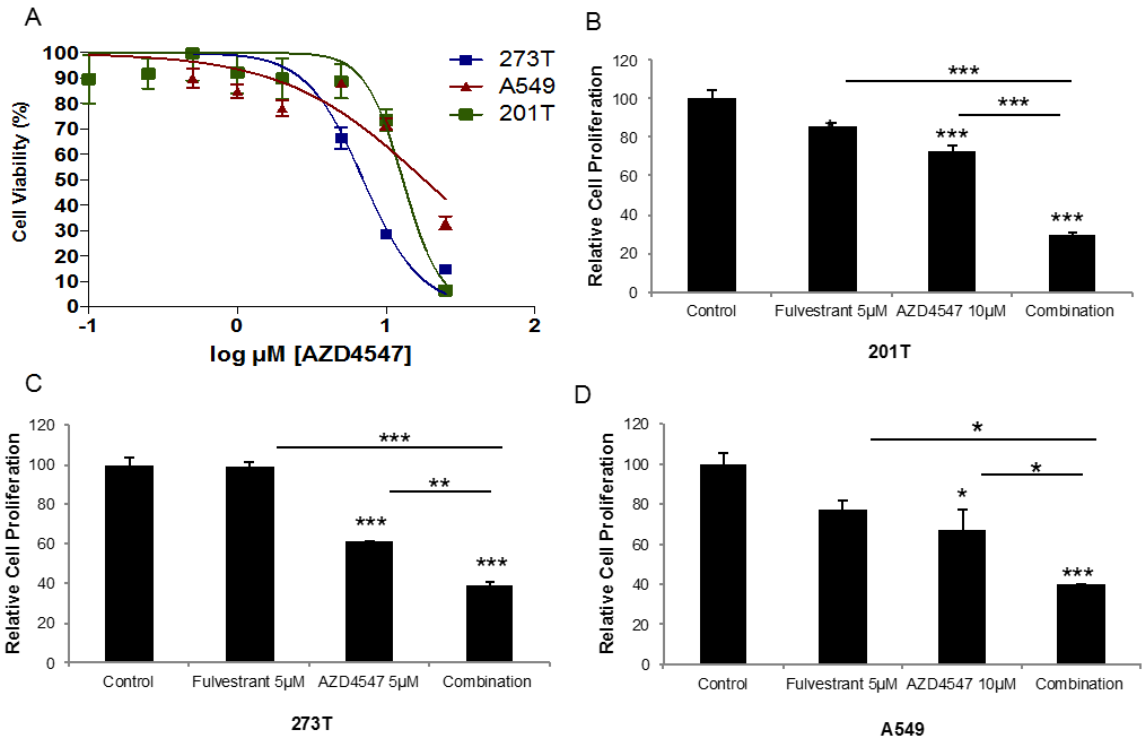

Figure 11. Fulvestrant Increases the Anti-Proliferative Effects of Pan-FGFR Inhibitor AZD4547. (A). Representative IC_{50} curves for AZD4547 in 201T, 273T and A549 cells. (B-D). NSCLC cells were treated with 5µM fulvestrant, 5 or 10µM AZD4547, or the combination for 72 hours. Cells were incubated for 1 hour, analyzed at 490nm wavelength following addition of 20µL of Cell Titer 96 Aqueous One MTS Solution to each well. Results are presented as the mean ± S.E. from three separate experiments with six independent samples per treatment group. ANOVA, * P < .05; ** P < .01;***P < .001. (B). 201T; (C) 273T; (D). A549.

2.3.6 Co-targeting ER and FGFR Signaling Maximally Inhibits Phosphorylation of FGFR Docking Protein FRS2

Since the NSCLC cell lines were not reliant on one particular FGFR or FGF ligand for activation of the FGFR signaling axis, we chose phosphorylation of the FRS2 docking protein as a marker of pathway activation [112]. Levels of phospho-FRS2 (pFRS2) expression were probed for in 201T and 273T cells following treatment with vehicle control (DMSO), AZD4547,

fulvestrant, or the combination. Levels of pFRS2 expression were normalized to constitutively expressed glyceraldehyde 3-phosphate dehydrogenase (GAPDH) and reported as band densities relative to the control. Singularly, AZD4547 effectively inhibited phosphorylation by 60% and 40% in 201T and 273T cells respectively. Fulvestrant alone had marginal effects on FRS2 phosphorylation with only a 10% inhibition observed in 201T cells and 30% inhibition in 273T cells. The greatest inhibitory effect on FRS2 phosphorylation was observed in the combination treatment groups in both cell lines with 98% inhibition in 201T and 70% in 273T and suggestive of crosstalk between these two pathways.

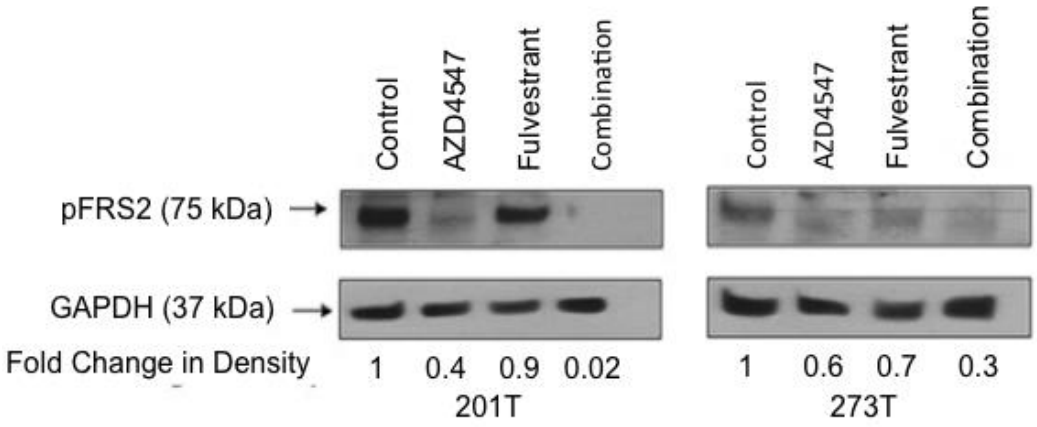

Figure 12. Inhibitory Effect of Fulvestrant and AZD4547 on Phosphorylation of FGFR Docking Protein FRS2. Following 24 hour serum deprivation 201T and 273T cells were treated with DMSO (control), AZD4547, fulvestrant, or the combination. Whole cell lysates were collected following 72-hour treatment. pFRS2 levels were assessed by immunoblotting and quantified by densitometry with normalization to GAPDH. *Experiment was performed by Mariya Farooqui, PhD.

2.3.7 Combined Targeting of the ER and FGFR Pathway Enhances Anti-tumor Activity in NSCLC Xenograft Models

The identification of crosstalk between the ER and FGFR pathways in NSCLC and enhanced anti-proliferative effects when targeting both pathways led us to evaluate co-inhibition of the ER and FGFR pathways using fulvestrant and AZD4547 *in vivo*. Female athymic nude mice bearing ERβ-positive NSCLC tumors began treatment once xenografts reached an average volume of 100mm^3. In A549 xenografts, mice were randomized into four treatment groups receiving vehicle control, AZD4547, fulvestrant, or the combination for 24 days at which point mice were sacrificed and tumors were harvested for IHC analysis. Both single agent therapies reduced tumor volume by 33% compared to placebo ($P<0.05$, Fig. 13). Combined fulvestrant and AZD4574 therapy using both inhibitors resulted in an even more significant anti-tumor effect with an 85% reduction in tumor volume after 24 days of treatment when compared to control ($P<0.001$) and 52% reduction compared to single agent therapies ($P<0.01$). Mouse weight and gait was maintained and no signs of toxicity were observed in any of the treatment groups.

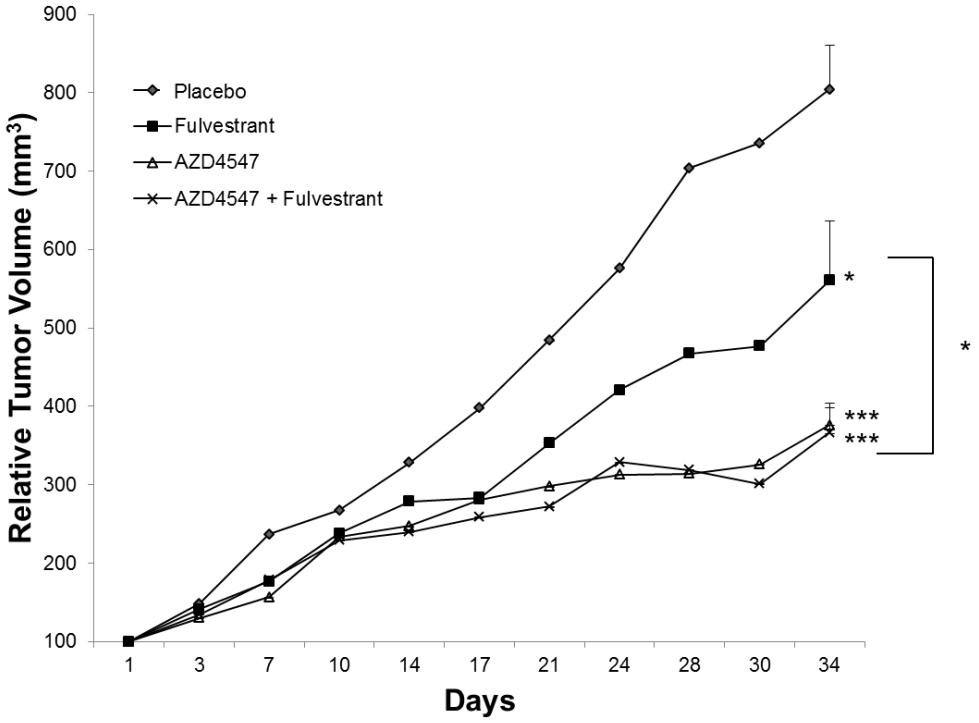

Figure 13. Combined Targeting of ER and FGFR Enhances Inhibition of A549 Tumor Growth *In Vivo*. A549 cells ($1x10^6$) were injected into immunocompromised nude mice and grown for approximately two weeks until xenografts reached an average volume of $100mm^3$. Mice were randomized and received one of four treatments for 24 days: Control (4% DMSO/30%PEG in sterile deionized water), AZD4547 (12.5mg.kg daily via oral gavage), fulvestrant (30mg/kg s.c. injection 2x/week), or combination. Tumor growth was measured using calipers twice a week and results are reported as the relative mean tumor volume ± S.E. or 6-8 tumors per group. ANOVA *P<.05, **P<0.01, ***P<0.001.

Immunohistochemical analysis of the xenografts following sacrifice revealed important histological changes among treatment groups. Examination of H&E staining revealed increased stromal content and fewer neoplastic cells comprising the tumors receiving treatment with the greatest changes observed in the combination therapy group (Fig. 14A). Measurement of Ki67 protein expression was also performed as a quantitative assessment of actively proliferating tumor cells. A significant reduction in Ki67 expression was observed across treatment groups when

compared to placebo, with the most significant loss of S-phase labeling observed in the combination treatment group. A mean value of 70 cells per field stained positive for Ki67 in the control placebo tumors, while combined AZD4547 and fulvestrant treatment showed significantly reduced staining compared to placebo (P<0.001) and single treatments (P<0.05 Fulvestrant; P<0.01 AZD4547) with an average of 18.5 Ki67 positive cells per field (Fig. 14B).

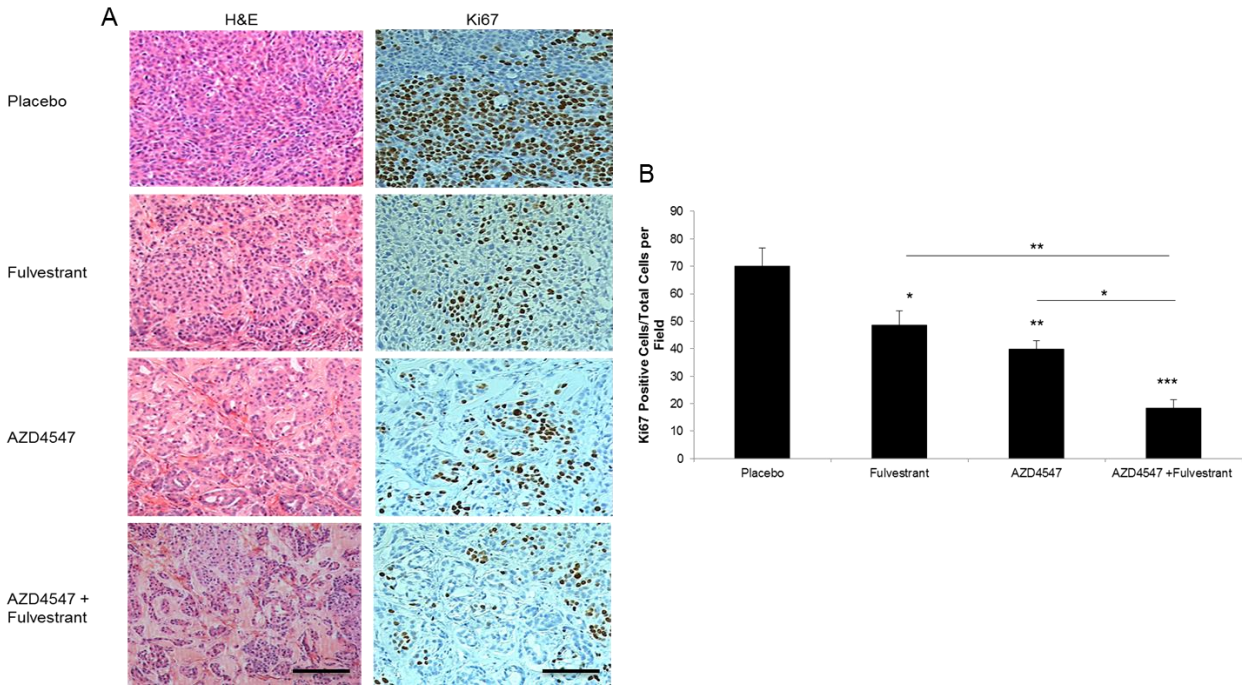

Figure 14. Combined Targeting of ER and FGFR Altered Tumor Histology and Reduced Ki67 Proliferative Index in A549 Xenografts. (A) Representative H&E and Ki67 stained sections of xenograft tumors harvested from the four treatment groups imaged at 40X magnification. Scale bars represent 150 μm.(B) Quantitation of Ki67 labeling was performed by counting 5 fields per tumor and represented as the average of three independent tumors per experimental group ANOVA *P<0.05; ** P < .01;*** P < .001.

Combination treatment was also assessed in a 273T xenograft model. In this study, a 30% reduction in tumor volume was observed with fulvestrant treatment alone (P<0.05), with both the AZD4547 single agent treatment and combination treatment groups showed a 67% reduction in

tumor growth compared to placebo (P<0.001) (Fig. 15). Mouse weight and mobility was maintained in all treatment groups, with no signs of toxicity.

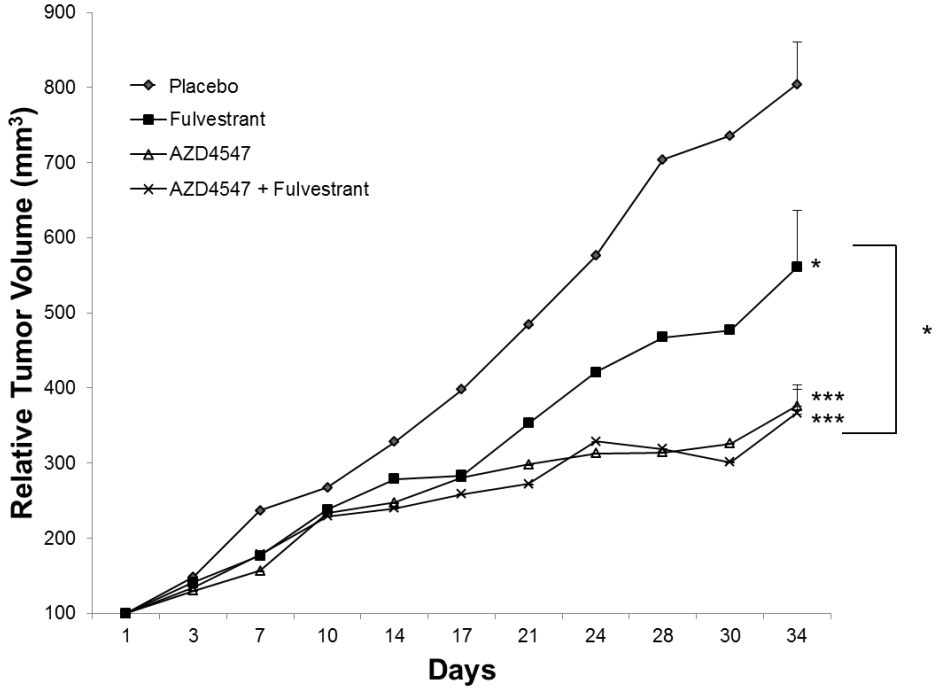

Figure 15. No Enhanced Effect on Tumor Growth with Combined ER and FGFR Targeting in 273T Xenografts. 273T cells ($1x10^6$) were injected into immunocompromised nude mice and grown until xenografts reached an average volume of $100mm^3$. Mice were randomized and treated for 34 days according to protocol described in Figure 13. Tumor growth was recorded twice a week using calipers and results are reported as the relative mean tumor volume ± S.E. or 6-8 tumors per group. ANOVA *P<.05, **P<0.01 ***P<0.001.

Interestingly in the study, tumor volumes were the same among AZD4547 treatment and combination treatment groups. However, similar to the A549 xenografts, IHC analysis revealed increased stromal content from single treatment groups to the combination treatment, suggesting that despite similar tumor volumes the combination therapy treated tumors were composed of fewer malignant cells (Fig. 16A). Ki67 protein expression supported this observation with the most

significant reduction in Ki67 labeling observed in the combination treatment group compared to placebo (P<0.001) and significantly less staining in combination treatment compared to AZD4547 alone (P<0.01) and fulvestrant alone (P<0.001, Fig. 16B).

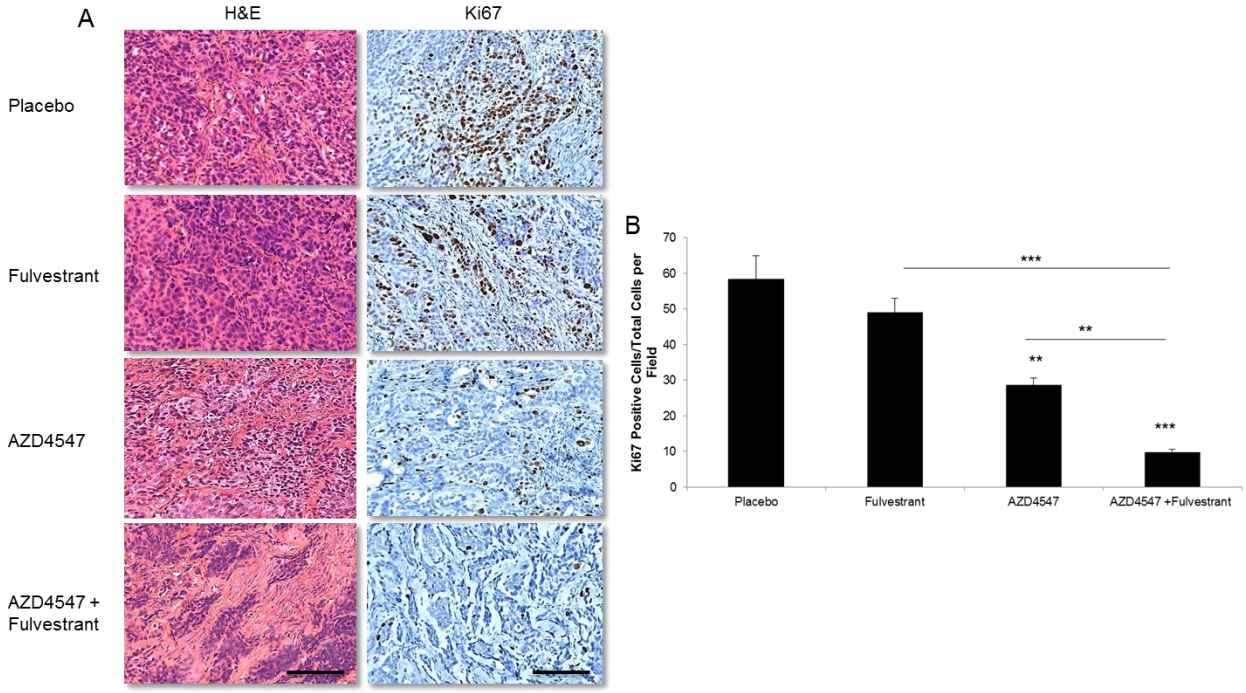

Figure 16. Combined Targeting of ER and FGFR Altered Tumor Histology and Reduced Ki67 Proliferative Index in 273T Xenografts. (A) Representative H&E and Ki67 stained sections of xenograft tumors from the four treatment groups imaged at 40X magnification. Scale bars represent 150µm. (B) Quantitation of Ki67 labeling was performed by counting 5 fields per tumor and represented as the average of three independent tumors per experimental group ANOVA ** P < .01;*** P < .001

Expression of ERα and ERβ were also probed in both the 273T and A549 xenografts using IHC. Analysis of staining revealed undetectable levels of ERα in all experimental groups, while ERβ was ubiquitously expressed among treatment groups with slight reduction in fulvestrant treated groups. Levels were similar among both the 273T and A549 xenografts, with representative staining shown for 273T in Figure 17.

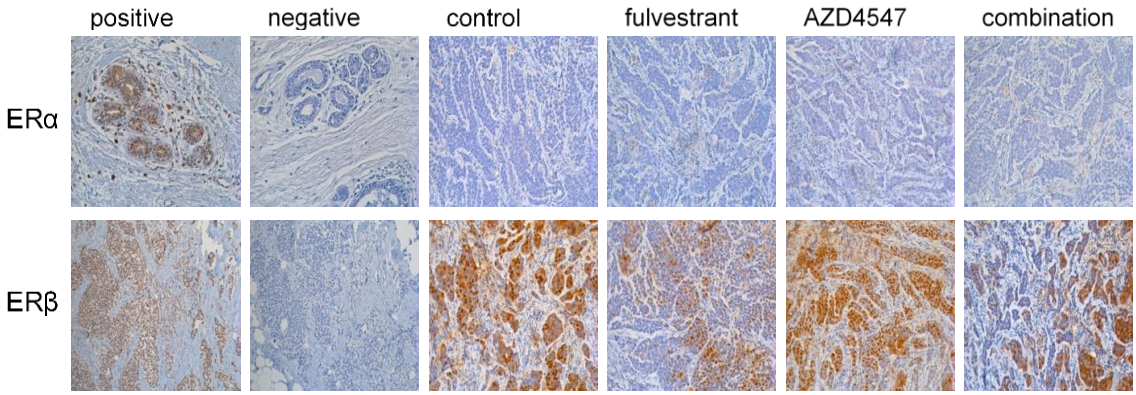

Figure 17. ERα and ERβ Protein Expression in 273T Xenografts. Representative staining of both ERα and ERβ expression in 273T tumors from the four treatment groups with positive and negative controls for comparison.

2.4 CONCLUSIONS AND FUTURE DIRECTIONS

Bleak improvement in the 5-year survival rate for lung cancer patients over the past decade necessitates continued development of novel therapies and treatment strategies. The clinical success of drugs selectively targeted against molecular alterations driving certain NSCLCs provides rationale for further identification and targeted inhibition of pathways promoting lung tumorigenesis. Both ER and FGFR signaling have identified roles in proliferation and lung carcinogenesis largely through activation of similar downstream pathways such as RAS-Raf – MEK and PI3k-AKT-ERK. To fully abrogate activation of these signaling cascades promoting cell proliferation and survival, combinational strategies targeting multiple upstream activators are being clinically evaluated in NSCLC patients. Our lab previously identified crosstalk between the ER and EGFR pathway and observed enhanced anti-tumor effects when co-targeting these pathways compared to single pathway inhibition [70]. This led to phase II clinical evaluation of the EGFR TKI erlotinib in combination with the anti-estrogen fulvestrant in advanced NSCLC

patients and while the combination treatment failed to statistically improve response rates compared to erlotinib alone, a significantly improved clinical benefit rate with the combination was interestingly observed in wild-type EGFR patients [108]. Here we sought to elucidate potential crosstalk between ER and FGFR signaling in NSCLC and whether co-inhibition of these pathways would enable enhanced anti-tumor activity in NSCLC cell lines lacking FGFR genetic alterations.

From our mRNA analysis comparing ERβ high expressing NSCLC patient tumors to ERβ low expressing tumors, *FGFR1* was identified as one of the top ten differentially expressed genes with significant up-regulation in the ERβ high expressing tumors. Pathway analysis of the most differentially expressed genes revealed they were involved in one interacting network connected to STAT3 and PTEN signaling as well. While FGFs are fundamental in normal lung development, deregulated FGFR signaling is involved in pathogenesis and promotion of lung cancer. Therefore, upregulated *FGFR1* in ERβ high expressing tumors associated with poorer prognosis provided initial rationale for further investigation of a targetable interaction between these pathways in NSCLC.

We focused our investigation on ERβ expressing NSCLC cell lines lacking *FGFR1* amplification under the hypothesis that enhanced activity of combined inhibition may be more prevalent and targetable in a non-amplified setting. In amplified cell lines we were unable to show ER-dependence on FGF2 secretion, and saw no enhanced anti-proliferative or anti-tumor effects when blocking both FGFR signaling and estrogen synthesis (data not shown). An interaction between ER and FGFR signaling is therefore more challenging to identify and target among cell lines harboring FGFR abnormalities since they may be more singularly reliant on FGFR signaling. This observation parallels the clinical results of co-targeting ER and EGFR in NSCLC, indicating combinational strategy may provide more clinical benefit to patients lacking FGFR abnormalities because *FGFR1* amplified patients are likely more sensitive to FGFR inhibitors alone.

Characterization of the non-*FGFR1* amplified NSCLC cell lines reveled expression of multiple FGFRs, invariably FGFR2 and FGFR5 and detectable levels of at least two other FGFRs in each cell line. Similarly, FGF secretion profiles revealed basal release of multiple FGFs indicating activity of FGF/FGFR signaling in these cells was not reliant on one particular receptor or ligand. Expression of multiple receptors in these cells provided rationale for utilizing a pan-FGFR inhibitor to target the pathway in our investigation. Following the establishment of FGFR signaling and ERβ expression in each cell line we demonstrated cross-communication among the pathways by showing E2 stimulated significantly increased FGF2 secretion in multiple cell lines. ER dependence on FGF2 release was further evidenced when the induced effect was completely blocked with the addition of fulvestrant. In addition, maximal inhibition of FRS2 phosphorylation, was achieved when combining fulvestrant and AZD4547, further indicating an interaction between the two pathways in NSCLC. In separate studies (data not shown) assessing the effects of estrogen signaling on lung tumorigenesis in a tobacco-carcinogen (4-(methylnitrosoamino)-1-(3-pyridyl)-1-butanone; NNK) induced murine model we demonstrated that ER blocking agents significantly reduced FGF ligand and FGF-dependent stem cell marker (SOX2 and Nanog) expression in both pre-neoplasias and adenomas. Alternatively, in a separate NNK murine model in which mice were supplemented with E2 or placebo alongside exposure to NNK, expression of FGF2, FGF9, SOX2, and Nanog all significantly increased in preneoplasia tissue [123].

Identification of crosstalk between FGFR and ER signaling in these studies led us to evaluate whether co-inhibition of these pathways may have a greater anti-tumor effect compared to single agent therapies. The addition of fulvestrant to AZD4547 treatment *in vitro* significantly enhanced sensitivity of the cells to the anti-proliferative effects of the FGFR inhibitor. Fulvestrant alone had no effect on cell viability at concentrations as high as 30μM. While half-maximal inhibition of proliferation using AZD4547 varied among the cell lines, but was consistently higher

in our non-amplified cells compared to more sensitive FGFR1 amplified cells. Simultaneous targeting of ER and FGFR *in vivo* revealed improved anti-tumor effects including enhanced inhibition of tumor proliferation, increased stromal component, and reduced Ki67 labeling compared to placebo and single agent treatments in the A549 xenografts. While 273T xenografts showed no significant difference in final tumor volumes between AZD4547 treatment and combination treatment, changes in tumor histology suggested increased stromal content and fewer actively dividing malignant cells. Differential responses to growth inhibition may be attributed to the increased sensitivity of the 273T cells to AZD4547 alone. In the *in vitro* studies evaluating the combination treatment, A549 and 201T cells required twice as much AZD4547 compared to 273T cells in order to obtain a significant combination effect, explaining the decreased combination effect *in vivo.* Furthermore, A549 cells are *KRAS* (G12S) mutant while 273T are wild-type for *KRAS* [127]. *KRAS* mutations result in constitutive activation of the RAS-Raf-MEK cascade that is downstream of ER and FGFR signaling. Lateral targeting of both ER and FGFR pathways in the A549 cell line therefore potentially enabled greater inhibition of hyper-activated downstream signaling involved in cellular proliferation.

While both ER isoforms are involved in estrogen signaling, IHC revealed undetectable levels of ERα expression in all of our xenografts, and clearly detectable ERβ expression in each of the treatment groups. Numerous studies have identified ERβ as the predominant isoform in lung cancer [93], and our observations herein indicate communication between ER and FGFR signaling in these NSCLC cell lines is largely conducted through the β isoform, which upon further clinical evaluation may act as a biomarker for therapeutic decision-making.

Taken together these studies demonstrate simultaneously co-targeting ER and FGFR signaling enhanced the anti-tumor and inhibitory effects of AZD4547 in non-*FGFR1* amplified NSCLC cell lines. These results suggest combined inhibition of the ER and FGFR pathways may

act as a novel therapeutic strategy and provide clinical benefit for NSCLC patients lacking FGFR1 genetic abnormalities.

Clinical evaluation of this combination strategy is an evident future direction, while other future studies are warranted as well. Herein, we demonstrated an interaction between the ER and FGFR pathway, but did not identify specifically which FGFR receptor was the point of interplay. Additional studies utilizing gene silencing techniques would be beneficial to demonstrate the exact location of crosstalk by individually knocking down each receptor and evaluating estrogen stimulation of FGF2 or altered co-targeting effects on proliferation. Furthermore, the Ingenuity pathway analysis of differentially expressed genes could be utilized to evaluate other pathways within the network connecting ER and FGFR such as STAT3.

3.0 ELUCIDATING INTERACTIONS AMONG ESTROGEN SIGNALING, THE TUMOR MIVROENVIRONMENT, AND EPITHELIAL-MESENCHYMAL TRANSITION IN NSCLC

Greater examination of solid tumor composition over the past decade has highlighted the immense complexity and heterogeneity of tumor biology. Progression of neoplastic disease is reliant not only on actively dividing neoplastic cells, but also neovasculature that recruits infiltration of stromal cells enabling fluid interaction with the local tumor microenvironment. In addition to the intracellular effects of ER signaling, recent reports indicate the pathway may also interact with elements of the local tumor microenvironment. In a murine tobacco-induced lung carcinogenesis prevention model, Stabile et.al. demonstrated the use of ER blocking agents anastrozole and fulvestrant, especially when in combination, significantly reduced tobacco carcinogen-induced lung tumor formation and size [128]. In addition, the study reported infiltration of inflammatory macrophage cells in the lung neoplasias, and that aromatase expression was exclusively observed in the macrophages and not in the tumor cells, while ERβ was expressed in both [128]. Furthermore, AIs such as exemestane have proven efficacy when used as chemopreventive agents in post-menopausal women at elevated risk for breast cancer, with preclinical evidence eluding to a potential anti-oxidant and anti-inflammatory mechanism through activation of cytoprotective nuclear receptor erythroid-2 related factor 2 (NRF2)/ antioxidant response element (ARE) signaling (Figure 18) [129,130]. The role of inflammation in the development of several carcinomas including lung is well established[131], but this observation of potential interplay between the inflammatory response and estrogen synthesis presents as another novel co-targeting strategy for lung cancer.

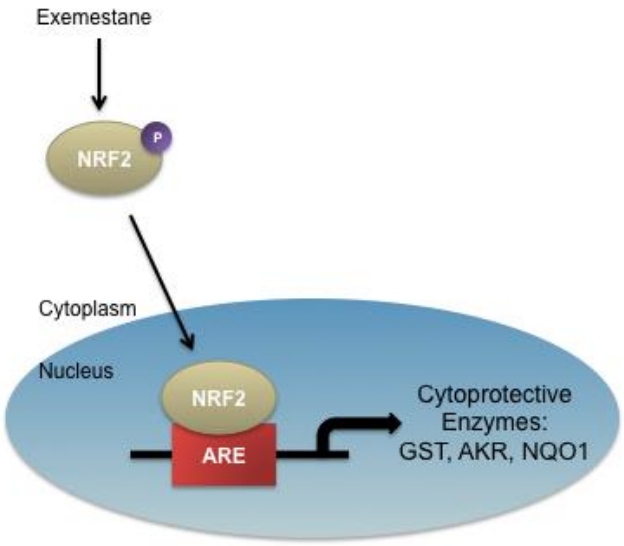

Figure 18. Proposed Mechanism of Exemestane Activated NRF2 Signaling in NSCLC. Figure is based on *in vitro* studies reporting increased nuclear receptor erythroid-2 related factor 2 (NRF2) signaling and NAD(P)H:quinone oxidoreductase 1 (NQO1) activity in response to exemestane, [130]. Schema represents potential mechanism by which exemestane leads to phosphorylated NRF2 activation inducing translocation to the nucleus and binding to antioxidant response elements (ARE) which subsequently upregulates transcription of cytoprotective enzymes

Estrogen signaling within the lung tumor microenvironment may also abrogate tumor immunosurveillance. Recently, Svoronos et.al. reported a potential interaction between estrogen and anti-tumor immunity in an ovarian mouse model. The study found that estrogen signaling mobilizes and enhances the immunosuppressive effects of myeloid derived suppressor cells (MDSCs) ultimately promoting ovarian carcinogenesis [132]. Evidence this interaction may also exist in lung cancer comes from a quantitative high-throughput screen of more than 2,000 compounds that identified fulvestrant as the lead candidate for enhancing lung cancer cell sensitivity to immuno- and chemotherapies. The study showed that fulvestrant was capable of re-sensitizing immunoresistant lung cancer cells to immune-mediated lysis with TNF-related apoptosis inducing ligand (TRAIL) [133]. The study also reported downregulation of

mesenchymal markers in lung cancer cells treated with fulvestrant, suggesting inhibition of ER signaling may not only restore immunocompetence, but also reverse the morphogenic epithelial-mesenchymal transition (EMT) process that is often associated with drug resistance and more aggressive disease [133]. Here, using both types of estrogen blocking agents, we evaluated the potential interactions among estrogen signaling, inflammation, drug resistance, and EMT in NSCLC.

3.1 METHODS AND MATERIALS

3.1.1 Cell Lines and Reagents

A549 cells were purchased from American Type Culture Collection (ATCC; Manassas, VA). H460 and ganetespib resistant A549GR-100 cells were generously gifted from Dr. Timothy Burns and generated as previously described [134]. A549 cells were grown in RPMI 1640 + 10% FBS and A549GR-100 cells were grown in RPMI 1640 + 10% FBS supplemented with ganetesib (100nM). Both cell lines were maintained at 37^0C in 5% CO_2. Fulvestrant, exemestane, letrozole, and androstenedione were purchased from Sigma-Aldrich (St. Louis, MO). Ganetespib was also generously gifted from Dr. Timothy Burns and originally sourced from Synta Pharmaceutical Corp. Recombinant soluble TRAIL was purchased from Peprotech (Rocky Hill, NJ). E-cadherin, Vimentin, and Actin antibodies were acquired from Cell Signaling Technology (Danvers, MA).

3.1.2 Evaluation of AI Therapies in a Xenograft Model of NSCLC

Ovariectomized female immunocompromised athymic nude mice were purchased from Harlan (Indianapolis, IN). A549 cells were grown, harvested, and resuspended in a 50% sterile serum-free PBS 50% matrigel (BD Biosciences, San Jose, CA). Cells ($2.5x10^6$) and injected into the rear flank on both sides of each mouse. Mice were supplemented with subcutaneous injections of androstenedione (0.1mg/mouse in peanut oil) 3x/week for two weeks prior to AI treatment initiation. Once tumors reached approximately $100mm^3$, blood was collected via the saphenous vein for serum analysis and mice were randomized into four treatment groups (n=12-14): (a) vehicle control 0.1mL/mouse daily (5%DMSO/ 0.3%hydroxypropylcellulose/0.9%NaCL) (b) exemestane 150μg/0.1ml/mouse daily via oral gavage (Exemestane-L) (c) exemestane 250μg/0.1ml/mouse daily via oral gavage (Exemestane-H) (d) letrozole 10μg/0.1mL/mouse daily via oral gavage. Doses were selected based on previous lung and breast cancer xenograft studies evaluating these compounds and demonstrating tumor growth inhibition at these concentrations [135,136]. Administration of androstenedione (0.1mg/mouse) continued 3x/week throughout the duration of the treatment period. Tumor volume was measured 2x/week and recorded as a relative tumor volume as previously described in methods 2.2.7. Treatment concluded after 28 days at which point half of the mice were sacrificed following cardiac puncture blood collection and tumors were harvested and processed as described in 2.2.7. Remaining mice were monitored for two weeks post-treatment with continued androstenedione injections (3x/week) and tumor growth measurements twice weekly. At day 42 remaining mice were sacrificed following cardiac puncture blood collection and tumors were harvested for IHC and protein analysis. All blood samples were processed by centrifugation within 1 hour of collection and serum supernatant was collected. Animal care was in compliance with IACUC and University of Pittsburgh DLAR guidelines.

3.1.3 Immunohistochemistry

Immunohistochemical analysis for H&E and Ki67 stained slides was performed as described in 2.2.8 methods. For p-NRF2 staining, slides were rinsed with PBS and blocked in background sniper (Biocare Medical), then incubated with p-NRF2 primary antibody (ab76026; 1:500; Abcam) for 50 minutes at room temperature. Slides were then incubated for 24 hour with horseradish peroxidase labeled secondary antibody (1:1000) and cell nuclei were counterstained with hematoxylin. Images were obtained as described in 2.2.8. pNRF2 was quantitated by taking into account staining positivity and intensity. Staining intensity was classified as strong, moderate, or low and proportions were attributed to the total score (ranging 0-300) utilizing the following formula: (3 x % strongly stained nuclei) + (2 x % moderately stained nuclei) + (% of weakly stained nuclei). Mean *H*-scores are represented as the average score of four fields from three independent samples per treatment.

3.1.4 Serum Cytokine Analysis

Serum was collected from blood samples by 10-minute centrifugation at 1300 rpm in serum collection tubes (BD Lifesciences). Samples were analyzed using a commercially available VPlex Pro-inflammatory Panel 1 Mouse Kit for IFN-γ, IL-10, IL-1β, IL-6, TNF-α from Meso Scale Delivery (Rockville, MD).

3.1.5 Cell Viability Assays

For TRAIL cell viability assays H460 cells were seeded at density of 1000 cells/well in a 96-well plate. Following 24-hour incubation half of the wells were pre-treated with 5μM of

fulvestrant or ethanol vehicle control for 48 hours. TRAIL was then added to all wells at increasing concentration (0-100nM) and fulvestrant was replenished in wells that were pre-treated. Cells were incubated 24 hours following TRAIL addition and cell viability was evaluated by adding 20µL of Cell Titer 96 Aqueous One reagent to each well and measuring at 490nm within 1 hour. For ganetespib cell viability assays A549 cells were seeded at a density of 2,000cells/well in a 96 well plate and incubated for 24 hours. Half of the plate was subjected to 5µM of fulvestrant or ethanol vehicle control for 48 hours. Ganetespib was then added to all wells at increasing concentration (0-100nM) and fulvestrant was replenished in wells that were pre-treated. Following 72-hour incubation cell viability was measured the same way as TRAIL assays.

3.1.6 Protein Extraction and Western Blot Analysis

Basal levels of e-cadherin and vimentin protein levels was conducted using cells grown to 80-90% confluency in T75 flasks and whole cell lysate collection, quantitation and immunoblotting analysis was performed as previously detailed in 2.2.4. Primary antibodies and dilutions used included: e-cadherin (1:1000; 3195s; Cell Signaling Technology), Vimentin (1:1000; 5741; Cell Signaling Technology), actin (1:5000; Clone C4; Millipore). For fulvestrant treated experiment, cells were plated at 75% confluency in 100mm dishes and incubated for 24 hours post attachment. Cells were then treated with ethanol vehicle control or fulvestrant (5µM) for 6-48 hours. Cells were harvested at time point.

3.1.7 Wound Healing Assays

A549 and A549-GR100 cells (500,000) were seeded into 6-well plates and incubated 24 hours post-seeding. Cells were then pre-treated for 48 hours with fulvestrant (5µM) or ethanol

vehicle control. Following 48 hour pre-treatment, and once 90-95% confluent, wells were scratched using a p200 tip in three vertical strokes. Wells were rinsed with DPBS to remove any floating cells and wells were imaged using 20x magnification light microscopy at 0 and 72 hours. Wounds were measured in μm using the measure tool on Leica Application suite. Percent migration was calculated by comparing wound measurements at 72 hours to 0 hours.

3.1.8 Statistical Analyses

Statistical analysis was performed for these studies as described in 2.2.9

3.2 RESULTS

3.2.1 Aromatase Inhibitors Suppress Tumor Growth in A549 Xenografts

Since the aromatase enzyme is responsible for the conversion of hormonal intermediates to estrogens, the *in vitro* assessment of AI efficacy is challenging with 2-D cell cultures lacking requisite supplies of endogenous substrates. However, even with the addition of the aromatase substrate androstenedione to cell proliferation assays evaluating exemestane and letrozole, we failed to observe any effect on cell viability up through 100μM in multiple NSCLC cell lines (data not shown). Therefore, to investigate the effect of AIs on tumor proliferation and inflammation in NSCLC we utilized an *in vivo* xenograft model using ovariectomized female mice regularly supplemented with androstenedione, ensuring elements of the tumor microenvironment and aromatase substrates were fully intact. Furthermore, since both steroidal and non-steroidal class AIs have been developed we treated mice bearing A549 flank tumors with two doses of hormonal

mimetic exemestane, the nonsteroidal letrozole, or vehicle control, to identify if AI classification affects anti-tumor efficacy or inflammation in NSCLC.

Compared with placebo, each AI treatment group significantly ($P<0.05$, Fig. 19) inhibited tumor proliferation when treatment was stopped at day 28 and half of the mice were sacrificed, tumors were fixed for IHC, and blood was collected for post-treatment serum analysis. Tumor measurements of all the mice at the end of treatment showed exemestane at a dose of 150μg/day inhibited tumor growth by 45%, exemestane at dose of 250μg/day inhibited tumor growth by 50%, and letrozole treatment inhibited tumor volume by 52% when compared to placebo. Relative tumor volume at the end of treatment was comparable among the AI treated groups, indicating exemestane (at both doses) and letrozole were all similarly effective at inhibiting NSCLC tumor growth in this study. Mouse weight and mobility were monitored and maintained throughout study among all treatment groups.

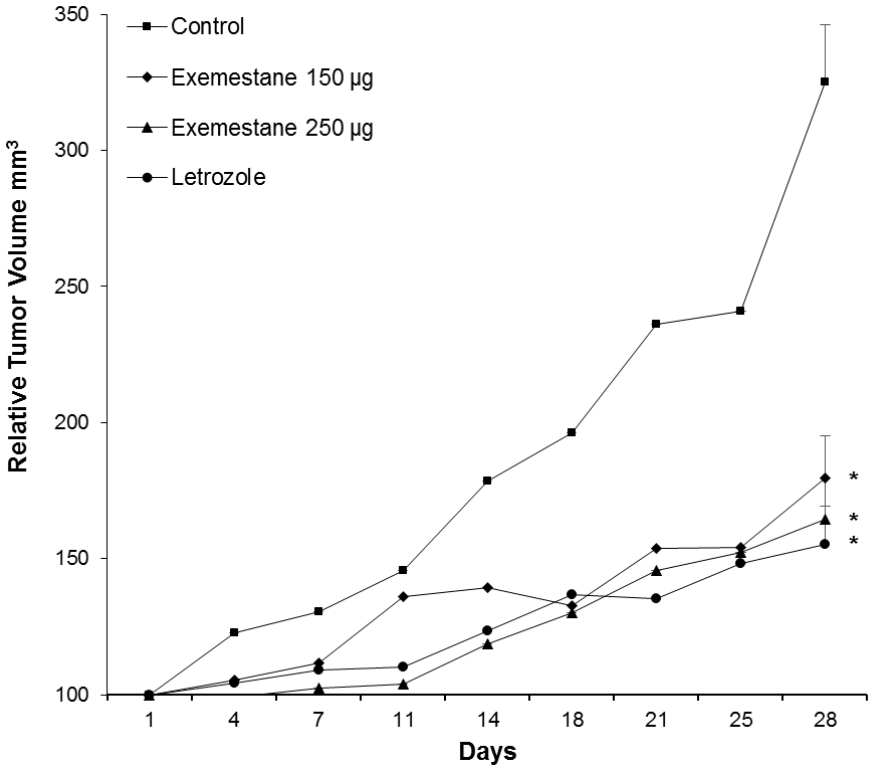

Figure 19. Exemestane and Letrozole Inhibit *In Vivo* A549 Xenograft Tumor Growth. Ovariectomized female athymic nude mice bearing A549 tumors were supplemented with androstenedione (0.1mg/3x/week) two weeks prior to initiation of AI treatment. Once tumors reached an average volume of 100mm^3, mice were randomized into four treatment groups: vehicle control, low-dose exemestane (150µg/daily, exemestane-L), high-dose exemestane (250µg/daily, exemestane-H), or letrozole (10µg/daily). Mice continued to receive subcutaneous injections of androstenedione three times per week for the duration of AI treatment. Tumor growth was measured twice weekly and results are reported as the relative mean tumor volume ± S.E. for 6-8 tumors per group. ANOVA *P<.05.

To evaluate long-term efficacy of AI therapies, tumor growth in the remaining half of mice was monitored an additional two weeks (Fig.20). During this time mice continued to receive androstenedione. At 14 days post-treatment, the only experimental group that exhibited significant tumor growth was the placebo group which had a 45% increase in relative tumor volume from day 28 to day 42 ($P<0.05$). Both the exemestane and letrozole treated groups showed no significant

increase in tumor growth two weeks following termination of treatment. Comparison of relative tumor volumes from day 42 with day 28 showed even more significant anti-tumor effects in the AI treated groups compared to placebo, indicating both AI therapies exhibit cytostatic efficacy in suppressing NSCLC tumor proliferation.

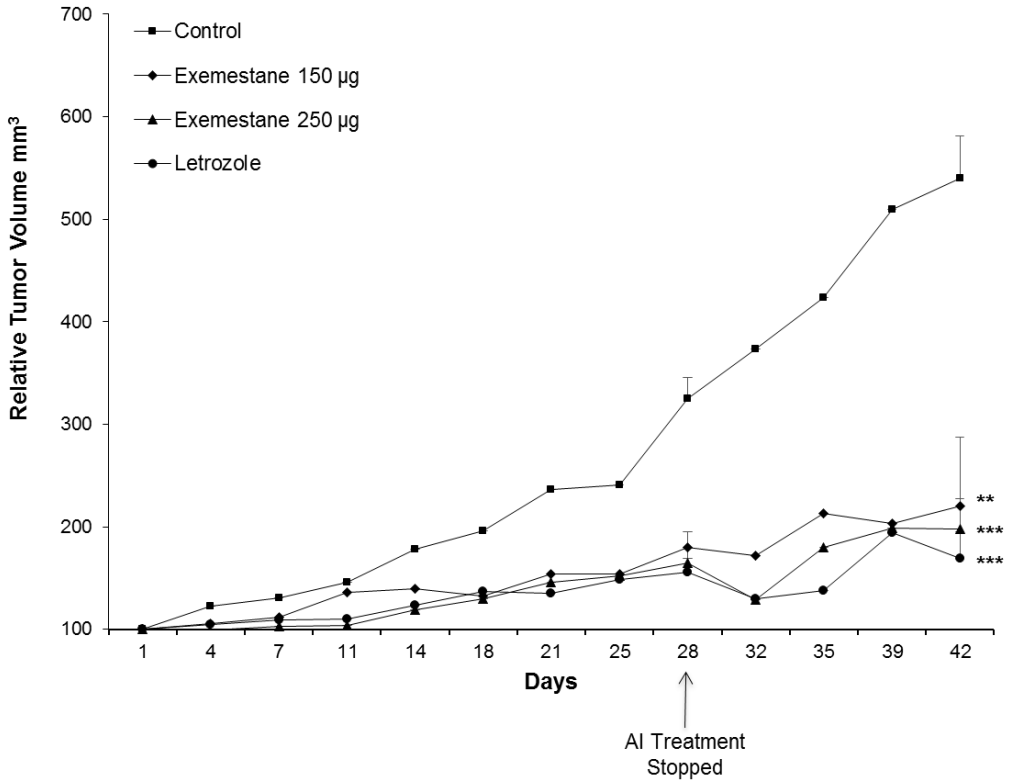

Figure 20. AI Therapies Exhibit Prolonged Tumor Growth Inhibition Post-Treatment. Tumor growth was evaluated in mice (n=3-4 per group) two weeks after AI treatment was stopped. Mice continued to receive regular androstenedione injections. Tumor growth was measured twice a week and reported as relative tumor volume ± S.E. ANOVA **P<0.01, ***P<0.001.

3.2.2 Exemestane and Letrozole Treated Xenografts Show Reduced Ki67 Staining and Increased Phosphorylated-NRF2 Staining

Immunohistochemical analysis was performed to assess changes in tumor histology and measure levels of Ki67 staining and phosphorylated-NRF2 (p-NRF2) in tissue harvested from

mice sacrificed at day 28 and day 42. Histologically, both exemestane and letrozole treated xenografts revealed increased stromal content compared to placebo, with similar levels of stroma observed irregardless of AI treatment group (Fig. 21). The Ki67 proliferative index was calculated for each experimental group to further assess the effects of AI therapy on tumor proliferation. Ki67 staining supported the tumor growth inhibition observed among AI treated mice with 60% reduced s-phase labeling in the exemestane and letrozole treated groups compared to placebo (P<0.001). All three AI treated groups showed similar reductions in Ki67 positive cells when compared with each other.

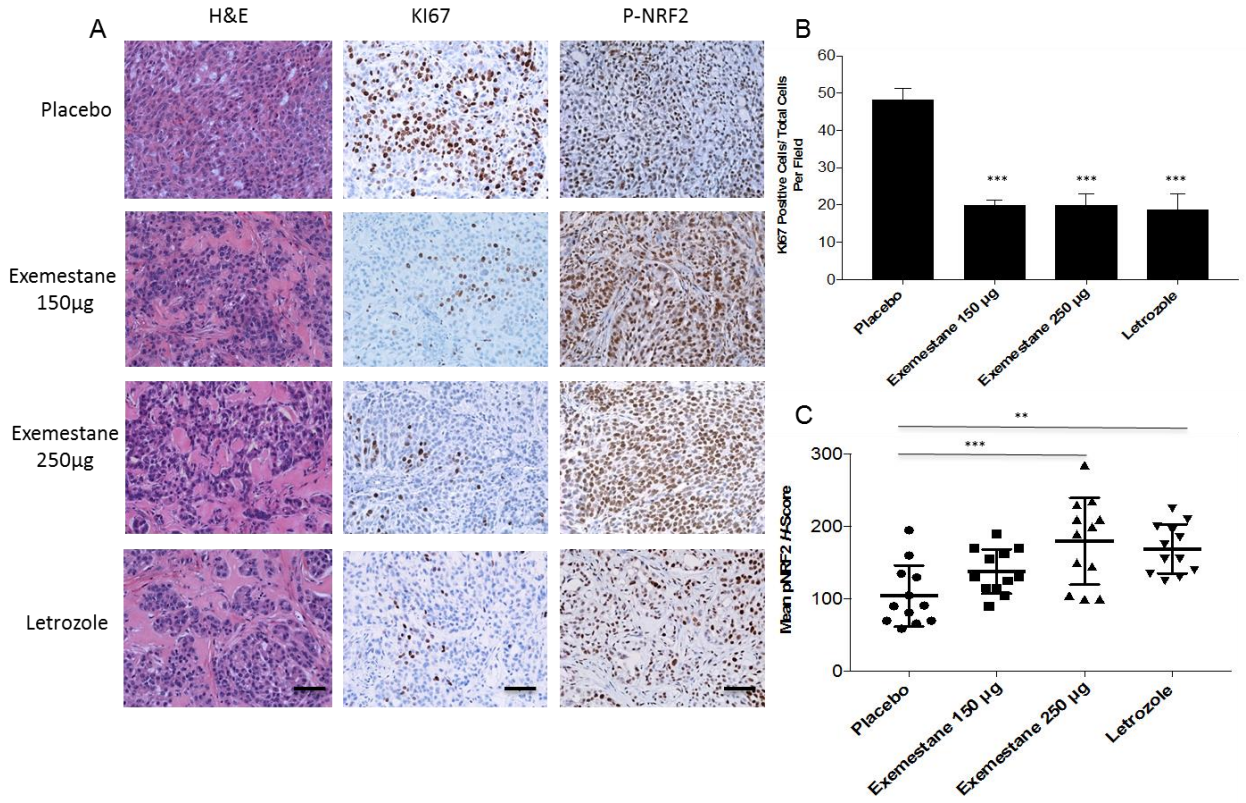

Figure 21. AI Treatments Show Decreased Ki67 Staining and Increased Stromal Content and p-NRF2 Staining. (A) Representative H&E, Ki67, and p-NRF2 stained sections from different xenograft treatment groups at day 28 imaged at 20X magnification. Scale bars represent 115µm. (B) Ki67 quantitation performed by counting four fields per tumor for three tumors per treatment group. (C) p-NRF2 quantitation representes mean pNRF2 *H*-Scores, determined by counting high, medium, and low intensity stained tumor cells from four fields of three separate tumors per treatment group. ANOVA **P<0.01, ***P<0.001.

To address whether aromatase inhibition increased anti-oxidant NRF2 signaling, protein levels of p-NRF2 were assessed (Fig. 21C). *H*-score quantitation of p-NRF2 revealed a significant 1.7-fold increase in staining in the high-dose exemestane treated mice ($P<0.001$) and a 1.62-fold increase in the letrozole treated mice ($P<0.01$) compared to placebo. While a significant increase was not demonstrated in the low-dose exemestane treatment group, an increase in staining was still observed, indicating the activation may increase with increasing dose. These results suggest both exemestane and letrozole stimulate activation of the anti-inflammatory NRF2/ARE pathway in this xenograft model and warrant continued investigation to further validate this potential interaction. Finally, we compared the IHC of tissue from the end of treatment to tissue two weeks post-treatment and found no observable changes in histology, Ki67 staining, or phospho-NRF2 staining.

3.2.3 AI Treatments Did Not Alter Circulating Pro-Inflammatory Cytokine Levels in A549 Xenografts

For a more comprehensive analysis of the potential anti-inflammatory effects of exemestane and letrozole treatment, a panel of pro-inflammatory cytokines was screened in serum collected from the mice. For an internal control, serum was collected for each mouse just before AI treatment was initiated and again prior to sacrifice either at the end of the treatment period or two weeks post treatment. Concentrations of circulating cytokines commonly implicated in inflammation including: IFN-γ, IL-1β, IL-6, IL-10, and TNFα, were evaluated using a multiplex assay kit. Trends were evaluated among pre-treatment serum, serum at the conclusion of the treatment period, and serum two-weeks post-treatment. When compared with placebo, both

exemestane and letrozole failed to demonstrate statistically significant alterations in the serum levels of circulating cytokines evaluated. Combined post-treatment (day 28 and day 42) serum IL-6 levels showed a decreased trend with mean the concentration observed in the high-dose exemestane treated mice 53.7 pg/mL, compared to a mean concentration of 91.93 pg/mL in placebo (P=0.17, Fig. 22).

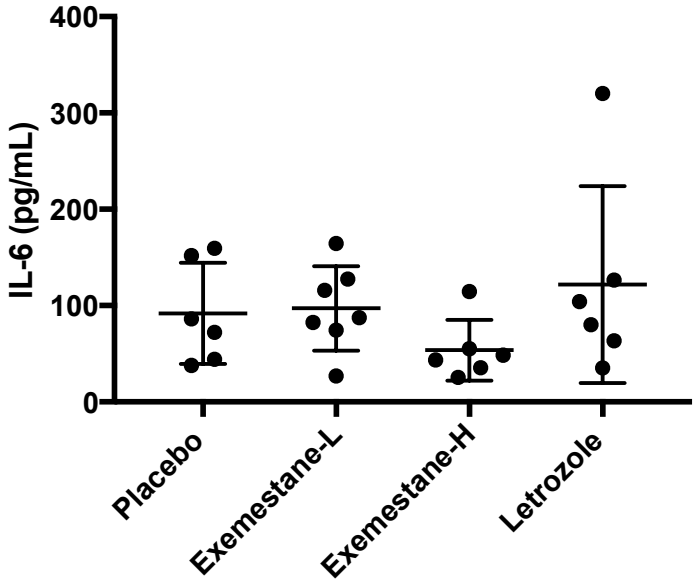

Figure 22. Decreasing Trend in Serum IL-6 of Exemestane Treated Mice. Post-treatment IL-6 serum levels were evaluated for differences among treatment groups. Blood was collected via cardiac puncture prior to sacrifice and serum was isolated following centrifugation in serum microcontainers. Cytokine concentrations were analyzed using a validated multiplex pro-inflammatory cytokine detection assay. Serum levels are reported as pg/mL and line represents the mean**.**

Interestingly, serum collected from mice at the end of the letrozole treatment period showed increased levels of every cytokine screened when compared to placebo, including IL-6. However, serum two-weeks post-letrozole treatment then showed decreasing levels of each cytokine relative to placebo, suggesting perhaps letrozole has a delayed effect on the inflammatory response following treatment. Variability in cytokine levels among mice in each experimental

group, both before and after treatment, greatly attributed to difficulty in evaluating significant mediation of inflammatory markers with exemestane and letrozole therapy.

3.2.4 Fulvestrant Enhances Immune-Mediated Lysis of H460 Cells

To further address a potential immune-modulating effect of endocrine therapies we evaluated the inhibitor effects of fulvestrant in combination with immune-based TRAIL therapy. A recent study demonstrated fulvestrant was capable of re-sensitizing H460 NSCLC cells exhibiting EMT-related drug resistance to immune-mediated apoptosis with TRAIL [133]. We sought to further investigate this observation with prior studies indicating TRAIL is regulated by IFN-γ, mediates immune surveillance, and potently induces death-receptor mediated apoptosis in certain NSCLC neoplastic cells [137,138]. While the cells utilized by the previous study were clonally selected based on a mesenchymal phenotype, protein analysis of our H460 cells (Figure 25) showed exclusive expression of the mesenchymal marker vimentin suggesting our cells were characteristically mesenchymal as well. Following the protocol utilized by Hamilton et.al. [133], H460 cells in this study were subjected to either fulvestrant or vehicle control pre-treatment for 48 hours prior to and during TRAIL treatment. Based on cell viability results from the previous chapter, prior unpublished studies in our laboratory, and published results reporting an IC_{50} well beyond 10μM for fulvestrant in H460 cells, we chose to again use a concentration of 5μM for the anti-estrogen [125]. Cell viability was evaluated 24 hours following the addition of TRAIL and showed significantly enhanced sensitivity to TRAIL-mediated apoptosis in cells pre-treated with fulvestrant (Figure 23). A nearly 2.5-fold enhancement of TRAIL-induced cytotoxicity in H460 cells with fulvestrant treatment implicates a potential role of ER signaling in immune-based drug resistance ($P<0.001$).

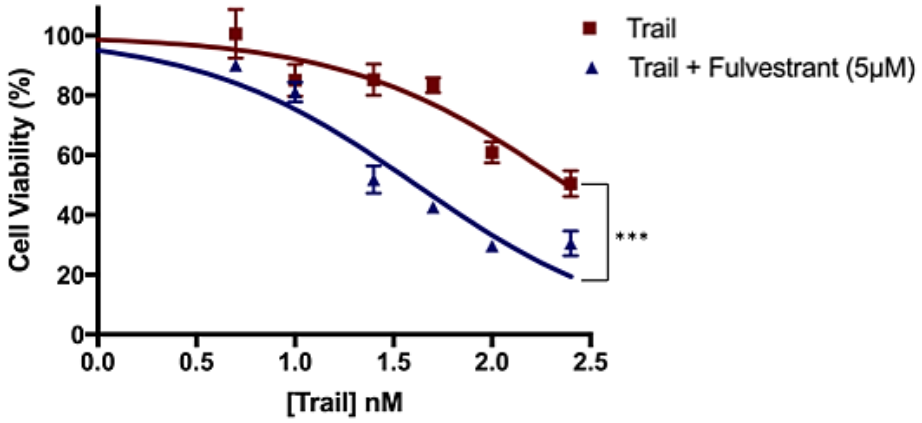

Figure 23. Fulvestrant Pre-Treatment Enhances TRAIL Mediated Apoptosis in H460 Cells.H460 cells were seeded and pre-treated with 5μM fulvestrant or ethanol for 48 hours. TRAIL was then added at increasing concentrations (0.5-100nM) to each well while fulvestrant was maintained in combination with TRAIL in pre-treated wells. Following 24 hour incubation, 20μL of Cell Titer 96 Aqueous One reagent was added to each well and the plate was read at 490nm. Cell viability at each concentration is the mean ± S.E. of three samples from one independent trial. ANOVA ***P<0.001.

3.2.5 Enhanced Therapeutic Sensitivity of Ganetespib-Resistant Cells with Fulvestrant Treatment is Not Reliant on EMT Reversal

While the complex mechanisms underlying drug resistance are still under investigation, recent studies show the broadly classified morphogenic process of EMT may be involved in conferring resistance to targeted and traditional chemotherapies in neoplastic cells [139,140]. It was demonstrated that chemoresistant NSCLC cells could be re-sensitized to cytotoxic chemotherapies such as cisplatin with fulvestrant treatment, resulting not only in downregulation of ERs but also the reversal of an EMT phenotype [133]. To further elucidate the effects of ER inhibition on drug resistance and mediation of EMT we utilized NSCLC cells with acquired resistance to the heat shock protein 90 (HSP90) inhibitor ganetespib. HSP90 is a molecular chaperone for several client proteins including ER, and pathways modulated by ER, such as EGFR,

AKT [141]. While HSP90 inhibitors revealed promising preclinical efficacy in lung cancer, these therapies remain clinically limited due to nearly inevitable acquired and intrinsic drug resistance [142]. While hyper-activation of pathways downstream of ER signaling are identified compensatory mechanisms involved in acquired resistance of NSCLC cells to ganetespib therapy [134], our primary focus for using the ganetespib-resistant (GR) NSCLC model was as a tool. The focus of these studies was to evaluate fulvestrant's effects on EMT and drug resistance rather than pharmacologic interactions between ER antagonists and HSP90.

Cell proliferation assays were performed to establish ganetespib resistance and determine whether fulvestrant would subsequently re-sensitize GR cells to the HSP90 inhibitor. An initial fulvestrant dose-response revealed no effect on GR cell viability up through 100μM, and fulvestrant (5μM) in combination with increasing doses of ganetespib also had no significant effect on the GR cells in a 72-hour proliferation assay (data not shown). However, based on the results of the TRAIL experiment, evaluation of a 48-hour pre-treatment with 5μM fulvestrant prior to a combined fulvestrant and ganetespib treatment, re-sensitized GR cells to ganetespib therapy. This treatment strategy was evaluated in both H460 and A549 cells with acquired resistance to ganetespib, however, greater effects of fulvestrant treatment on ganetespib sensitivity were observed in resistant A549 cells (A549-GR100) shifting the IC_{50} from over 250nM to 30nM ($P<0.001$, Figure 23).

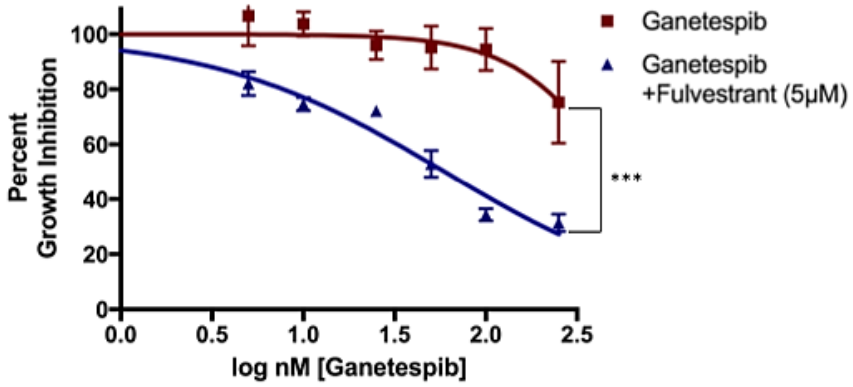

Figure 24. Fulvestrant Pre-Treatment Enhanced Sensitivity of A549-GR100 Cells to Combined Ganetespib and Fulvestrant Treatment. A549-GR100 cells were seeded and subjected to fulvestrant or vehicle control for 48 hours prior to addition of increasing concentrations of ganetespib (0.5-250μM). Fulvestrant was replenished in pre-treated cells with the addition of ganetespib. Cell proliferation was measured following 72-hour incubation and subsequent addition of Cell Titer 96 Aqueous One reagent. Results are plotted as the average percent growth inhibition ± S.E. ***P<0.001.

Following demonstration that fulvestrant could re-sensitize GR cells to ganetespib, we characterized a panel of parental non-resistant NSCLC cell lines to evaluate basal levels of EMT markers e-cadherin and vimentin. Expression of e-cadherin, a cell surface transmembrane protein identified for its role in cell-cell adhesion, is a commonly used identifier of an epithelial phenotype [143]. Whereas expression of vimentin, an intermediate filament protein associated with increased motility and migration, is a marker associated with a mesenchymal phenotype [144].

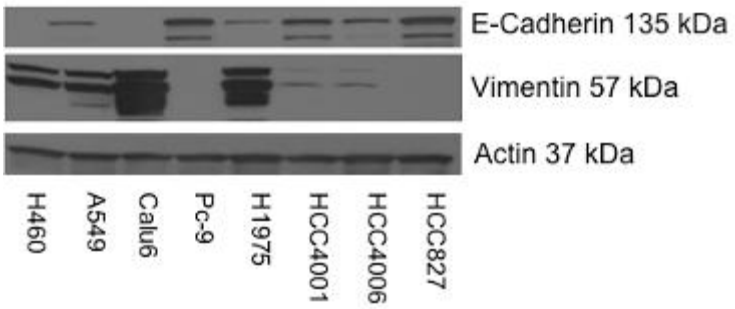

Figure 25. Basal EMT Marker Expression in NSCLC Cell Panel. Immunoblotting analysis of e-cadherin and vimentin expression in whole cell lysates collected from NSCLC cell lines. Blot was also probed for actin as a loading control.

Traditionally, studies have characterized cell lines based on their exclusive expression of either mesenchymal or epithelial markers. However, we observed a hybrid EMT phenotype with both epithelial and mesenchymal markers expressed in A549 cells and to a lesser extent in H1975, HCC4001 and HCC4006 cells. We chose to move forward with A549 and A549-GR100 cells based on this dual EMT marker profile and previous studies showing upregulated expression of ERβ and vimentin in A549-G100 cells compared to parental (data not shown).

To determine whether fulvestrant's ability to enhance therapeutic sensitivity of GR cells is reliant on reversal of EMT, we evaluated alterations in e-cadherin and vimentin expression with and without fulvestrant treatment at multiple time points (Figure 26)

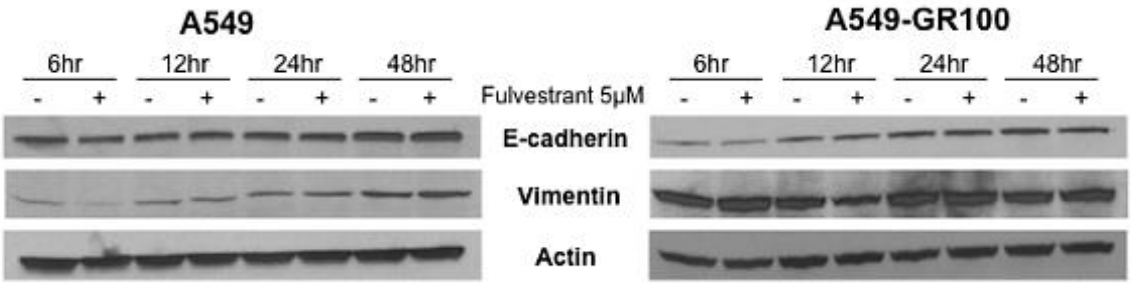

Figure 26. Fulvestrant Treatment Demonstrates Limited Modulation of Vimentin Expression in A549 and A549-GR100 Cells. A549 and A549-GR100 cells were seeded and treated with fulvestrant (5μM) or ethanol for 6-48 hours. Whole cell lysates were collected at each time point and probed for EMT markers using immunoblotting. Blots were stripped and probed for actin protein to confirm equal loading.

Fulvestrant down-regulated vimentin expression by 23% relative to control at the 12-hour time point in A549-GR100 cells. This effect was transient, however, with expression returning to basal levels by 24 hours. While fulvestrant had no apparent effect on e-cadherin expression at any particular time point in GR cells, overall e-cadherin expression increased 2.5-fold from 6 to 48 hours. Samples were also collected in the more epithelial A549 parental line to act as a phenotypic control. Fulvestrant treatment markedly reduced vimentin expression by 48% in A549 cells at 6 hours. However, the inhibitory effect was again short-term with basal expression returning by 12 hours. Furthermore, regardless of fulvestrant treatment total vimentin expression increased 2.3-fold in A549 cells throughout the duration of the time course. Based on these results, and several repeated efforts, fulvestrant treatment had no consistent or robust effect on the expression of these EMT markers in either the more mesenchymal GR or epithelial parental cell lines. Independent upregulation of the markers observed in each cell line over time may potentially be attributed to increased cell density by the 48 hour mark compared to the shorter time points.

3.2.6 Fulvestrant Inhibits Migration in A549-GR100 NSCLC Cells

Loss of e-cadherin expression is associated with enhanced migration, a hallmark phenotype of EMT in mesenchymal cells [145]. Aside from modulation of protein markers associated with epithelial and mesenchymal phenotypes, we were interested to further characterize the functional EMT phenotypes of the parental and resistant cells by assessing their migratory capacity. Migration patterns for A549 parental and A549-GR100 cells were evaluated in wound-healing assays. In addition to basal un-treated migration, we assessed whether pharmacologic inhibition of ER signaling with fulvestrant treatment impacted migration in either the parental or GR cells. Un-treated A549-GR100 cells exhibited 1.7-fold increased migration by 72 hours following wounding compared to A549 cells (Figure 27). In this study, cells receiving fulvestrant were pre-treated 48 hours prior to wounding and then maintained in fulvestrant for the 72 hours following wounding. A549-GR100 cells treated with fulvestrant in this way showed 35% less migration compared to control, while no statistically significant effect on migration was observed with fulvestrant treatment in A549 parental cells.

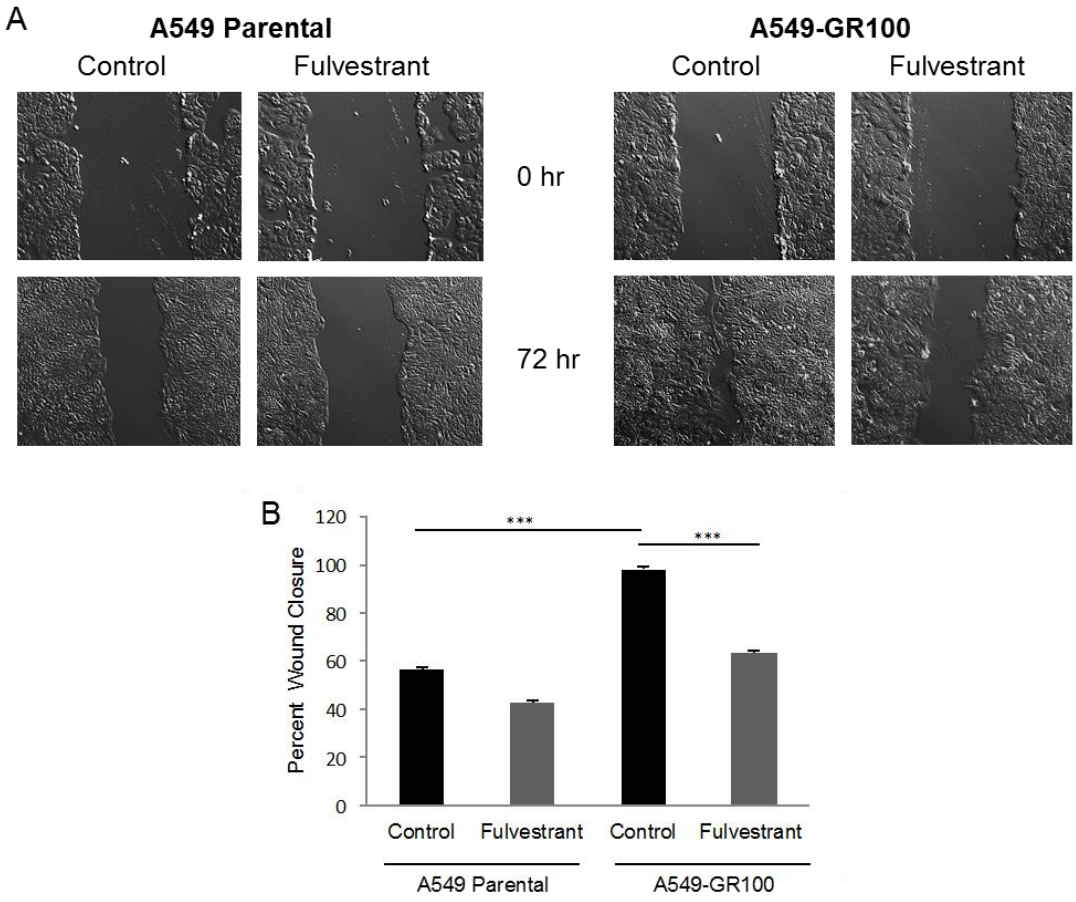

Figure 27. Fulvestrant Treatment Inhibits Migration in A549-GR100 Cells. (A) Representative images of wound healing at 0 and 72 hours in A549 and A549-GR100 cells. (B) Mean migration in A549 and A549-GR100 cells +/- fulvestrant treatment. Cells were grown on 6-well plates and treated with 5μM fulvestrant or ethanol for 48 hours prior to and during the 72 hours following wounding. Wounds were imaged at 0 and 72 hours with 20X light microscopy. Migration was measured by comparing wound size at three different locations for each sample at 72 hours versus 0 hours and is reported as a percentage of wound closure for three independent samples ± S.E. per experimental group. ANOVA ***P<0.001.

3.3 CONCLUSIONS AND FUTURE DIRECTIONS

Preclinical studies have consistently demonstrated that estrogen signaling promotes lung tumorigenesis by inducing cellular proliferation through both genomic and non-genomic mechanisms [70,100]. However, recent efforts focused on targeting this pathway indicate an increasingly pervasive role of estrogen signaling as a driver of the disease with interactions among not only growth factor pathways, but also inflammation, EMT, therapeutic resistance, and immunosurveillance. In this portion of the study, we used selective agents targeted against the synthesis and signaling of estrogen to evaluate these associations and the potential added benefits of inhibiting the pathway in NSCLC.

Our results further demonstrated the potential clinical benefit of aromatase inhibitors exemestane and letrozole in NSCLC by showing both agents significantly inhibited tumor proliferation in an A549 NSCLC xenograft model for up to two weeks post-treatment. These results revealed that regardless of chemical structure both steroidal and nonsteroidal aromatase inhibitors function as anti-tumor agents in NSCLC effectively blocking tumor growth, reducing actively proliferating cells, and increasing tumor stroma. Furthermore, in this study the higher dose of exemestane did not statistically improve tumor growth inhibition compared to the low-dose, suggesting further evaluation of dose-dependent effects on tumor proliferation. Together, these results provide further rationale for current phase I evaluations of AIs in post-menopausal with late-stage NSCLC (NCT01664754).

Utilizing the *in vivo* model also enabled examination of a potential interaction between the ER signaling and the inflammatory response. Based on the hypothesis that AI therapies would exhibit anti-inflammatory effects, our analysis of NRF2 phosphorylation revealed increased activation of the pathway in high-dose exemestane ($P<0.001$) and letrozole treated mice ($P<0.01$)

compared to placebo. These results suggest AI therapies may upregulate NRF2 signaling and further evaluation of an interaction between the E2 and NRF2 pathways should be conducted through IHC staining and immunoblotting analysis of downstream effector molecules and cytoprotective enzymes. Furthermore, while we failed to identify any significant shifts in circulating pro-inflammatory cytokine serum levels in response to either AI, a trend towards decreased IL-6 in the high-dose exemestane treated group warrants further exploration since IL-6 is an identified regulator of tumor associated macrophage (TAM) aromatase activity in breast cancer and aromatase expression is reported in infiltrating TAMs in NSCLC [146]. Furthermore, IL-6 is a well-known activator of the tumor promoting STAT3 signaling pathway [147], and evaluation of phosphorylated STAT3 in the xenografts may be beneficial for assessing whether exemestane abrogates STAT3 signaling as well. Additionally, recently submitted work from our laboratory showed AIs combined with non-steroidal anti-inflammatory drugs (NSAIDS) prevented tumor development following carcinogen exposure in a murine model, suggesting this combined approach should be further analyzed for the potential prevention and treatment of lung cancer. Finally, it is important to note that the use of an immunocompromised mouse model likely impacted our evaluation of the adaptive immune response and future studies elucidating this interaction should utilize immunocompetent mice in a syngeneic or carcinogen-induced murine model.

In our investigation of an immunoregulatory effect with ER inhibition, we show that fulvestrant significantly enhances sensitivity of H460 cells to TRAIL-mediated apoptosis. Pre-treatment with the fulvestrant followed by combination treatment with recombinant TRAIL shifted the IC_{50} nearly 4-fold from the TRAIL treated control. However, because H460 cells are *KRAS-STK11-PIK3CA* triple mutant and TRAIL signaling alternatively has been shown to actually promote cancer progression through PI3K signaling in *KRAS* mutant cells with elevated TRAIL-

Receptor 2 (TRAIL-R2), the expression of TRAIL-R2 should be evaluated in these cells to determine whether ER blockade is interacting with the immune response or inhibiting a compensatory mechanism of resistance [148]. While performed in triplicate, the results for this study are only from one independent trial necessitating additional studies to ensure accuracy of the pharmacologic response of H460 cells to TRAIL following fulvestrant pre-treatment. However, the results for this study were in support of previously published data [133] and prompted our continued investigation of fulvestrant in a NSCLC drug-resistant setting.

Previous studies showing enhanced TRAIL sensitivity with fulvestrant treatment attributed the increased therapeutic response to fulvestrant's effect on EMT reversal [133]. Therefore, we examined the role of fulvestrant and ER inhibition on EMT in A549-GR100 cells. While neoplastic cells are often categorized as epithelial or mesenchymal based on their expression of either e-cadherin or vimentin, immunoblotting revealed dual expression of both markers in our A549 and A549-GR100 cells. An emerging theory of partial EMT versus complete EMT has been recently reported by a few studies also demonstrating co-expression of epithelial and mesenchymal markers in NSCLC cell lines [149]. Cells characterized by partial EMT in these studies exhibited more aggressive, resistant, and migratory behavior compared with strictly mesenchymal cells, and in breast cancer identification of hybrid EMT cells was associated with poorer prognosis [149]. Based on the EMT marker expression in our cells H460 appeared to have already undergone EMT, while A549/A549-GR100 cells were characteristic of partial EMT.

The hypothesis that fulvestrant treatment was re-sensitizing A549-GR100 cells through modulation of EMT was partially disproved by minimal alteration of vimentin expression throughout a time course. While vimentin expression decreased with fulvestrant treatment at 12 hours, the effect was limited and expression returned by 24 hours. Since therapeutic enhancement with fulvestrant treatment was observed at 48 hours, the data suggests this is not due to modulation

of EMT. However, our inability to detect changes in these markers may include the fact that marker modulation may be less evident in hybrid cells, since most studies focus on strictly changes in marker expression in complete EMT cells. Furthermore, we only evaluated two markers when several others are representative of the various phases of EMT morphogenesis and a larger screen of EMT markers is warranted. Also, as mentioned previously, the HSP90 drug-resistant model was used primarily as a tool, but using a model with resistance to a therapy selectively targeting a mediator of ER may have impacted our ability to detect anti-estrogen modulatory effects on EMT. Moreover, with time in culture the resistant cells became less responsive to fulvestrant treatment, indicating the cells became more resistant over time and in the future a more stable model should be used. Despite these confounding experimental variables, the results from these studies support the continued debate over whether the EMT is a mediator or merely an accompanying phenotype of drug resistance. Future studies are required to elucidate other methods by which fulvestrant is capable of enhancing therapeutic sensitivity across such a broad range of therapeutics. While cellular senescence and arrest are usually identified for their negative effects on therapeutic response, fulvestrant was only capable of enhancing therapeutic sensitivity to either compound with a 48-hour pre-treatment, suggesting future studies should evaluate cell cycle mediation during fulvestrant pre-treatment periods.

Increased migratory and invasive behavior is associated with down-regulated e-cadherin expression and indicative of EMT. As anticipated, the more mesenchymal A549-GR100 cells exhibited significantly greater migration compared to parental A549. Enhanced migratory behavior in the GR cells was inhibited by fulvestrant, implicating ER signaling in NSCLC migration, specifically cells exhibiting mesenchymal characteristics. Since fulvestrant potently targets both ER isoforms, we also attempted to identify which receptor was responsible for modulation of migration through a genetic approach. A549-GR100 cells were transiently

transfected with ERα and ERβ siRNA pools (data not shown). Both siRNA transfection pools failed to appropriately and selectively down-regulate each receptor individually, requiring the experiment to be optimized and repeated in order to make valid conclusions. In this experiment, cells transfected with ERα siRNA exhibited knockdown of ERβ, which may likely be due to off-target effects since a comparison of sequences in each pool failed to show significant homology. Despite this off-target effect, we observed acquisition of a spindle-like morphology in the transfected cells expressing down-regulated ERβ and 36% decreased migration (data not shown). As mentioned, future studies are required to draw conclusions regarding which receptor is responsible for migration, and a more effective approach would instead utilize stably knocked down cell lines due to the extended period of the wound healing experiment.

Ultimately, inhibition of estrogen synthesis with AI therapy presents as a novel mechanism for tumor growth inhibition in NSCLC. In other ongoing studies in our laboratory, the combination of the AI anastrozole with either aspirin or ibuprofen has been shown to have enhanced anti-tumor effects in murine models of lung carcinogenesis, meriting continued investigation of this combination in NSCLC, not only in regards to tumor growth, but also NRF2 activation. Exciting results showing fulvestrant enhances therapeutic sensitivity in several cell models prompts continued investigation of other settings in which this anti-estrogen therapy may restore therapeutic sensitivity and by which mechanisms it is doing so. Furthermore, while not an apparent mediator of e-cadherin and vimentin expression, fulvestrant may modulate other markers associated with EMT. Finally, ER inhibition significantly reduces migration, the specifics of which have potential impact on the invasive and metastatic capacity of NSCLC cells [144]. Taken together these findings highlight an expanding network of interactions between estrogen signaling and various elements of the tumor microenvironment, affirming the need to further elucidate the widespread therapeutic effects of estrogen inhibition in NSCLC.

4.0 DISCUSSION

The primary focus of this study was to utilize estrogen-blocking agents to identify and target interactions between estrogen signaling and tumor promoting mechanisms such as growth factor pathways, inflammation, and EMT in NSCLC. Our efforts in this study were concentrated on identifying additional druggable mechanisms by which the estrogen signaling pathway promotes lung tumor progression.

The first aspect of this study involved the identification and targeted inhibition of crosstalk between ER and FGFR signaling. Having previously published that elevated ERβ expression in lung tumors is a poor prognostic indicator, an mRNA study comparing ERβ high expressing lung tumors with ERβ low expressing tumors identified the *FGFR1* gene significantly upregulated in the ERβ high tumors. The FGFR signaling pathway is also well characterized in lung cancer with several therapies such as AZD4547 already under clinical evaluation for NSCLC patients [119,150]. These results coupled with recent reports of estrogen mediated FGFR signaling in breast cancer prompted our investigation of a non-genomic interaction between the two pathways in NSCLC as well. Following characterization of a panel of NSCLC cell lines for *FGFR1* amplification and FGFR/FGF expression and secretion profiles, we chose to focus our studies on non-amplified cells since they were less solely reliant on FGFR as a molecular driver making crosstalk more readily identified and targeted in these cells. We demonstrated estrogen treatment significantly stimulated FGF2 secretion and fulvestrant was capable of blocking this effect, suggesting FGF ligand secretion was reliant on estrogen. We also established crosstalk between the pathways by showing greater abrogation of FGFR signaling with AZD4547 combined with fulvestrant compared to AZD4547 alone. Preclinical studies showed significantly enhanced anti-

proliferative effects of the combined ER and FGFR inhibitor both *in vitro* and *in vivo* compared to either single agent treatment or placebo. Combined with the additional data (covered in detail in reference [123]) that showed the co-targeting strategy also significantly inhibited the acquisition of a stem cell-like phenotype, the results of this study provide rationale for clinical evaluation of a pan-FGFR inhibitor combined with an ER targeting agent in NSCLC patients lacking *FGFR1* amplification. Having selected inhibitors for this study with established safety and tolerability profiles, renders these results and combination strategy even more readily translatable to the clinic. Furthermore, with studies having now identified interactions between ERβ and EGFR [70] and ERβ and FGFR, these results suggest continued investigation of interactions between estrogen signaling and additional growth factor pathways.

The second aspect of this study focused on using AIs and ER antagonists to broadly evaluate interactions between estrogen signaling and: inflammation, therapeutic resistance, EMT, and migration in NSCLC. Already under early clinical evaluation in post-menopausal women with advanced NSCLC (NCT01664754), we further demonstrated the potential clinical benefit of AIs, by showing both exemestane and letrozole significantly inhibited NSCLC *in vivo* tumor growth. While AI therapies exhibited inhibition of tumor proliferation, the estrogen synthesis inhibitors did not significantly alter the serum levels of pro-inflammatory cytokines, but did significantly enhance activation of NRF2 signaling. Failure to observe modulation of pro-inflammatory proteins with AI treatment may be attributed to the fact that AI therapies may require being combined with NSAIDs to observe an effect on circulating cytokines. Additionally, our use of an immunocompromised mouse model distorted the adaptive immune and inflammatory response, whereas most murine models assessing inflammation are conducted in mice with intact immune systems. Regardless, we were still able to observe enhanced NRF2 phosphorylation with both high-dose exemestane and letrozole treatments. IHC and protein analysis of cytoprotective

enzymes downstream of NRF2 activation will help to further validate whether the anti-inflammatory response is fully initiated by exposure to the AI therapies. This initial evidence of estrogen inhibition inciting an immune response in NSCLC supports further investigation of E2 mediation of inflammation and other components of tumor immune regulation such as PD-L1 expression. The clinical efficacy of PD-L1 targeted therapies in lung cancer has sparked several research efforts to evaluate other interacting elements for potential combination strategies. Most recently, preliminary results in our laboratory evaluating whether estrogen treatment stimulates PD-L1 cell surface expression in NSCLC cells showed increased expression with E2 treatment in 2 out of 3 cell lines assessed. We not only plan to repeat and expand these studies, but also determine if fulvestrant alternatively down-regulates PD-L1 and whether anti-estrogens can enhance the clinical utility of PD-L1 immunotherapies.

The final aspect of this study focused on evaluating fulvestrant's effects on drug resistance and EMT phenotypes. Our evaluation was based on results from a study showing fulvestrant was capable of enhancing the therapeutic sensitivity of mesenchymal/resistant NSCLC cells to chemo- and immune therapies, and did so by reversing EMT [133]. We were able to demonstrate that fulvestrant treatment has the potential to enhance sensitivity of H460 mesenchymal cells to TRAIL mediated cytotoxicity. In addition, while the GR model became increasingly resistant to both ganetespib and fulvestrant throughout the entirety of this investigation, fulvestrant was initially capable of re-sensitizing GR cells to ganetespib therapy. Furthermore, because we did not observe robust modulation of e-cadherin and vimentin expression following fulvestrant treatment, therapeutic enhancement in GR cells was not solely due to a reversal of EMT. Here we chose to focus on modulation of just one epithelial and one mesenchymal marker, however, there are up to 20 other identified markers representative of these associated phenotypes [144] and fulvestrant may not directly mediate the markers we selected. Ultimately, conclusive remarks regarding

whether estrogen signaling, or inhibition thereof, mediates EMT are challenging to make based on our limited evaluation of associated markers and use of a model with acquired resistance to the molecular chaperone HSP90. In addition to EMT protein studies, however, we also evaluated cell migration as it is a representative functional phenotype of mesenchymal cells. Wound healing assays revealed GR cells were more mesenchymal than parental A549 by exhibiting significantly increased migration. Observations that fulvestrant treatment significantly blocked migration in the resistant cells, but had no protective effect against migration in the epithelial parental cells, implicates ER signaling in migration and a potential role for anti-estrogens specifically in the metastatic setting. While our final experiments assessing the impact of ER specific knockdown on migration encountered several challenges and require re-evaluation, a recent publication successfully demonstrated with RNAi that migration in NSCLC is reliant on the ERβ isoform and matrix-metalloproteinase-2 protein expression, supporting continued investigation of the beta receptor [151]. Further analysis of fulvestrant's effects on NSCLC migration should also be conducted using three-dimensional tumor spheroids since key elements of the tumor microenvironment are conserved in these models.

In summary, the results of this study indicate the estrogen signaling pathway is implicated in a wide-range of tumor promoting mechanisms in NSCLC. While each of the interactions outlined in this study require further investigation, the overall findings provide rationale for the use of combination strategies involving hormonal therapies as novel therapeutic approaches for the treatment of lung cancer.

APPENDIX A

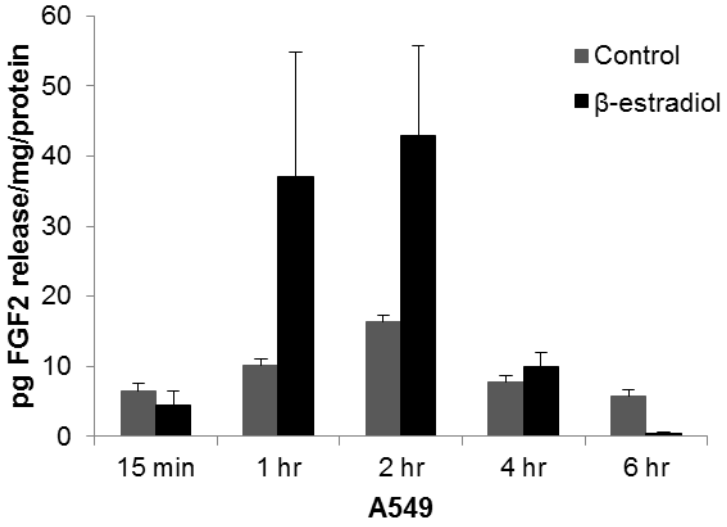

Figure 28. Complete Time Course for FGF2 Release in A549 Cells. Representative time course data for A549 cells. Initially performed in 201T and 273T cells as well. Media was collected and concentrated 4-fold for ELISA analysis and corresponding whole cell lysates were collected for protein normalization.

BIBLIOGRAPHY

1. American, S.C. Cancer facts & figures 2017. American Cancer Society Atlanta, 2017.
2. Kris, M.G.; Johnson, B.E.; Berry, L.D.; Kwiatkowski, D.J.; Iafrate, A.J.; Wistuba, II; Varella-Garcia, M.; Franklin, W.A.; Aronson, S.L.; Su, P.F., *et al.* Using multiplexed assays of oncogenic drivers in lung cancers to select targeted drugs. *Jama* **2014**, *311*, 1998-2006.
3. Borghaei, H.; Paz-Ares, L.; Horn, L.; Spigel, D.R.; Steins, M.; Ready, N.E.; Chow, L.Q.; Vokes, E.E.; Felip, E.; Holgado, E., *et al.* Nivolumab versus docetaxel in advanced nonsquamous non-small-cell lung cancer. *The New England journal of medicine* **2015**, *373*, 1627-1639.
4. Reck, M.; Rodriguez-Abreu, D.; Robinson, A.G.; Hui, R.; Csoszi, T.; Fulop, A.; Gottfried, M.; Peled, N.; Tafreshi, A.; Cuffe, S., *et al.* Pembrolizumab versus chemotherapy for pd-l1-positive non-small-cell lung cancer. *The New England journal of medicine* **2016**, *375*, 1823-1833.
5. Herbst, R.S.; Heymach, J.V.; Lippman, S.M. Lung cancer. *The New England journal of medicine* **2008**, *359*, 1367-1380.
6. Lewis, D.R.; Check, D.P.; Caporaso, N.E.; Travis, W.D.; Devesa, S.S. Us lung cancer trends by histologic type. *Cancer* **2014**, *120*, 2883-2892.
7. Song, M.A.; Benowitz, N.L.; Berman, M.; Brasky, T.M.; Cummings, K.M.; Hatsukami, D.K.; Marian, C.; O'Connor, R.; Rees, V.W.; Woroszylo, C., *et al.* Cigarette filter ventilation and its relationship to increasing rates of lung adenocarcinoma. *Journal of the National Cancer Institute* **2017**, *109*.
8. Alberg, A.J.; Samet, J.M. Epidemiology of lung cancer. *Chest* **2003**, *123*, 21S-49S.
9. Durham, A.L.; Adcock, I.M. The relationship between copd and lung cancer. *Lung cancer* **2015**, *90*, 121-127.
10. Massion, P.P.; Carbone, D.P. The molecular basis of lung cancer: Molecular abnormalities and therapeutic implications. *Respiratory research* **2003**, *4*, 12.
11. Cheng, Y.W.; Chiou, H.L.; Sheu, G.T.; Hsieh, L.L.; Chen, J.T.; Chen, C.Y.; Su, J.M.; Lee, H. The association of human papillomavirus 16/18 infection with lung cancer among nonsmoking taiwanese women. *Cancer research* **2001**, *61*, 2799-2803.
12. Testa, J.R.; Carbone, M.; Hirvonen, A.; Khalili, K.; Krynska, B.; Linnainmaa, K.; Pooley, F.D.; Rizzo, P.; Rusch, V.; Xiao, G.H. A multi-institutional study confirms the presence and expression of simian virus 40 in human malignant mesotheliomas. *Cancer research* **1998**, *58*, 4505-4509.
13. Matakidou, A.; Eisen, T.; Houlston, R.S. Systematic review of the relationship between family history and lung cancer risk. *British journal of cancer* **2005**, *93*, 825-833.
14. Schwartz, A.G.; Siegfried, J.M.; Weiss, L. Familial aggregation of breast cancer with early onset lung cancer. *Genetic epidemiology* **1999**, *17*, 274-284.
15. Burns, T.F.; Stabile, L.P. Targeting the estrogen pathway for the treatment and prevention of lung cancer. *Lung Cancer Manag* **2014**, *3*, 43-52.
16. Thomas, A.; Liu, S.V.; Subramaniam, D.S.; Giaccone, G. Refining the treatment of nsclc according to histological and molecular subtypes. *Nature reviews. Clinical oncology* **2015**, *12*, 511-526.

17. Network, N.C.C. Nccn guidelines version 6.2017 non-small cell lung cancer. https://http://www.nccn.org/professionals/physician_gls/pdf/nscl.pdf (June 18, 2017),
18. Network, N.C.C. Nccn guidelines version 3.2017 small cell lung cancer https://http://www.nccn.org/professionals/physician_gls/pdf/sclc.pdf (June 20,2018),
19. Rossi, A.; Di Maio, M.; Chiodini, P.; Rudd, R.M.; Okamoto, H.; Skarlos, D.V.; Fruh, M.; Qian, W.; Tamura, T.; Samantas, E., *et al.* Carboplatin- or cisplatin-based chemotherapy in first-line treatment of small-cell lung cancer: The cocis meta-analysis of individual patient data. *Journal of clinical oncology : official journal of the American Society of Clinical Oncology* **2012**, *30*, 1692-1698.
20. Tiseo, M.; Ardizzoni, A. Current status of second-line treatment and novel therapies for small cell lung cancer. *Journal of thoracic oncology : official publication of the International Association for the Study of Lung Cancer* **2007**, *2*, 764-772.
21. Yang, P. Epidemiology of lung cancer prognosis: Quantity and quality of life. *Methods in molecular biology* **2009**, *471*, 469-486.
22. Strebhardt, K.; Ullrich, A. Paul ehrlich's magic bullet concept: 100 years of progress. *Nature reviews. Cancer* **2008**, *8*, 473-480.
23. Cancer Genome Atlas Research, N. Comprehensive genomic characterization of squamous cell lung cancers. *Nature* **2012**, *489*, 519-525.
24. Cancer Genome Atlas Research, N. Comprehensive molecular profiling of lung adenocarcinoma. *Nature* **2014**, *511*, 543-550.
25. Miettinen, P.J.; Berger, J.E.; Meneses, J.; Phung, Y.; Pedersen, R.A.; Werb, Z.; Derynck, R. Epithelial immaturity and multiorgan failure in mice lacking epidermal growth factor receptor. *Nature* **1995**, *376*, 337-341.
26. Scaltriti, M.; Baselga, J. The epidermal growth factor receptor pathway: A model for targeted therapy. *Clinical cancer research : an official journal of the American Association for Cancer Research* **2006**, *12*, 5268-5272.
27. Bethune, G.; Bethune, D.; Ridgway, N.; Xu, Z. Epidermal growth factor receptor (egfr) in lung cancer: An overview and update. *Journal of thoracic disease* **2010**, *2*, 48-51.
28. Veale, D.; Kerr, N.; Gibson, G.J.; Kelly, P.J.; Harris, A.L. The relationship of quantitative epidermal growth factor receptor expression in non-small cell lung cancer to long term survival. *British journal of cancer* **1993**, *68*, 162-165.
29. Salomon, D.S.; Brandt, R.; Ciardiello, F.; Normanno, N. Epidermal growth factor-related peptides and their receptors in human malignancies. *Critical reviews in oncology/hematology* **1995**, *19*, 183-232.
30. Lynch, T.J.; Bell, D.W.; Sordella, R.; Gurubhagavatula, S.; Okimoto, R.A.; Brannigan, B.W.; Harris, P.L.; Haserlat, S.M.; Supko, J.G.; Haluska, F.G., *et al.* Activating mutations in the epidermal growth factor receptor underlying responsiveness of non-small-cell lung cancer to gefitinib. *The New England journal of medicine* **2004**, *350*, 2129-2139.
31. Zhou, C.; Wu, Y.L.; Chen, G.; Feng, J.; Liu, X.Q.; Wang, C.; Zhang, S.; Wang, J.; Zhou, S.; Ren, S., *et al.* Erlotinib versus chemotherapy as first-line treatment for patients with advanced egfr mutation-positive non-small-cell lung cancer (optimal, ctong-0802): A multicentre, open-label, randomised, phase 3 study. *The Lancet. Oncology* **2011**, *12*, 735-742.
32. Lee, C.K.; Brown, C.; Gralla, R.J.; Hirsh, V.; Thongprasert, S.; Tsai, C.M.; Tan, E.H.; Ho, J.C.; Chu da, T.; Zaatar, A., *et al.* Impact of egfr inhibitor in non-small cell lung cancer on progression-free and overall survival: A meta-analysis. *Journal of the National Cancer Institute* **2013**, *105*, 595-605.

33. Suda, K.; Mizuuchi, H.; Maehara, Y.; Mitsudomi, T. Acquired resistance mechanisms to tyrosine kinase inhibitors in lung cancer with activating epidermal growth factor receptor mutation--diversity, ductility, and destiny. *Cancer metastasis reviews* **2012**, *31*, 807-814.
34. Koivunen, J.P.; Mermel, C.; Zejnullahu, K.; Murphy, C.; Lifshits, E.; Holmes, A.J.; Choi, H.G.; Kim, J.; Chiang, D.; Thomas, R., *et al.* Eml4-alk fusion gene and efficacy of an alk kinase inhibitor in lung cancer. *Clinical cancer research : an official journal of the American Association for Cancer Research* **2008**, *14*, 4275-4283.
35. Gainor, J.F.; Shaw, A.T. Novel targets in non-small cell lung cancer: Ros1 and ret fusions. *The oncologist* **2013**, *18*, 865-875.
36. Solomon, B.J.; Mok, T.; Kim, D.W.; Wu, Y.L.; Nakagawa, K.; Mekhail, T.; Felip, E.; Cappuzzo, F.; Paolini, J.; Usari, T., *et al.* First-line crizotinib versus chemotherapy in alk-positive lung cancer. *The New England journal of medicine* **2014**, *371*, 2167-2177.
37. Shaw, A.T.; Ou, S.H.; Bang, Y.J.; Camidge, D.R.; Solomon, B.J.; Salgia, R.; Riely, G.J.; Varella-Garcia, M.; Shapiro, G.I.; Costa, D.B., *et al.* Crizotinib in ros1-rearranged non-small-cell lung cancer. *The New England journal of medicine* **2014**, *371*, 1963-1971.
38. Huber, K.V.; Salah, E.; Radic, B.; Gridling, M.; Elkins, J.M.; Stukalov, A.; Jemth, A.S.; Gokturk, C.; Sanjiv, K.; Stromberg, K., *et al.* Stereospecific targeting of mth1 by (s)-crizotinib as an anticancer strategy. *Nature* **2014**, *508*, 222-227.
39. Yasuda, H.; de Figueiredo-Pontes, L.L.; Kobayashi, S.; Costa, D.B. Preclinical rationale for use of the clinically available multitargeted tyrosine kinase inhibitor crizotinib in ros1-translocated lung cancer. *Journal of thoracic oncology : official publication of the International Association for the Study of Lung Cancer* **2012**, *7*, 1086-1090.
40. Pfeifer, G.P.; Denissenko, M.F.; Olivier, M.; Tretyakova, N.; Hecht, S.S.; Hainaut, P. Tobacco smoke carcinogens, DNA damage and p53 mutations in smoking-associated cancers. *Oncogene* **2002**, *21*, 7435-7451.
41. Halvorsen, A.R.; Silwal-Pandit, L.; Meza-Zepeda, L.A.; Vodak, D.; Vu, P.; Sagerup, C.; Hovig, E.; Myklebost, O.; Borresen-Dale, A.L.; Brustugun, O.T., *et al.* Tp53 mutation spectrum in smokers and never smoking lung cancer patients. *Frontiers in genetics* **2016**, *7*, 85.
42. Mandinova, A.; Lee, S.W. The p53 pathway as a target in cancer therapeutics: Obstacles and promise. *Science translational medicine* **2011**, *3*, 64rv61.
43. Planchard, D.; Besse, B.; Groen, H.J.; Souquet, P.J.; Quoix, E.; Baik, C.S.; Barlesi, F.; Kim, T.M.; Mazieres, J.; Novello, S., *et al.* Dabrafenib plus trametinib in patients with previously treated braf(v600e)-mutant metastatic non-small cell lung cancer: An open-label, multicentre phase 2 trial. *The Lancet. Oncology* **2016**, *17*, 984-993.
44. Administration, U.S.F.a.D. Fda grants regular approval to dabrafenib and trametinib combination for metastatic nsclc with braf v600e mutation. U.S. Department of Health and Human Services https://http://www.fda.gov/Drugs/InformationOnDrugs/ApprovedDrugs/ucm564331.htm, 2017.
45. Reungwetwattana, T.; Dy, G.K. Targeted therapies in development for non-small cell lung cancer. *Journal of carcinogenesis* **2013**, *12*, 22.
46. Woo, E.Y.; Yeh, H.; Chu, C.S.; Schlienger, K.; Carroll, R.G.; Riley, J.L.; Kaiser, L.R.; June, C.H. Cutting edge: Regulatory t cells from lung cancer patients directly inhibit autologous t cell proliferation. *Journal of immunology* **2002**, *168*, 4272-4276.
47. Brahmer, J.R. Harnessing the immune system for the treatment of non-small-cell lung cancer. *Journal of clinical oncology : official journal of the American Society of Clinical Oncology* **2013**, *31*, 1021-1028.

48. Kerr, K.M.; Nicolson, M.C. Non-small cell lung cancer, pd-l1, and the pathologist. *Archives of pathology & laboratory medicine* **2016**, *140*, 249-254.
49. Brahmer, J.; Reckamp, K.L.; Baas, P.; Crino, L.; Eberhardt, W.E.; Poddubskaya, E.; Antonia, S.; Pluzanski, A.; Vokes, E.E.; Holgado, E., *et al.* Nivolumab versus docetaxel in advanced squamous-cell non-small-cell lung cancer. *The New England journal of medicine* **2015**, *373*, 123-135.
50. Garon, E.B.; Rizvi, N.A.; Hui, R.; Leighl, N.; Balmanoukian, A.S.; Eder, J.P.; Patnaik, A.; Aggarwal, C.; Gubens, M.; Horn, L., *et al.* Pembrolizumab for the treatment of non-small-cell lung cancer. *The New England journal of medicine* **2015**, *372*, 2018-2028.
51. Villaruz, L.C.; Kalyan, A.; Zarour, H.; Socinski, M.A. Immunotherapy in lung cancer. *Translational lung cancer research* **2014**, *3*, 2-14.
52. Jure-Kunkel, M.; Masters, G.; Girit, E.; Dito, G.; Lee, F.; Hunt, J.T.; Humphrey, R. Synergy between chemotherapeutic agents and ctla-4 blockade in preclinical tumor models. *Cancer immunology, immunotherapy : CII* **2013**, *62*, 1533-1545.
53. Lee, F.; Jure-Kunkel, M.N.; Salvati, M.E. Synergistic activity of ixabepilone plus other anticancer agents: Preclinical and clinical evidence. *Therapeutic advances in medical oncology* **2011**, *3*, 11-25.
54. Women and smoking: A report of the surgeon general. Executive summary. *MMWR. Recommendations and reports : Morbidity and mortality weekly report. Recommendations and reports* **2002**, *51*, i-iv; 1-13.
55. Institute, N.C. Surveillance, epidemiology, and end results (seer) program 1974-2014. https://seer.cancer.gov/faststats/selections.php?#Output (June 24, 2017),
56. Patel, J.D.; Bach, P.B.; Kris, M.G. Lung cancer in us women: A contemporary epidemic. *Jama* **2004**, *291*, 1763-1768.
57. Risch, H.A.; Howe, G.R.; Jain, M.; Burch, J.D.; Holowaty, E.J.; Miller, A.B. Are female smokers at higher risk for lung cancer than male smokers? A case-control analysis by histologic type. *American journal of epidemiology* **1993**, *138*, 281-293.
58. Zang, E.A.; Wynder, E.L. Differences in lung cancer risk between men and women: Examination of the evidence. *Journal of the National Cancer Institute* **1996**, *88*, 183-192.
59. Perneger, T.V. Sex, smoking, and cancer: A reappraisal. *Journal of the National Cancer Institute* **2001**, *93*, 1600-1602.
60. Sun, S.; Schiller, J.H.; Gazdar, A.F. Lung cancer in never smokers--a different disease. *Nature reviews. Cancer* **2007**, *7*, 778-790.
61. Thun, M.J.; Hannan, L.M.; Adams-Campbell, L.L.; Boffetta, P.; Buring, J.E.; Feskanich, D.; Flanders, W.D.; Jee, S.H.; Katanoda, K.; Kolonel, L.N., *et al.* Lung cancer occurrence in never-smokers: An analysis of 13 cohorts and 22 cancer registry studies. *PLoS medicine* **2008**, *5*, e185.
62. Burns, T.F.S., L.P. Targeting the estrogen pathway for the treatment and prevention of lung cancer *Lung cancer Management* **2014**, *3*, 1-10.
63. Alexiou, C.; Onyeaka, C.V.; Beggs, D.; Akar, R.; Beggs, L.; Salama, F.D.; Duffy, J.P.; Morgan, W.E. Do women live longer following lung resection for carcinoma? *European journal of cardio-thoracic surgery : official journal of the European Association for Cardio-thoracic Surgery* **2002**, *21*, 319-325.
64. Stabile, L.P.; Siegfried, J.M. Sex and gender differences in lung cancer. *The journal of gender-specific medicine : JGSM : the official journal of the Partnership for Women's Health at Columbia* **2003**, *6*, 37-48.

65. Ryberg, D.; Hewer, A.; Phillips, D.H.; Haugen, A. Different susceptibility to smoking-induced DNA damage among male and female lung cancer patients. *Cancer research* **1994**, *54*, 5801-5803.
66. Mollerup, S.; Ryberg, D.; Hewer, A.; Phillips, D.H.; Haugen, A. Sex differences in lung cyp1a1 expression and DNA adduct levels among lung cancer patients. *Cancer research* **1999**, *59*, 3317-3320.
67. Wei, Q.; Cheng, L.; Amos, C.I.; Wang, L.E.; Guo, Z.; Hong, W.K.; Spitz, M.R. Repair of tobacco carcinogen-induced DNA adducts and lung cancer risk: A molecular epidemiologic study. *Journal of the National Cancer Institute* **2000**, *92*, 1764-1772.
68. Stapelfeld, C.; Neumann, K.T.; Maser, E. Different inhibitory potential of sex hormones on nnk detoxification in vitro: A possible explanation for gender-specific lung cancer risk. *Cancer letters* **2017**.
69. Yang, S.H.; Mechanic, L.E.; Yang, P.; Landi, M.T.; Bowman, E.D.; Wampfler, J.; Meerzaman, D.; Hong, K.M.; Mann, F.; Dracheva, T., *et al.* Mutations in the tyrosine kinase domain of the epidermal growth factor receptor in non-small cell lung cancer. *Clinical cancer research : an official journal of the American Association for Cancer Research* **2005**, *11*, 2106-2110.
70. Stabile, L.P.; Lyker, J.S.; Gubish, C.T.; Zhang, W.; Grandis, J.R.; Siegfried, J.M. Combined targeting of the estrogen receptor and the epidermal growth factor receptor in non-small cell lung cancer shows enhanced antiproliferative effects. *Cancer research* **2005**, *65*, 1459-1470.
71. Marquez-Garban, D.C.; Chen, H.W.; Fishbein, M.C.; Goodglick, L.; Pietras, R.J. Estrogen receptor signaling pathways in human non-small cell lung cancer. *Steroids* **2007**, *72*, 135-143.
72. Dogan, S.; Shen, R.; Ang, D.C.; Johnson, M.L.; D'Angelo, S.P.; Paik, P.K.; Brzostowski, E.B.; Riely, G.J.; Kris, M.G.; Zakowski, M.F., *et al.* Molecular epidemiology of egfr and kras mutations in 3,026 lung adenocarcinomas: Higher susceptibility of women to smoking-related kras-mutant cancers. *Clinical cancer research : an official journal of the American Association for Cancer Research* **2012**, *18*, 6169-6177.
73. The coronary drug project. Findings leading to discontinuation of the 2.5-mg day estrogen group. The coronary drug project research group. *Jama* **1973**, *226*, 652-657.
74. Global Burden of Disease Cancer, C.; Fitzmaurice, C.; Allen, C.; Barber, R.M.; Barregard, L.; Bhutta, Z.A.; Brenner, H.; Dicker, D.J.; Chimed-Orchir, O.; Dandona, R., *et al.* Global, regional, and national cancer incidence, mortality, years of life lost, years lived with disability, and disability-adjusted life-years for 32 cancer groups, 1990 to 2015: A systematic analysis for the global burden of disease study. *JAMA oncology* **2016**.
75. Adami, H.O.; Persson, I.; Hoover, R.; Schairer, C.; Bergkvist, L. Risk of cancer in women receiving hormone replacement therapy. *International journal of cancer* **1989**, *44*, 833-839.
76. Taioli, E.; Wynder, E.L. Re: Endocrine factors and adenocarcinoma of the lung in women. *Journal of the National Cancer Institute* **1994**, *86*, 869-870.
77. Ganti, A.K.; Sahmoun, A.E.; Panwalkar, A.W.; Tendulkar, K.K.; Potti, A. Hormone replacement therapy is associated with decreased survival in women with lung cancer. *Journal of clinical oncology : official journal of the American Society of Clinical Oncology* **2006**, *24*, 59-63.
78. Ramnath, N.; Menezes, R.J.; Loewen, G.; Dua, P.; Eid, F.; Alkhaddo, J.; Paganelli, G.; Natarajan, N.; Reid, M.E. Hormone replacement therapy as a risk factor for non-small cell lung cancer: Results of a case-control study. *Oncology* **2007**, *73*, 305-310.

79. Schabath, M.B.; Wu, X.; Vassilopoulou-Sellin, R.; Vaporciyan, A.A.; Spitz, M.R. Hormone replacement therapy and lung cancer risk: A case-control analysis. *Clinical cancer research : an official journal of the American Association for Cancer Research* **2004**, *10*, 113-123.
80. Baschnagel, A.M.; Williams, L.; Hanna, A.; Chen, P.Y.; Krauss, D.J.; Pruetz, B.L.; Akervall, J.; Wilson, G.D. C-met expression is a marker of poor prognosis in patients with locally advanced head and neck squamous cell carcinoma treated with chemoradiation. *International journal of radiation oncology, biology, physics* **2014**, *88*, 701-707.
81. Slatore, C.G.; Chien, J.W.; Au, D.H.; Satia, J.A.; White, E. Lung cancer and hormone replacement therapy: Association in the vitamins and lifestyle study. *Journal of clinical oncology : official journal of the American Society of Clinical Oncology* **2010**, *28*, 1540-1546.
82. Chlebowski, R.T.; Schwartz, A.G.; Wakelee, H.; Anderson, G.L.; Stefanick, M.L.; Manson, J.E.; Rodabough, R.J.; Chien, J.W.; Wactawski-Wende, J.; Gass, M., *et al.* Oestrogen plus progestin and lung cancer in postmenopausal women (women's health initiative trial): A post-hoc analysis of a randomised controlled trial. *Lancet* **2009**, *374*, 1243-1251.
83. Ishibashi, H.; Suzuki, T.; Suzuki, S.; Niikawa, H.; Lu, L.; Miki, Y.; Moriya, T.; Hayashi, S.; Handa, M.; Kondo, T., *et al.* Progesterone receptor in non-small cell lung cancer--a potent prognostic factor and possible target for endocrine therapy. *Cancer research* **2005**, *65*, 6450-6458.
84. Stabile, L.P.; Dacic, S.; Land, S.R.; Lenzner, D.E.; Dhir, R.; Acquafondata, M.; Landreneau, R.J.; Grandis, J.R.; Siegfried, J.M. Combined analysis of estrogen receptor beta-1 and progesterone receptor expression identifies lung cancer patients with poor outcome. *Clinical cancer research : an official journal of the American Association for Cancer Research* **2011**, *17*, 154-164.
85. Sprague, B.L.; Trentham-Dietz, A.; Cronin, K.A. A sustained decline in postmenopausal hormone use: Results from the national health and nutrition examination survey, 1999-2010. *Obstetrics and gynecology* **2012**, *120*, 595-603.
86. Bouchardy, C.; Benhamou, S.; Schaffar, R.; Verkooijen, H.M.; Fioretta, G.; Schubert, H.; Vinh-Hung, V.; Soria, J.C.; Vlastos, G.; Rapiti, E. Lung cancer mortality risk among breast cancer patients treated with anti-estrogens. *Cancer* **2011**, *117*, 1288-1295.
87. Lother, S.A.; Harding, G.A.; Musto, G.; Navaratnam, S.; Pitz, M.W. Antiestrogen use and survival of women with non-small cell lung cancer in manitoba, canada. *Hormones & cancer* **2013**, *4*, 270-276.
88. Hsu, L.H.; Feng, A.C.; Kao, S.H.; Liu, C.C.; Tsai, S.Y.; Shih, L.S.; Chu, N.M. Second primary lung cancers among breast cancer patients treated with anti-estrogens have a longer cancer-specific survival. *Anticancer research* **2015**, *35*, 1121-1127.
89. Chu, S.C.; Hsieh, C.J.; Wang, T.F.; Hong, M.K.; Chu, T.Y. Antiestrogen use in breast cancer patients reduces the risk of subsequent lung cancer: A population-based study. *Cancer epidemiology* **2017**, *48*, 22-28.
90. Niikawa, H.; Suzuki, T.; Miki, Y.; Suzuki, S.; Nagasaki, S.; Akahira, J.; Honma, S.; Evans, D.B.; Hayashi, S.; Kondo, T., *et al.* Intratumoral estrogens and estrogen receptors in human non-small cell lung carcinoma. *Clinical cancer research : an official journal of the American Association for Cancer Research* **2008**, *14*, 4417-4426.
91. Kawai, H.; Ishii, A.; Washiya, K.; Konno, T.; Kon, H.; Yamaya, C.; Ono, I.; Minamiya, Y.; Ogawa, J. Estrogen receptor alpha and beta are prognostic factors in non-small cell

lung cancer. *Clinical cancer research : an official journal of the American Association for Cancer Research* **2005**, *11*, 5084-5089.
92. Schwartz, A.G.; Prysak, G.M.; Murphy, V.; Lonardo, F.; Pass, H.; Schwartz, J.; Brooks, S. Nuclear estrogen receptor beta in lung cancer: Expression and survival differences by sex. *Clinical cancer research : an official journal of the American Association for Cancer Research* **2005**, *11*, 7280-7287.
93. Stabile, L.P.; Davis, A.L.; Gubish, C.T.; Hopkins, T.M.; Luketich, J.D.; Christie, N.; Finkelstein, S.; Siegfried, J.M. Human non-small cell lung tumors and cells derived from normal lung express both estrogen receptor alpha and beta and show biological responses to estrogen. *Cancer research* **2002**, *62*, 2141-2150.
94. Kuiper, G.G.; Enmark, E.; Pelto-Huikko, M.; Nilsson, S.; Gustafsson, J.A. Cloning of a novel receptor expressed in rat prostate and ovary. *Proceedings of the National Academy of Sciences of the United States of America* **1996**, *93*, 5925-5930.
95. Raso, M.G.; Behrens, C.; Herynk, M.H.; Liu, S.; Prudkin, L.; Ozburn, N.C.; Woods, D.M.; Tang, X.; Mehran, R.J.; Moran, C., *et al.* Immunohistochemical expression of estrogen and progesterone receptors identifies a subset of nsclcs and correlates with egfr mutation. *Clinical cancer research : an official journal of the American Association for Cancer Research* **2009**, *15*, 5359-5368.
96. Nose, N.; Sugio, K.; Oyama, T.; Nozoe, T.; Uramoto, H.; Iwata, T.; Onitsuka, T.; Yasumoto, K. Association between estrogen receptor-beta expression and epidermal growth factor receptor mutation in the postoperative prognosis of adenocarcinoma of the lung. *Journal of clinical oncology : official journal of the American Society of Clinical Oncology* **2009**, *27*, 411-417.
97. Verma, M.K.; Miki, Y.; Abe, K.; Nagasaki, S.; Niikawa, H.; Suzuki, S.; Kondo, T.; Sasano, H. Co-expression of estrogen receptor beta and aromatase in japanese lung cancer patients: Gender-dependent clinical outcome. *Life sciences* **2012**, *91*, 800-808.
98. Abe, K.; Miki, Y.; Ono, K.; Mori, M.; Kakinuma, H.; Kou, Y.; Kudo, N.; Koguchi, M.; Niikawa, H.; Suzuki, S., *et al.* Highly concordant coexpression of aromatase and estrogen receptor beta in non-small cell lung cancer. *Human pathology* **2010**, *41*, 190-198.
99. Mah, V.; Seligson, D.B.; Li, A.; Marquez, D.C.; Wistuba, II; Elshimali, Y.; Fishbein, M.C.; Chia, D.; Pietras, R.J.; Goodglick, L. Aromatase expression predicts survival in women with early-stage non small cell lung cancer. *Cancer research* **2007**, *67*, 10484-10490.
100. Hershberger, P.A.; Vasquez, A.C.; Kanterewicz, B.; Land, S.; Siegfried, J.M.; Nichols, M. Regulation of endogenous gene expression in human non-small cell lung cancer cells by estrogen receptor ligands. *Cancer research* **2005**, *65*, 1598-1605.
101. Klinge, C.M. Estrogen receptor interaction with estrogen response elements. *Nucleic acids research* **2001**, *29*, 2905-2919.
102. Shen, L.; Li, Z.; Shen, S.; Niu, X.; Yu, Y.; Li, Z.; Liao, M.; Chen, Z.; Lu, S. The synergistic effect of egfr tyrosine kinase inhibitor gefitinib in combination with aromatase inhibitor anastrozole in non-small cell lung cancer cell lines. *Lung cancer* **2012**, *78*, 193-200.
103. Xu, R.; Shen, H.; Guo, R.; Sun, J.; Gao, W.; Shu, Y. Combine therapy of gefitinib and fulvestrant enhances antitumor effects on nsclc cell lines with acquired resistance to gefitinib. *Biomedicine & pharmacotherapy = Biomedecine & pharmacotherapie* **2012**, *66*, 384-389.
104. Siegfried, J.M.; Hershberger, P.A.; Stabile, L.P. Estrogen receptor signaling in lung cancer. *Seminars in oncology* **2009**, *36*, 524-531.
105. Nardulli, A.M.; Katzenellenbogen, B.S. Dynamics of estrogen receptor turnover in uterine cells in vitro and in uteri in vivo. *Endocrinology* **1986**, *119*, 2038-2046.

106. Long, X.; Nephew, K.P. Fulvestrant (ici 182,780)-dependent interacting proteins mediate immobilization and degradation of estrogen receptor-alpha. *The Journal of biological chemistry* **2006**, *281*, 9607-9615.
107. Miller, W.R.; Bartlett, J.; Brodie, A.M.; Brueggemeier, R.W.; di Salle, E.; Lonning, P.E.; Llombart, A.; Maass, N.; Maudelonde, T.; Sasano, H., *et al.* Aromatase inhibitors: Are there differences between steroidal and nonsteroidal aromatase inhibitors and do they matter? *The oncologist* **2008**, *13*, 829-837.
108. Garon, E.B.S., J.M.; Dubinett, S.M.; et al. In *Result of tori l-03, a randomized, multicenter phase ii clinical trial of erlotinib (e) or e + fulvestrant (f) in previously treated advanced non-small cell lung cancer (nsclc)*, AACR Annual Meeting Washington D.C., April 6-10, 2013; Washington D.C.
109. Brooks, A.N.; Kilgour, E.; Smith, P.D. Molecular pathways: Fibroblast growth factor signaling: A new therapeutic opportunity in cancer. *Clinical cancer research : an official journal of the American Association for Cancer Research* **2012**, *18*, 1855-1862.
110. Tiseo, M.; Gelsomino, F.; Alfieri, R.; Cavazzoni, A.; Bozzetti, C.; De Giorgi, A.M.; Petronini, P.G.; Ardizzoni, A. Fgfr as potential target in the treatment of squamous non small cell lung cancer. *Cancer treatment reviews* **2015**, *41*, 527-539.
111. Marek, L.; Ware, K.E.; Fritzsche, A.; Hercule, P.; Helton, W.R.; Smith, J.E.; McDermott, L.A.; Coldren, C.D.; Nemenoff, R.A.; Merrick, D.T., *et al.* Fibroblast growth factor (fgf) and fgf receptor-mediated autocrine signaling in non-small-cell lung cancer cells. *Molecular pharmacology* **2009**, *75*, 196-207.
112. Hadari, Y.R.; Gotoh, N.; Kouhara, H.; Lax, I.; Schlessinger, J. Critical role for the docking-protein frs2 alpha in fgf receptor-mediated signal transduction pathways. *Proceedings of the National Academy of Sciences of the United States of America* **2001**, *98*, 8578-8583.
113. Greulich, H.; Pollock, P.M. Targeting mutant fibroblast growth factor receptors in cancer. *Trends in molecular medicine* **2011**, *17*, 283-292.
114. Weiss, J.; Sos, M.L.; Seidel, D.; Peifer, M.; Zander, T.; Heuckmann, J.M.; Ullrich, R.T.; Menon, R.; Maier, S.; Soltermann, A., *et al.* Frequent and focal fgfr1 amplification associates with therapeutically tractable fgfr1 dependency in squamous cell lung cancer. *Science translational medicine* **2010**, *2*, 62ra93.
115. Seo, A.N.; Jin, Y.; Lee, H.J.; Sun, P.L.; Kim, H.; Jheon, S.; Kim, K.; Lee, C.T.; Chung, J.H. Fgfr1 amplification is associated with poor prognosis and smoking in non-small-cell lung cancer. *Virchows Archiv : an international journal of pathology* **2014**, *465*, 547-558.
116. Ueno, K.; Inoue, Y.; Kawaguchi, T.; Hosoe, S.; Kawahara, M. Increased serum levels of basic fibroblast growth factor in lung cancer patients: Relevance to response of therapy and prognosis. *Lung cancer* **2001**, *31*, 213-219.
117. Hibi, M.; Kaneda, H.; Tanizaki, J.; Sakai, K.; Togashi, Y.; Terashima, M.; De Velasco, M.A.; Fujita, Y.; Banno, E.; Nakamura, Y., *et al.* Fgfr gene alterations in lung squamous cell carcinoma are potential targets for the multikinase inhibitor nintedanib. *Cancer science* **2016**, *107*, 1667-1676.
118. Liao, R.G.; Jung, J.; Tchaicha, J.; Wilkerson, M.D.; Sivachenko, A.; Beauchamp, E.M.; Liu, Q.; Pugh, T.J.; Pedamallu, C.S.; Hayes, D.N., *et al.* Inhibitor-sensitive fgfr2 and fgfr3 mutations in lung squamous cell carcinoma. *Cancer research* **2013**, *73*, 5195-5205.
119. Gavine, P.R.; Mooney, L.; Kilgour, E.; Thomas, A.P.; Al-Kadhimi, K.; Beck, S.; Rooney, C.; Coleman, T.; Baker, D.; Mellor, M.J., *et al.* Azd4547: An orally bioavailable, potent, and selective inhibitor of the fibroblast growth factor receptor tyrosine kinase family. *Cancer research* **2012**, *72*, 2045-2056.

120. Garnier, M.; Giamarchi, C.; Delrieu, I.; Rio, M.C.; Chinestra, P.; Bayard, F.; Poirot, M.; Faye, J.C. Insulin and estrogen receptor ligand influence the fgf-2 activities in mcf-7 breast cancer cells. *Biochemical pharmacology* **2003**, *65*, 629-636.
121. Fillmore, C.M.; Gupta, P.B.; Rudnick, J.A.; Caballero, S.; Keller, P.J.; Lander, E.S.; Kuperwasser, C. Estrogen expands breast cancer stem-like cells through paracrine fgf/tbx3 signaling. *Proceedings of the National Academy of Sciences of the United States of America* **2010**, *107*, 21737-21742.
122. Turner, N.; Pearson, A.; Sharpe, R.; Lambros, M.; Geyer, F.; Lopez-Garcia, M.A.; Natrajan, R.; Marchio, C.; Iorns, E.; Mackay, A., *et al.* Fgfr1 amplification drives endocrine therapy resistance and is a therapeutic target in breast cancer. *Cancer research* **2010**, *70*, 2085-2094.
123. Siegfried, J.M.; Farooqui, M.; Rothenberger, N.J.; Dacic, S.; Stabile, L.P. Interaction between the estrogen receptor and fibroblast growth factor receptor pathways in non-small cell lung cancer. *Oncotarget* **2017**, *8*, 24063-24076.
124. Siegfried, J.M.; Krishnamachary, N.; Gaither Davis, A.; Gubish, C.; Hunt, J.D.; Shriver, S.P. Evidence for autocrine actions of neuromedin b and gastrin-releasing peptide in non-small cell lung cancer. *Pulmonary pharmacology & therapeutics* **1999**, *12*, 291-302.
125. Garon, E.B.; Pietras, R.J.; Finn, R.S.; Kamranpour, N.; Pitts, S.; Marquez-Garban, D.C.; Desai, A.J.; Dering, J.; Hosmer, W.; von Euw, E.M., *et al.* Antiestrogen fulvestrant enhances the antiproliferative effects of epidermal growth factor receptor inhibitors in human non-small-cell lung cancer. *Journal of thoracic oncology : official publication of the International Association for the Study of Lung Cancer* **2013**, *8*, 270-278.
126. Hershberger, P.A.; Stabile, L.P.; Kanterewicz, B.; Rothstein, M.E.; Gubish, C.T.; Land, S.; Shuai, Y.; Siegfried, J.M.; Nichols, M. Estrogen receptor beta (erbeta) subtype-specific ligands increase transcription, p44/p42 mitogen activated protein kinase (mapk) activation and growth in human non-small cell lung cancer cells. *The Journal of steroid biochemistry and molecular biology* **2009**, *116*, 102-109.
127. Zhang, W.; Stabile, L.P.; Keohavong, P.; Romkes, M.; Grandis, J.R.; Traynor, A.M.; Siegfried, J.M. Mutation and polymorphism in the egfr-tk domain associated with lung cancer. *Journal of thoracic oncology : official publication of the International Association for the Study of Lung Cancer* **2006**, *1*, 635-647.
128. Stabile, L.P.; Rothstein, M.E.; Cunningham, D.E.; Land, S.R.; Dacic, S.; Keohavong, P.; Siegfried, J.M. Prevention of tobacco carcinogen-induced lung cancer in female mice using antiestrogens. *Carcinogenesis* **2012**, *33*, 2181-2189.
129. Goss, P.E.; Ingle, J.N.; Ales-Martinez, J.E.; Cheung, A.M.; Chlebowski, R.T.; Wactawski-Wende, J.; McTiernan, A.; Robbins, J.; Johnson, K.C.; Martin, L.W., *et al.* Exemestane for breast-cancer prevention in postmenopausal women. *The New England journal of medicine* **2011**, *364*, 2381-2391.
130. Liu, H.; Talalay, P. Relevance of anti-inflammatory and antioxidant activities of exemestane and synergism with sulforaphane for disease prevention. *Proceedings of the National Academy of Sciences of the United States of America* **2013**, *110*, 19065-19070.
131. Gomes, M.; Teixeira, A.L.; Coelho, A.; Araujo, A.; Medeiros, R. The role of inflammation in lung cancer. *Advances in experimental medicine and biology* **2014**, *816*, 1-23.
132. Svoronos, N.; Perales-Puchalt, A.; Allegrezza, M.J.; Rutkowski, M.R.; Payne, K.K.; Tesone, A.J.; Nguyen, J.M.; Curiel, T.J.; Cadungog, M.G.; Singhal, S., *et al.* Tumor cell-independent estrogen signaling drives disease progression through mobilization of myeloid-derived suppressor cells. *Cancer discovery* **2017**, *7*, 72-85.

133. Hamilton, D.H.; Griner, L.M.; Keller, J.M.; Hu, X.; Southall, N.; Marugan, J.; David, J.M.; Ferrer, M.; Palena, C. Targeting estrogen receptor signaling with fulvestrant enhances immune and chemotherapy-mediated cytotoxicity of human lung cancer. *Clinical cancer research : an official journal of the American Association for Cancer Research* **2016**, *22*, 6204-6216.
134. Chatterjee, S.; Huang, E.H.; Christie, I.; Kurland, B.F.; Burns, T.F. Acquired resistance to the hsp90 inhibitor, ganetespib, in kras-mutant nsclc is mediated via reactivation of the erk-p90rsk-mtor signaling network. *Molecular cancer therapeutics* **2017**, *16*, 793-804.
135. Brodie, A.; Jelovac, D.; Macedo, L.; Sabnis, G.; Tilghman, S.; Goloubeva, O. Therapeutic observations in mcf-7 aromatase xenografts. *Clinical cancer research : an official journal of the American Association for Cancer Research* **2005**, *11*, 884s-888s.
136. Marquez-Garban, D.C.; Chen, H.W.; Goodglick, L.; Fishbein, M.C.; Pietras, R.J. Targeting aromatase and estrogen signaling in human non-small cell lung cancer. *Annals of the New York Academy of Sciences* **2009**, *1155*, 194-205.
137. Takeda, K.; Hayakawa, Y.; Smyth, M.J.; Kayagaki, N.; Yamaguchi, N.; Kakuta, S.; Iwakura, Y.; Yagita, H.; Okumura, K. Involvement of tumor necrosis factor-related apoptosis-inducing ligand in surveillance of tumor metastasis by liver natural killer cells. *Nature medicine* **2001**, *7*, 94-100.
138. Cretney, E.; Takeda, K.; Yagita, H.; Glaccum, M.; Peschon, J.J.; Smyth, M.J. Increased susceptibility to tumor initiation and metastasis in tnf-related apoptosis-inducing ligand-deficient mice. *Journal of immunology* **2002**, *168*, 1356-1361.
139. Mitra, A.; Mishra, L.; Li, S. Emt, ctcs and cscs in tumor relapse and drug-resistance. *Oncotarget* **2015**, *6*, 10697-10711.
140. Rho, J.K.; Choi, Y.J.; Lee, J.K.; Ryoo, B.Y.; Na, II; Yang, S.H.; Kim, C.H.; Lee, J.C. Epithelial to mesenchymal transition derived from repeated exposure to gefitinib determines the sensitivity to egfr inhibitors in a549, a non-small cell lung cancer cell line. *Lung cancer* **2009**, *63*, 219-226.
141. Chatterjee, S.; Bhattacharya, S.; Socinski, M.A.; Burns, T.F. Hsp90 inhibitors in lung cancer: Promise still unfulfilled. *Clinical advances in hematology & oncology : H&O* **2016**, *14*, 346-356.
142. Lu, X.; Xiao, L.; Wang, L.; Ruden, D.M. Hsp90 inhibitors and drug resistance in cancer: The potential benefits of combination therapies of hsp90 inhibitors and other anti-cancer drugs. *Biochemical pharmacology* **2012**, *83*, 995-1004.
143. Thiery, J.P. Epithelial-mesenchymal transitions in tumour progression. *Nature reviews. Cancer* **2002**, *2*, 442-454.
144. Davis, F.M.; Stewart, T.A.; Thompson, E.W.; Monteith, G.R. Targeting emt in cancer: Opportunities for pharmacological intervention. *Trends in pharmacological sciences* **2014**, *35*, 479-488.
145. Heerboth, S.; Housman, G.; Leary, M.; Longacre, M.; Byler, S.; Lapinska, K.; Willbanks, A.; Sarkar, S. Emt and tumor metastasis. *Clinical and translational medicine* **2015**, *4*, 6.
146. Reed, M.J.; Purohit, A. Breast cancer and the role of cytokines in regulating estrogen synthesis: An emerging hypothesis. *Endocrine reviews* **1997**, *18*, 701-715.
147. Dutta, P.; Sabri, N.; Li, J.; Li, W.X. Role of stat3 in lung cancer. *Jak-Stat* **2014**, *3*, e999503.
148. von Karstedt, S.; Conti, A.; Nobis, M.; Montinaro, A.; Hartwig, T.; Lemke, J.; Legler, K.; Annewanter, F.; Campbell, A.D.; Taraborrelli, L., *et al.* Cancer cell-autonomous trail-r signaling promotes kras-driven cancer progression, invasion, and metastasis. *Cancer cell* **2015**, *27*, 561-573.

149. Jolly, M.K.; Tripathi, S.C.; Jia, D.; Mooney, S.M.; Celiktas, M.; Hanash, S.M.; Mani, S.A.; Pienta, K.J.; Ben-Jacob, E.; Levine, H. Stability of the hybrid epithelial/mesenchymal phenotype. *Oncotarget* **2016**, *7*, 27067-27084.
150. Cihoric, N.; Savic, S.; Schneider, S.; Ackermann, I.; Bichsel-Naef, M.; Schmid, R.A.; Lardinois, D.; Gugger, M.; Bubendorf, L.; Zlobec, I., *et al.* Prognostic role of fgfr1 amplification in early-stage non-small cell lung cancer. *British journal of cancer* **2014**, *110*, 2914-2922.
151. Fan, S.; Liao, Y.; Liu, C.; Huang, Q.; Liang, H.; Ai, B.; Fu, S.; Zhou, S. Estrogen promotes tumor metastasis via estrogen receptor beta-mediated regulation of matrix-metalloproteinase-2 in non-small cell lung cancer. *Oncotarget* **2017**.